重力波観測とデータ解析

真貝寿明

大阪工業大学情報科学部

http://www.oit.ac.jp/is/~shinkai/

KAGRA

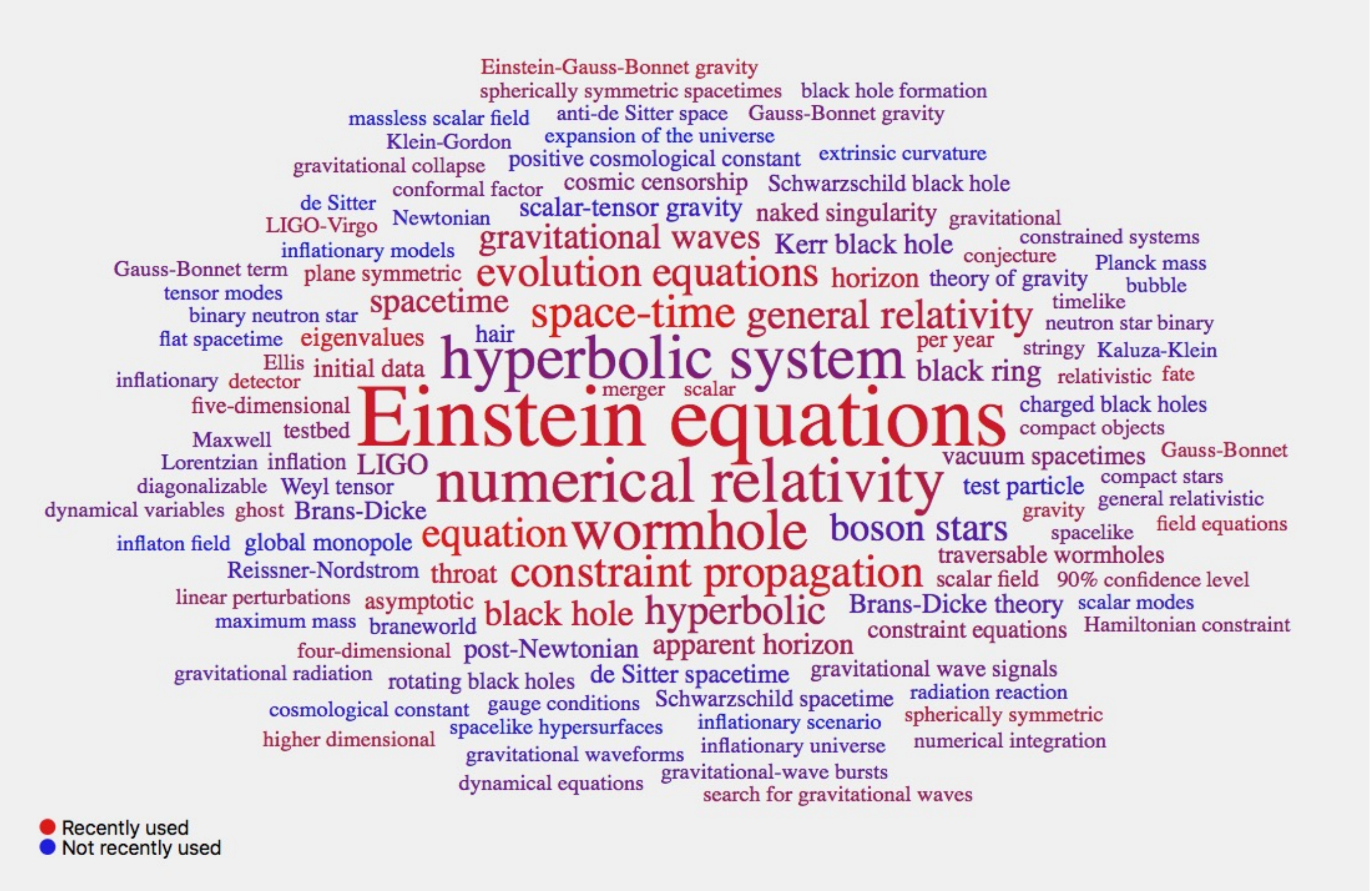

https://scimeter.org says.

1.重力波 / 2. KAGRA / 3. データ解析

1. 重力波

2016年2月，LIGOが重力波を初めて検出した，と発表　GW150914

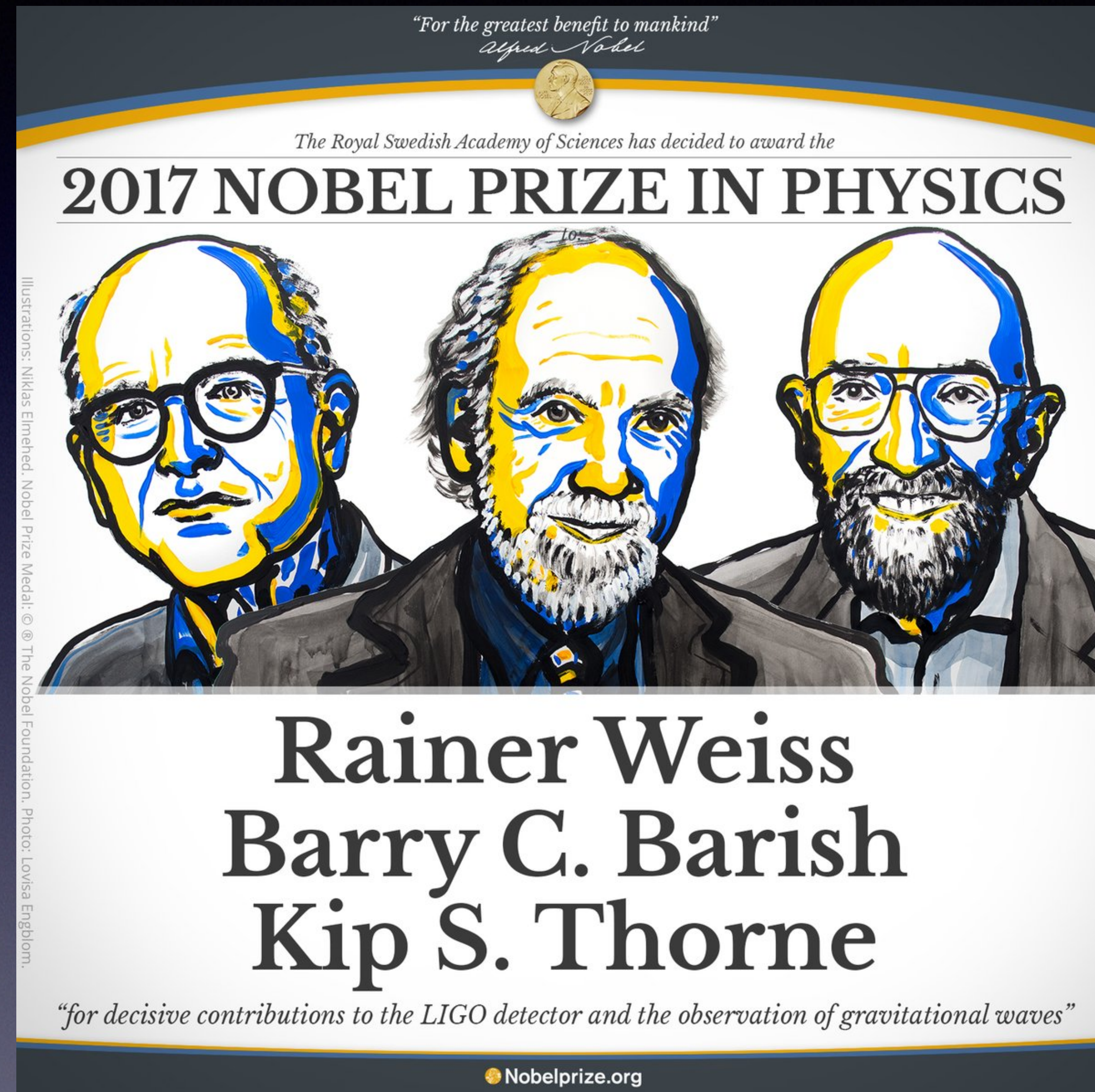

2017年10月，LIGO/Virgo
中性子星連星合体観測を発表
GW170817

2017年10月，ノーベル財団が，重力波検出に貢献した３名をノーベル物理学賞として顕彰

重力波の発生と伝播

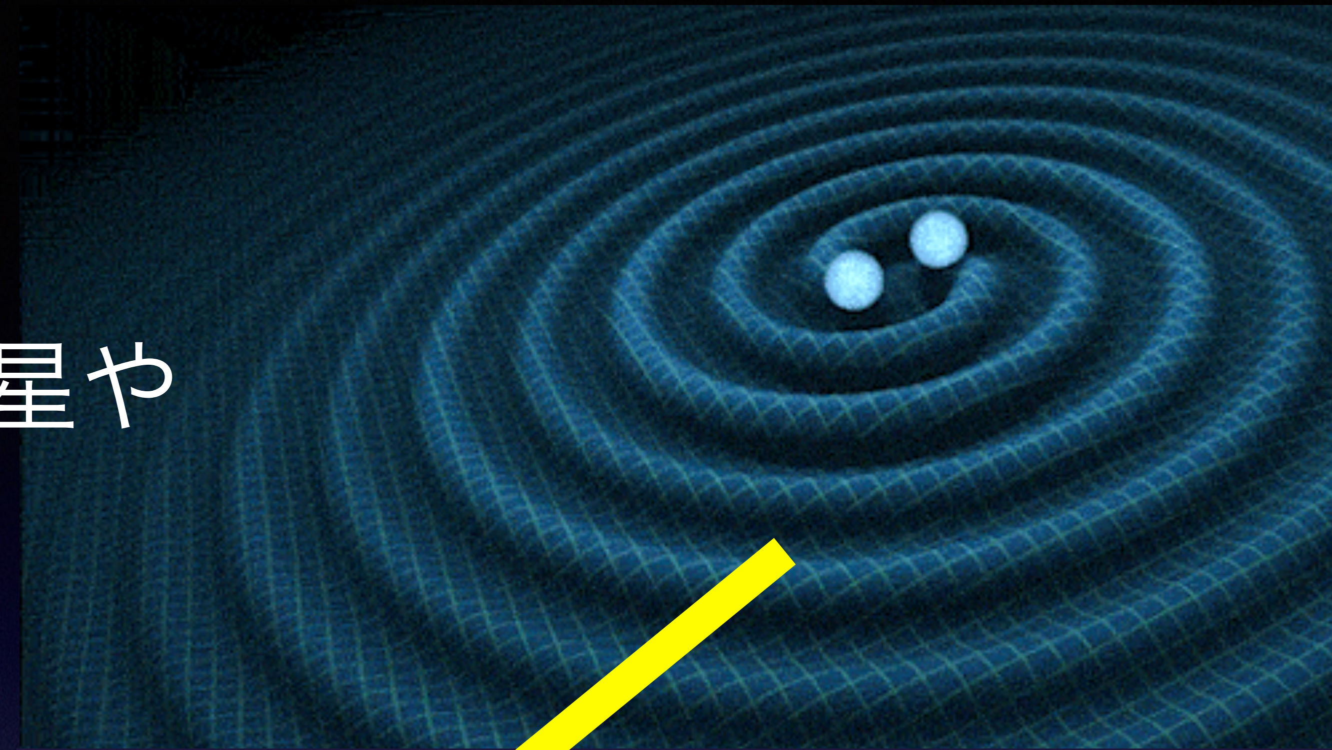

ブラックホール連星や
中性子星連星

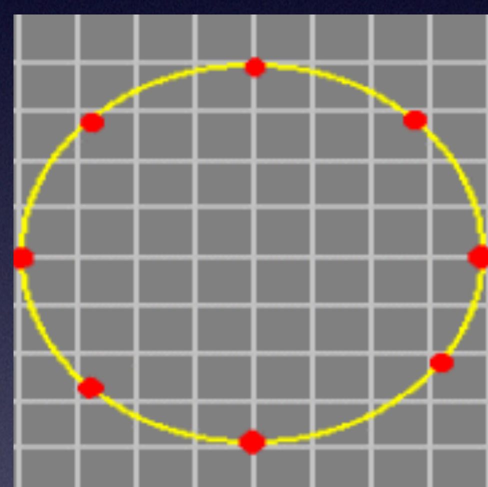

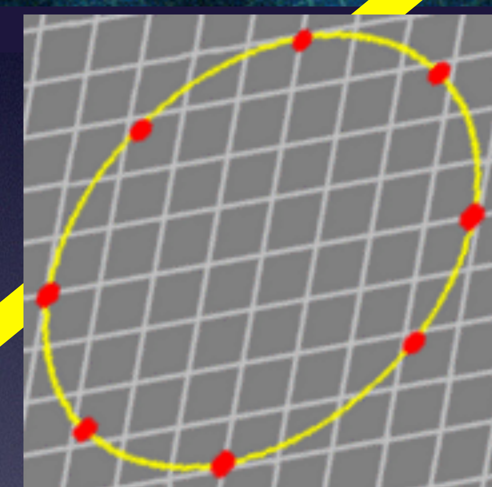

レーザー干渉計

LIGO＝Laser Interferometer
Gravitational-Wave Observatory

重力波の発生と伝播

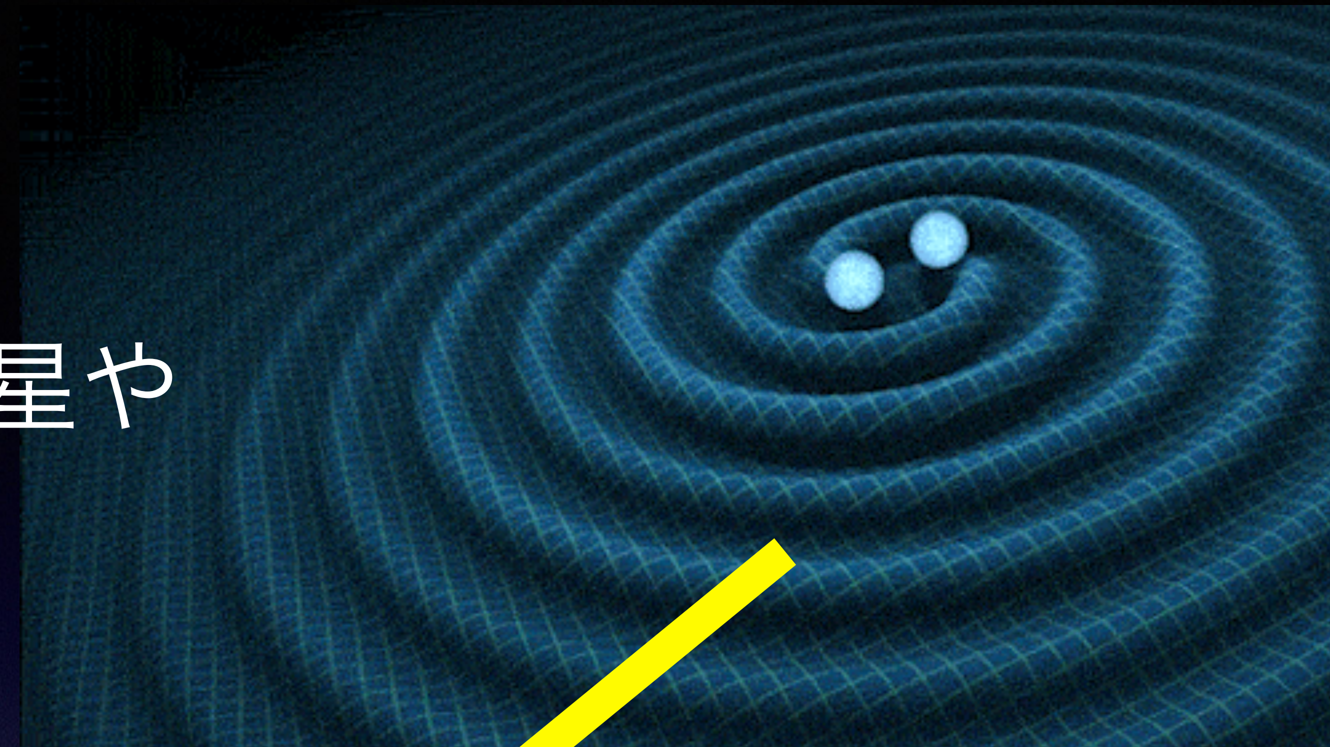

ブラックホール連星や
中性子星連星

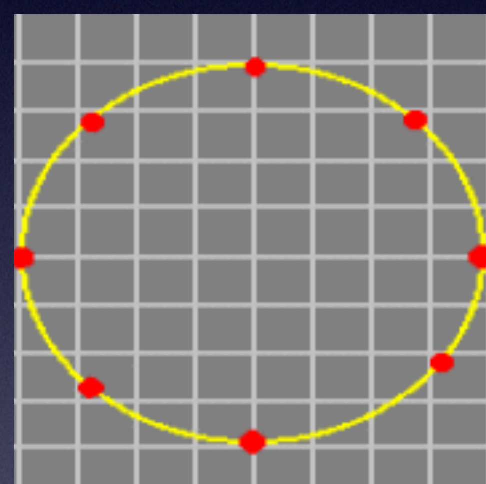

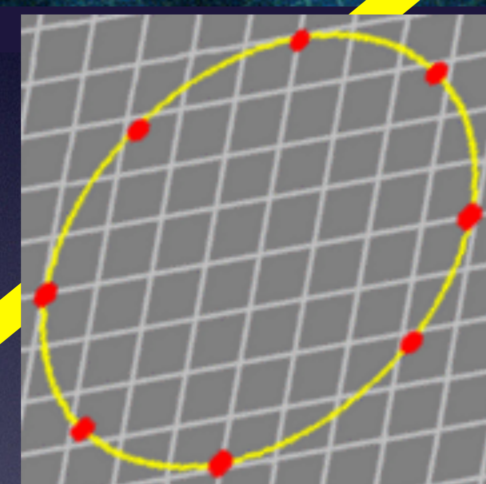

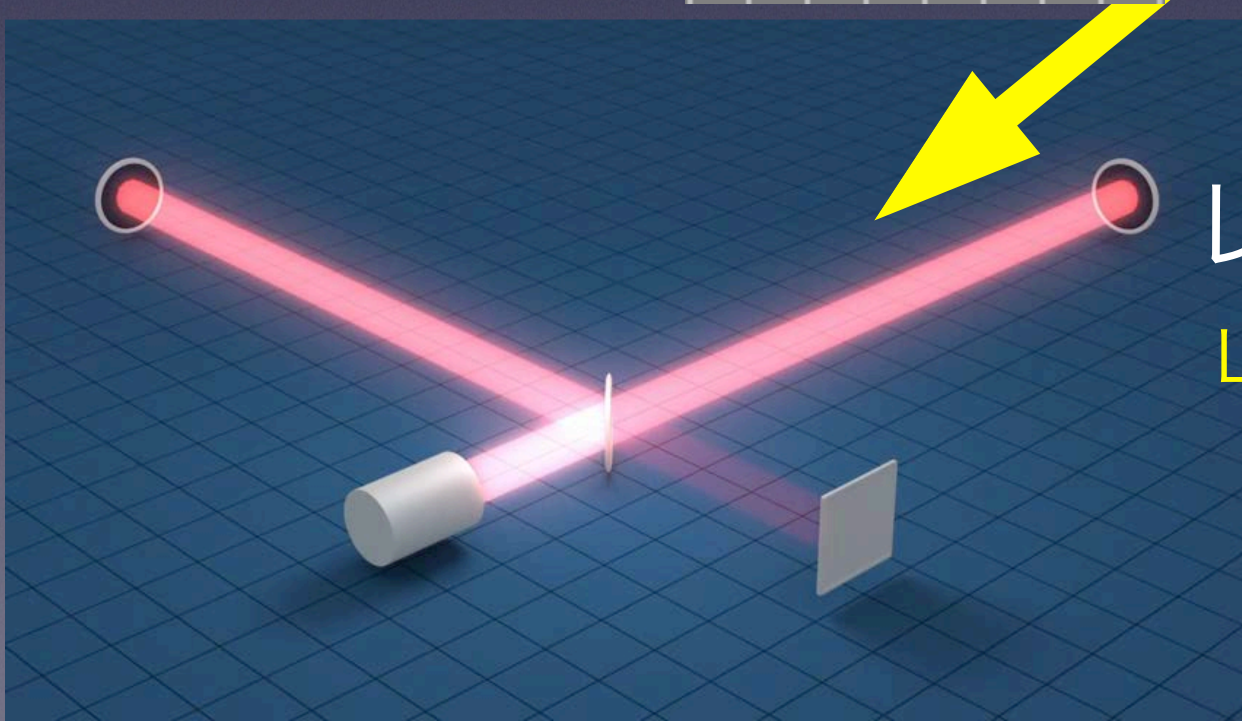

レーザー干渉計

LIGO＝Laser Interferometer
Gravitational-Wave Observatory

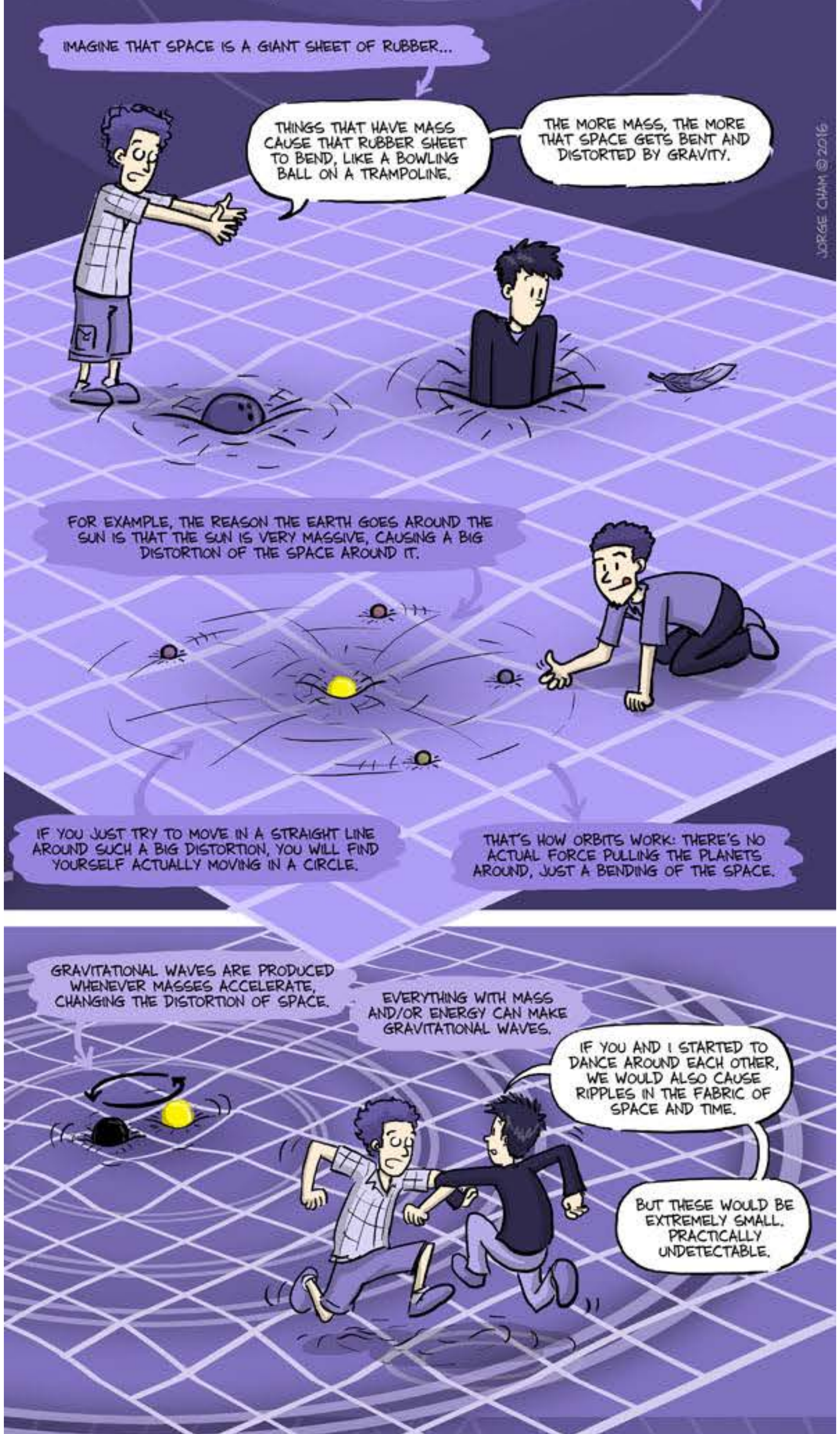

重力＝時空のゆがみ

質点が加速度運動
＝重力波発生

大質量の天体が激しく加速度運動
＝観測できる重力波が発生

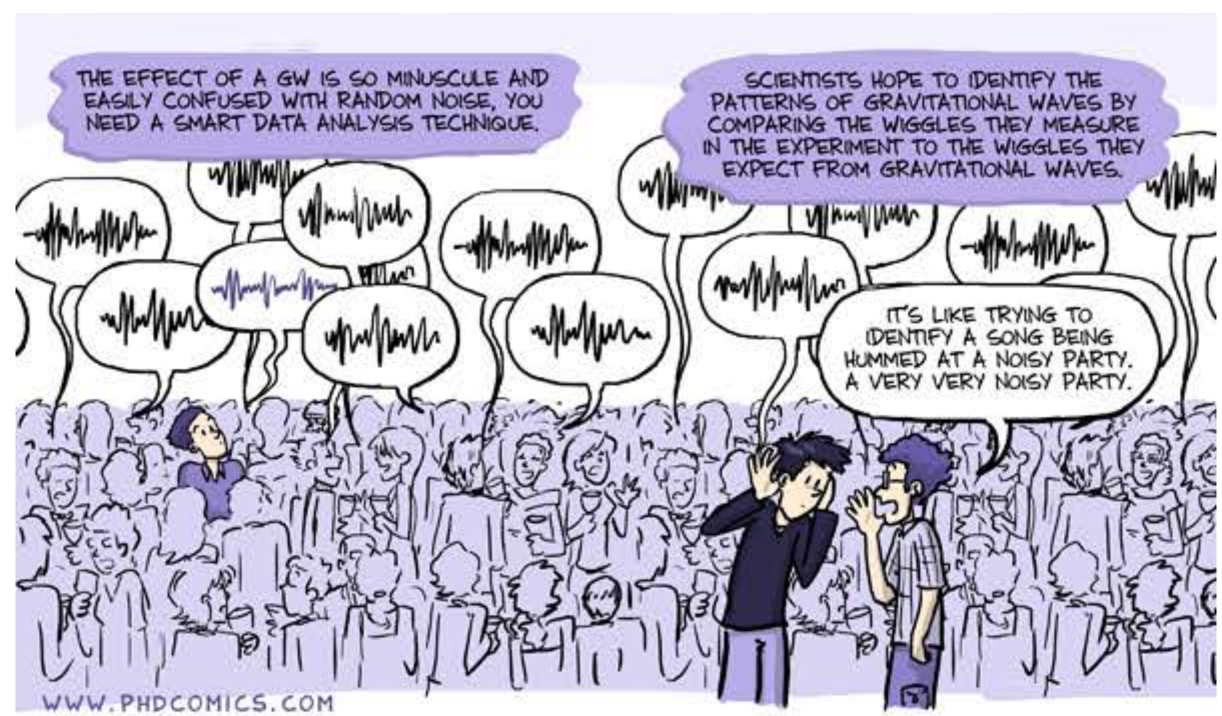

www.phdcomics.com
“gravitational waves explained”

重力波の波源

http://gwcenter.icrr.u-tokyo.ac.jp

超新星爆発（写真出典:NASA）

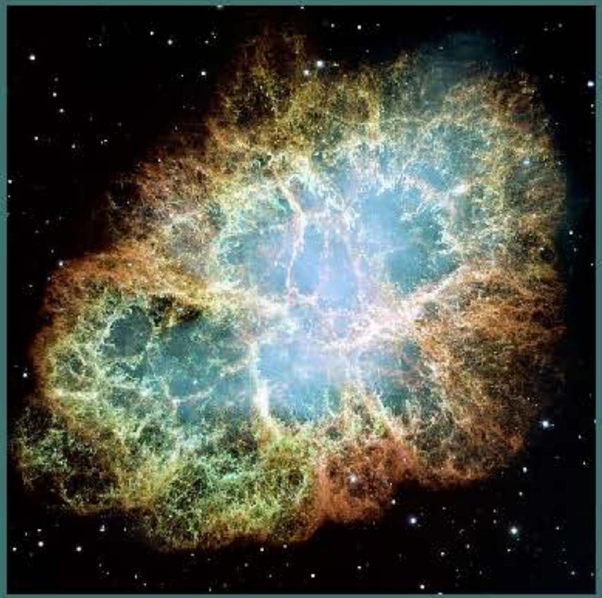

パルサー（写真出典:NASA）

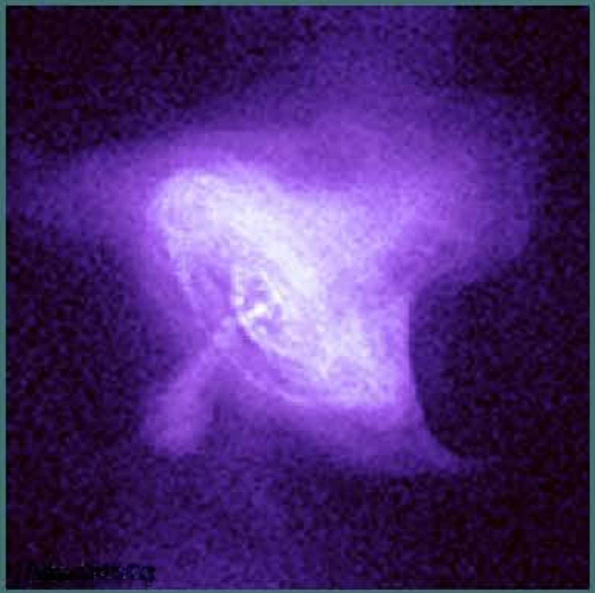

ブラックホール（想像図）

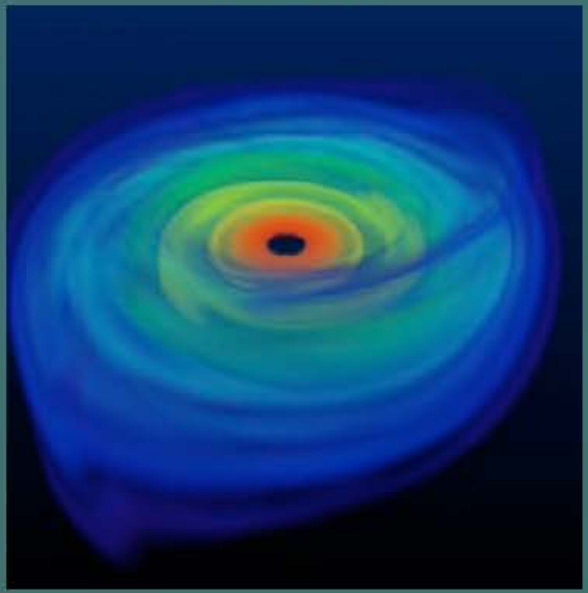

連星中性子星合体（想像図）

予測が難しい

振幅が小さい

振幅が小さい

連星合体をターゲットに

重力波観測によって解明できること

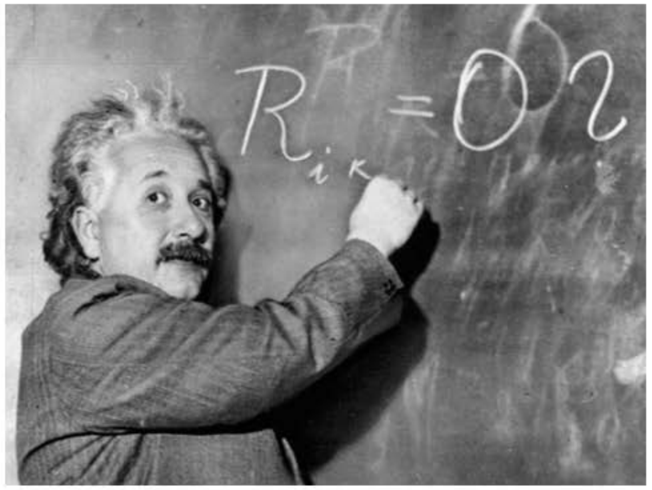

一般相対性理論は正しいか？

強い重力場で重力理論の検証ができる

ブラックホール合体後のふるまいは？

no hair になるか.

（質量，角運動量，電荷の3物理量のみか？）

ガンマ線バースト現象の起源は？

加速メカニズムは？

重力波観測によって解明できること

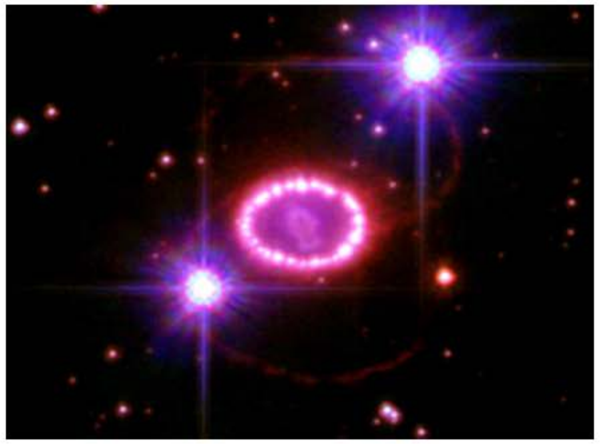

超新星爆発のメカニズムは？

ブラックホールと中性子星の質量差？

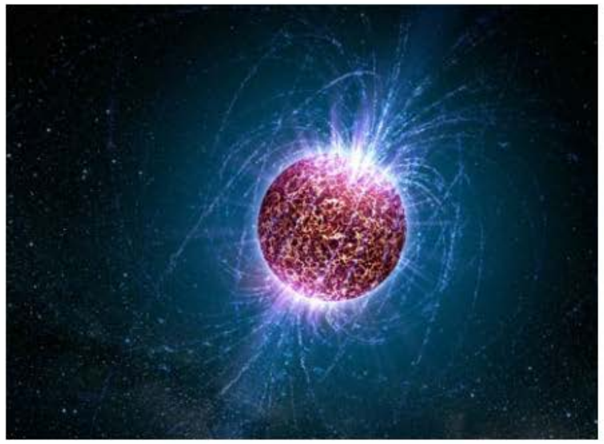

中性子星の最大質量は？

高密度物質の状態方程式は？

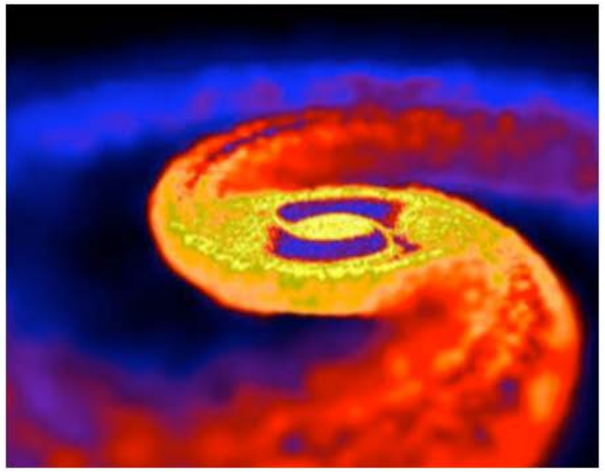

重元素の起源？

r-processは充分に発生するか？

重力波観測によって解明できること（ちょっと将来）

銀河中心の超巨大ブラックホールの起源は？

合体成長か，初期にできていたか？

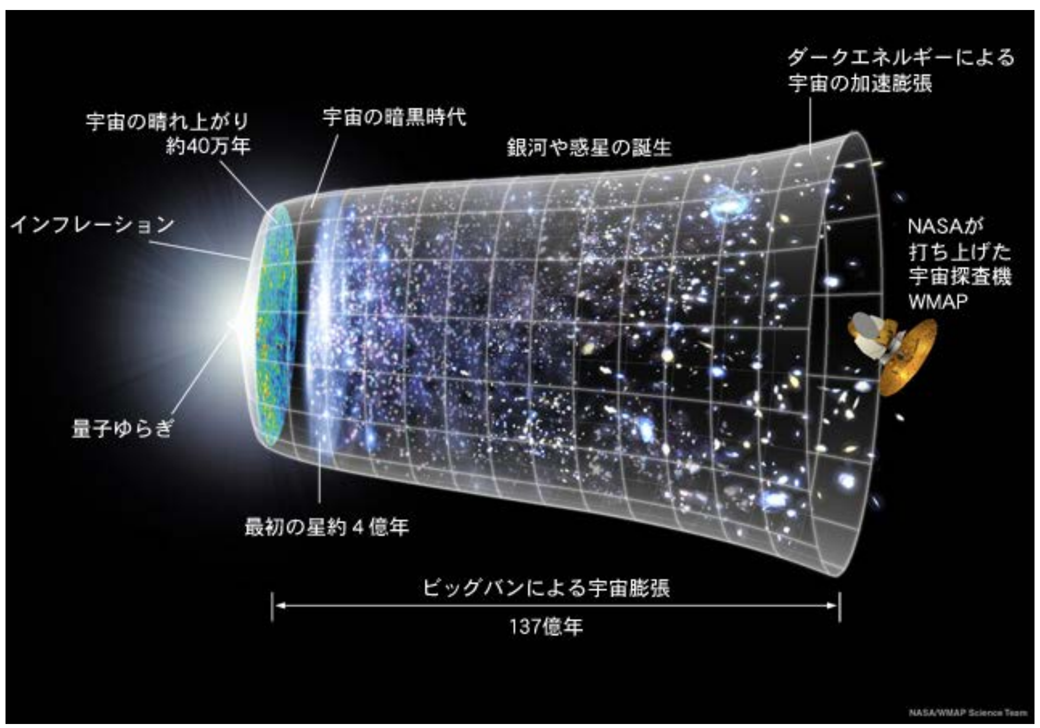

宇宙の膨張速度の測定
星形成モデルの特定
CMB以前の初期宇宙の解明

連星中性子星の発見 (1974)

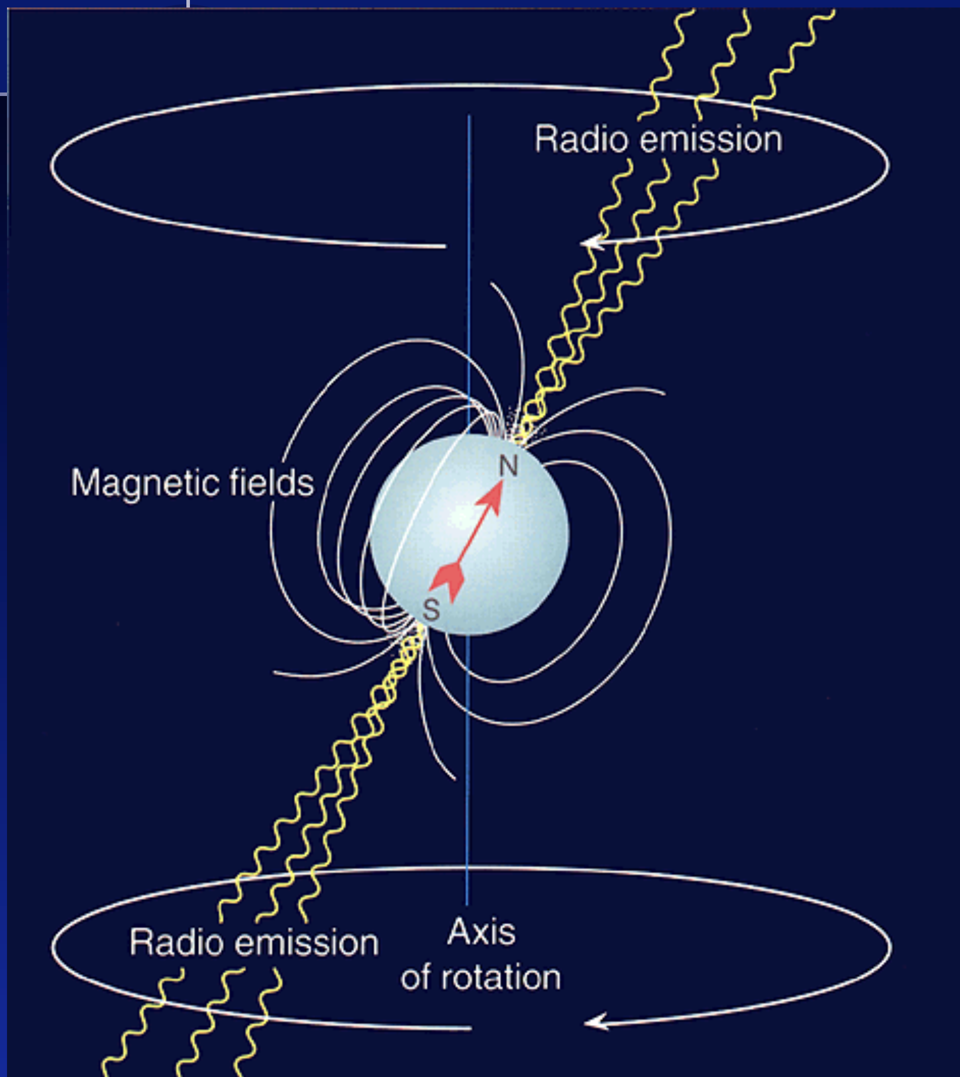

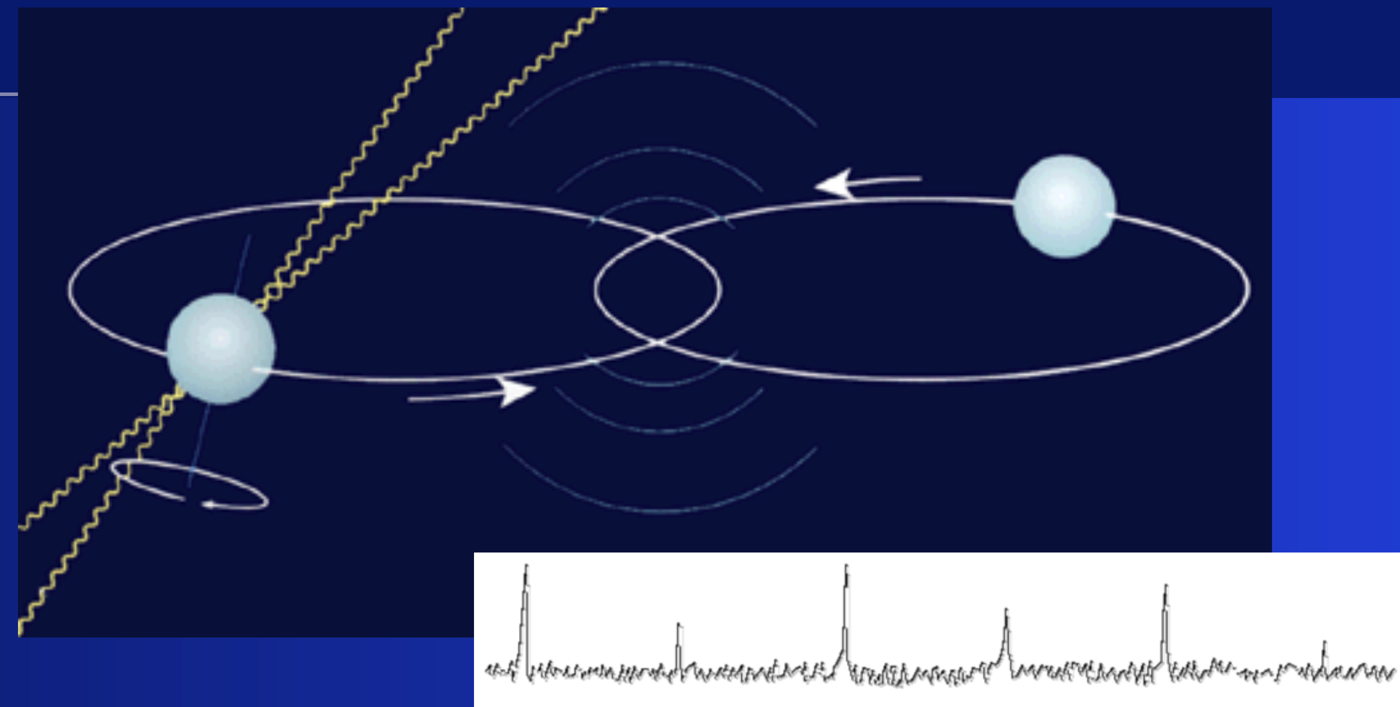


Arecibo, Puerto Rico

パルサー＝中性子星
半径 10km位
質量 1.4x太陽

http://www.nobelprize.org/nobel_prizes/physics/laureates/1993/illpres/discovery.html

連星中性子星の発見 (1974)

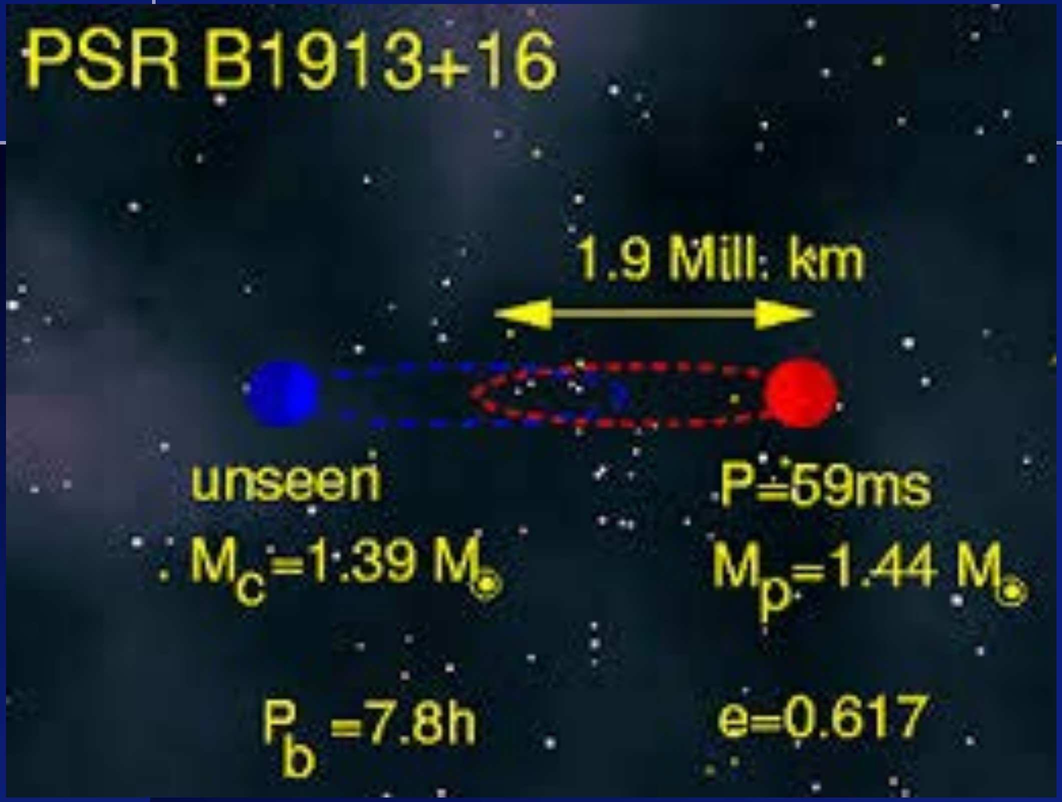

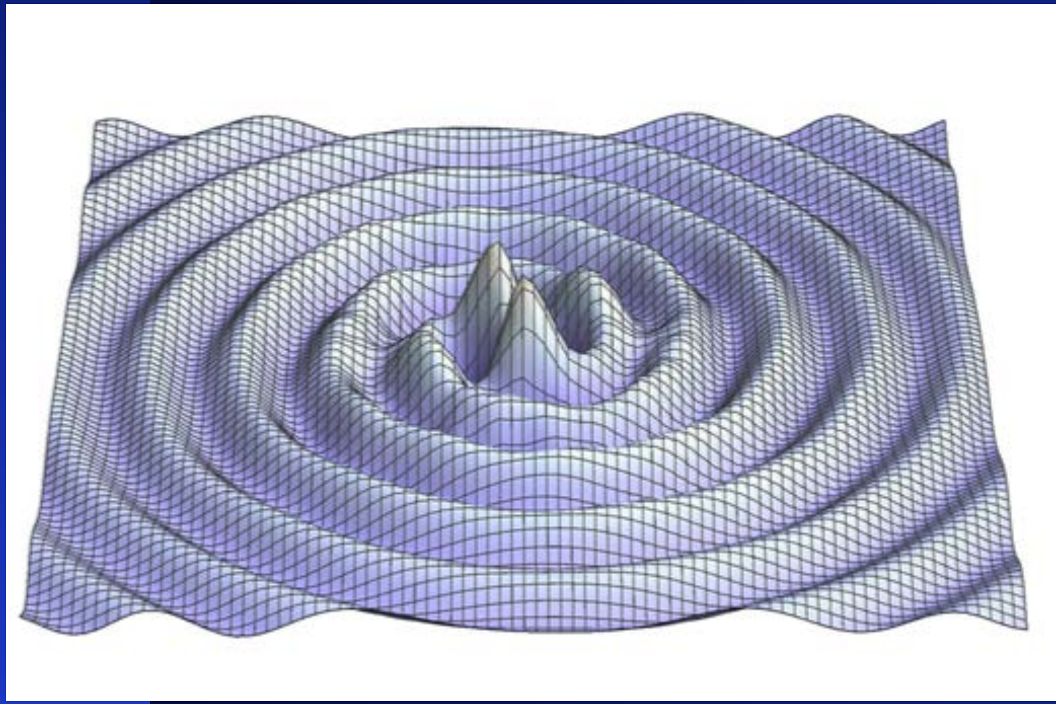

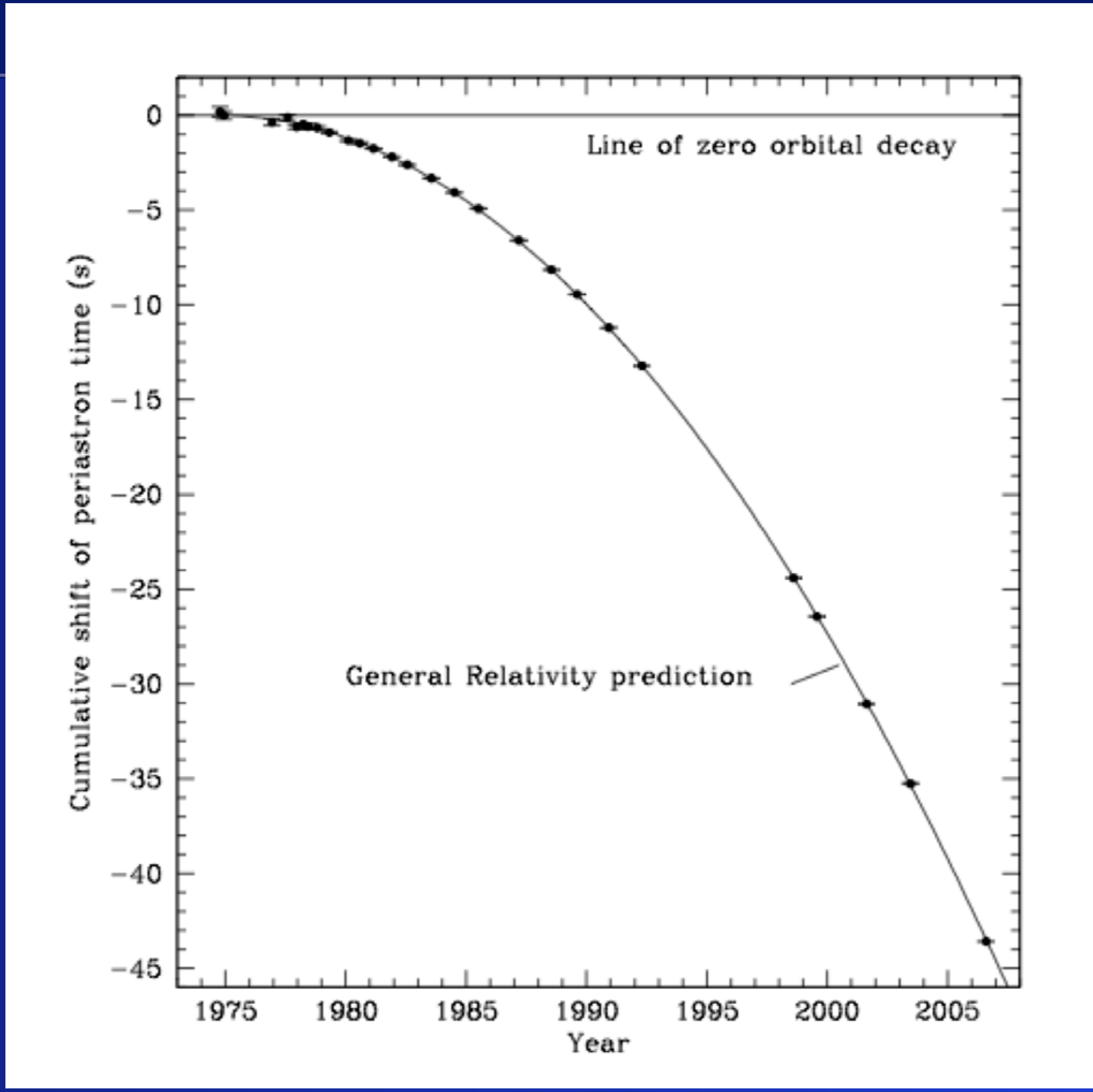

重力波を放出してエネルギーを失うので，星が近づいてゆく．

重力波の存在が間接的に確かめられた．

連星中性子星の発見 (1974)

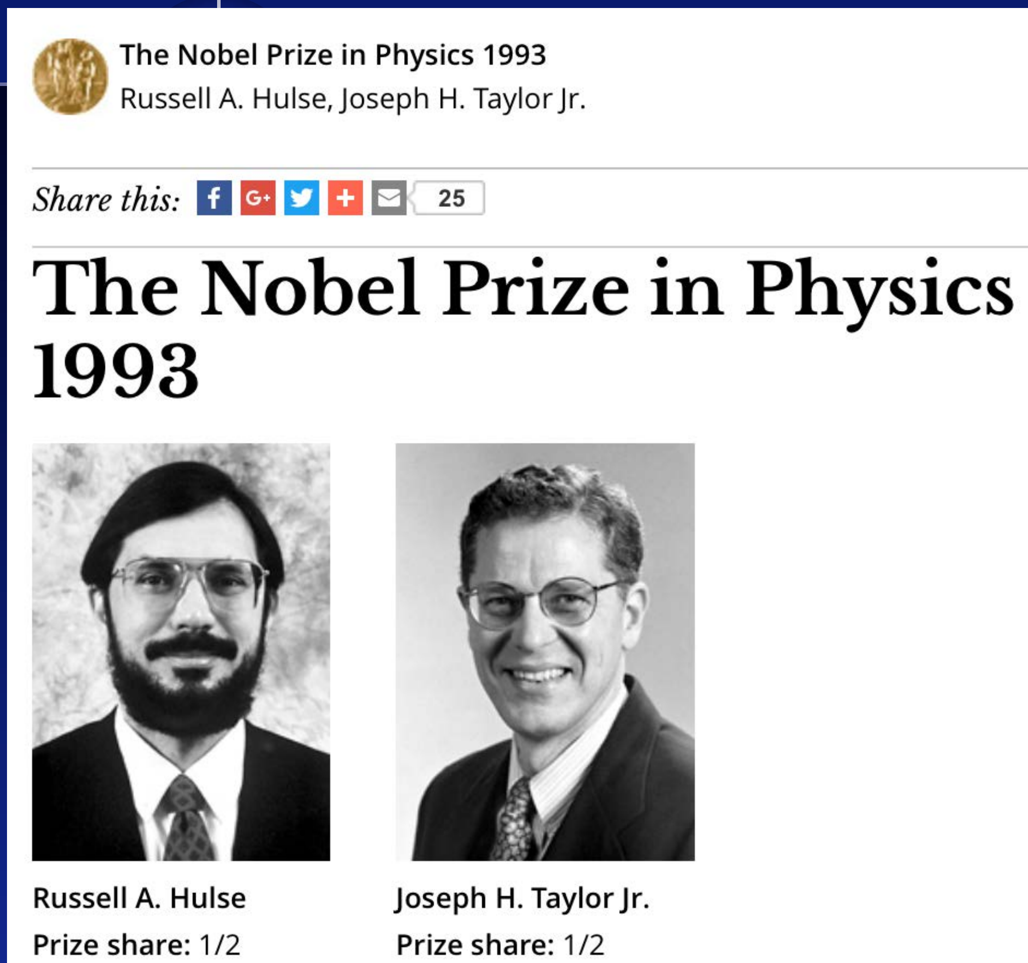

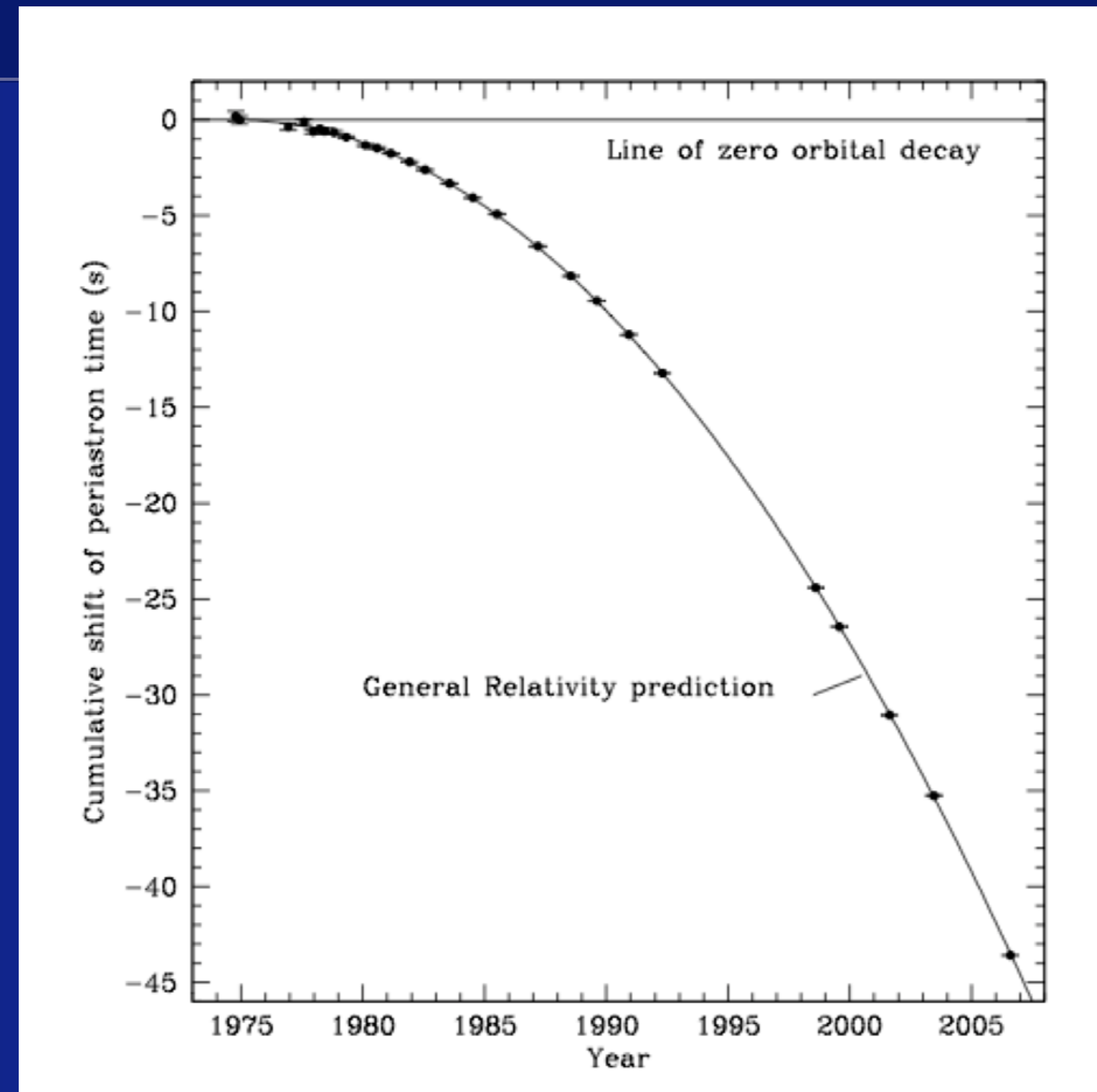

"for the discovery of a new type of pulsar, a discovery that has opened up new possibilities for the study of gravitation"

"重力についての新しい研究を開いた，新種のパルサーの発見に対して"

重力波の存在が間接的に確かめられた.

重力波の存在は連星パルサーの発見で,
間接的に確かめられていた.

重力波の直接観測をしたい！

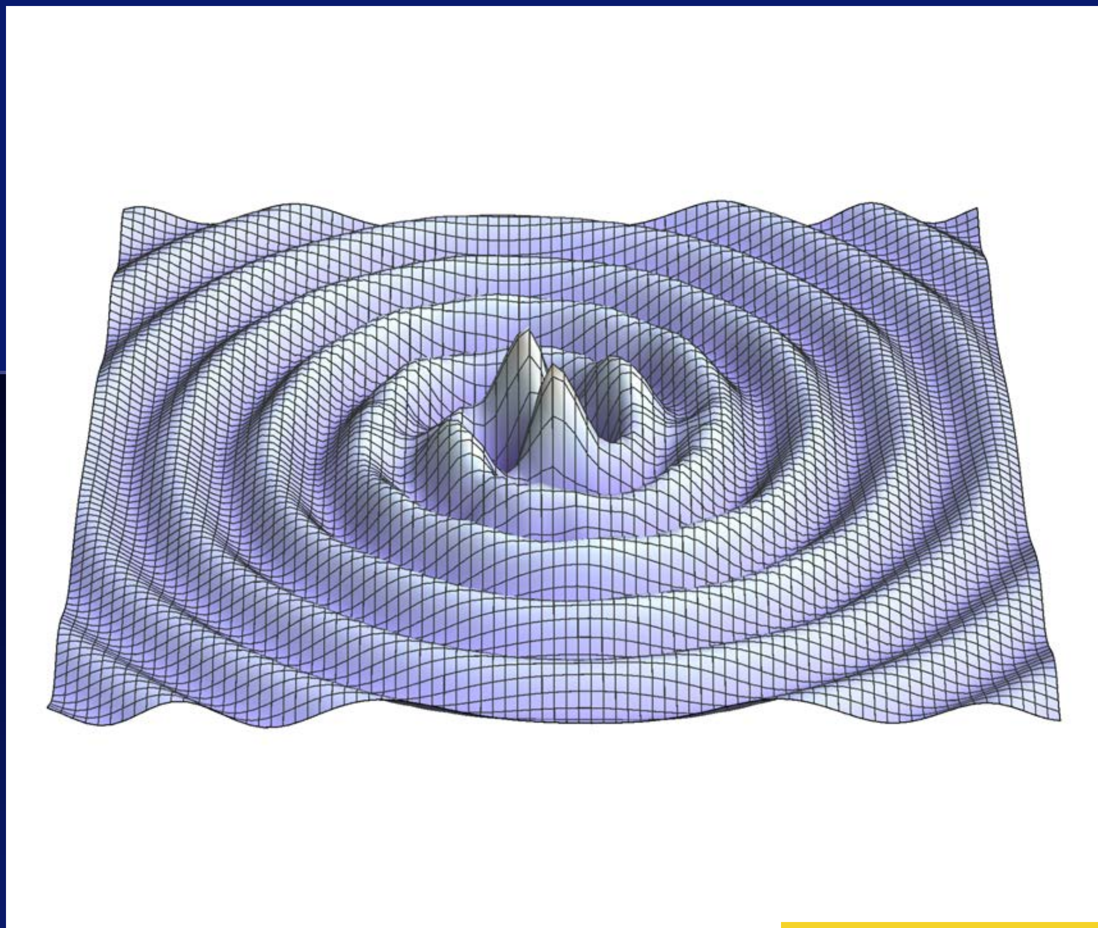

連星中性子星
連星ブラックホール

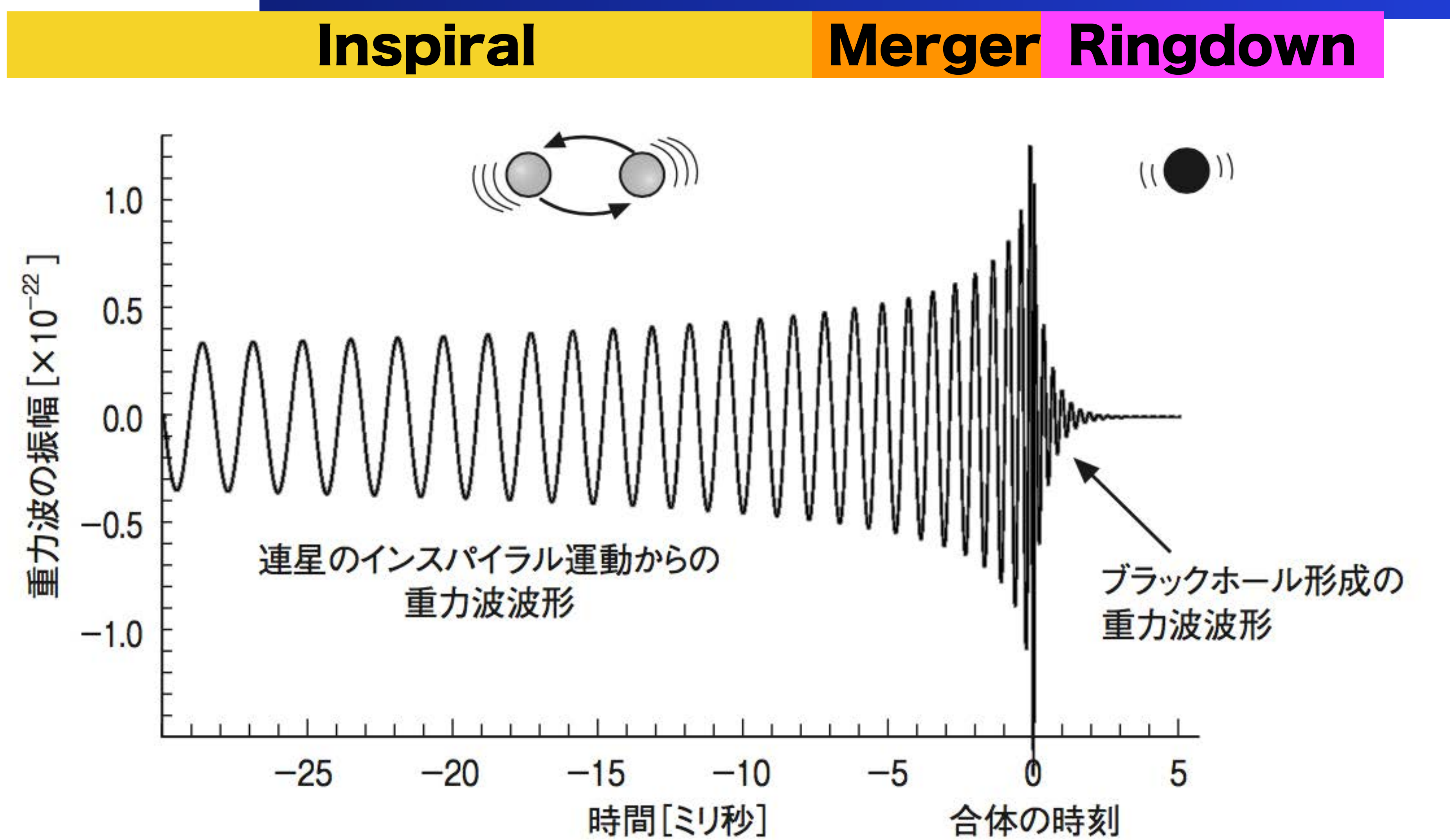

2015年9月14日

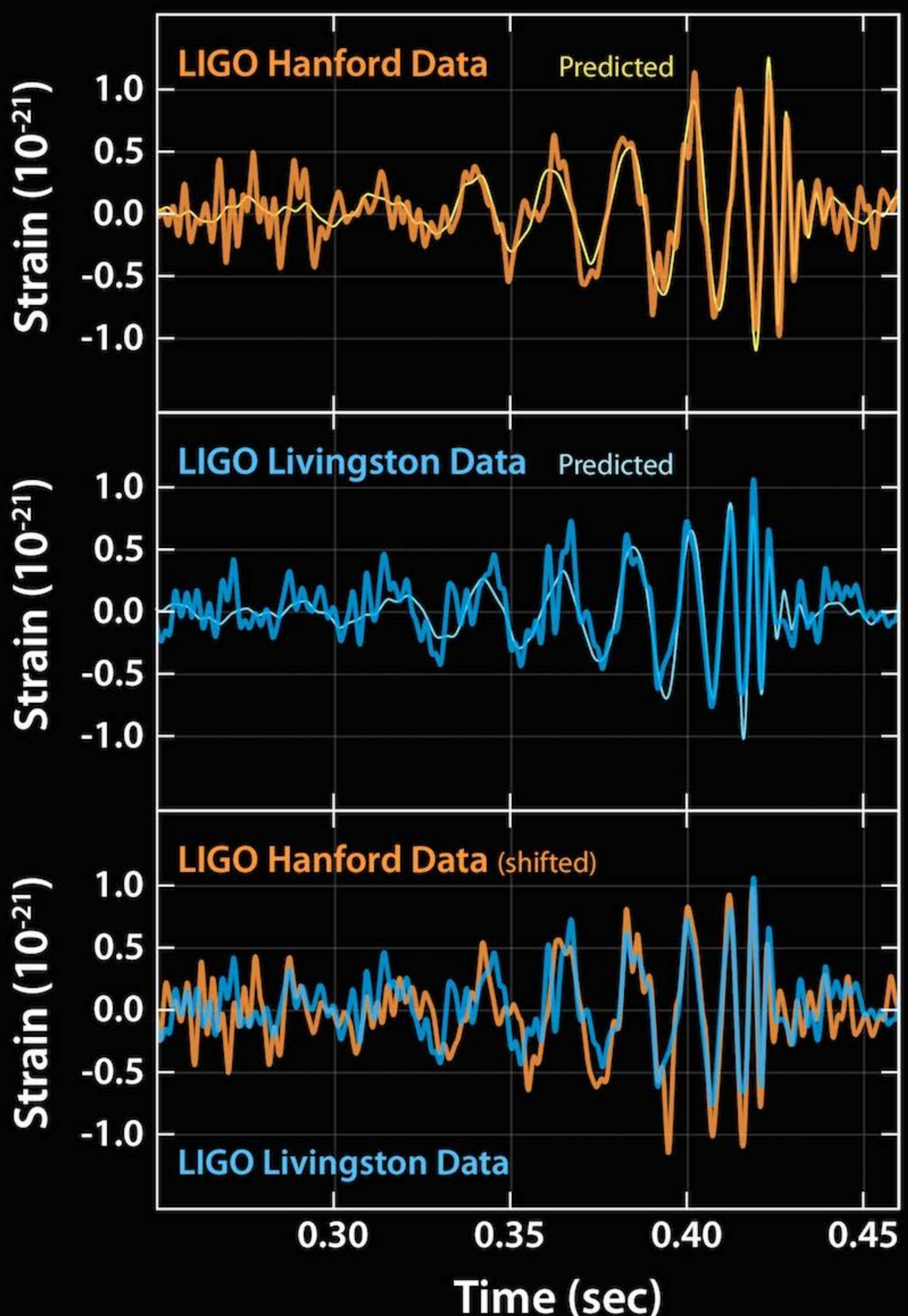

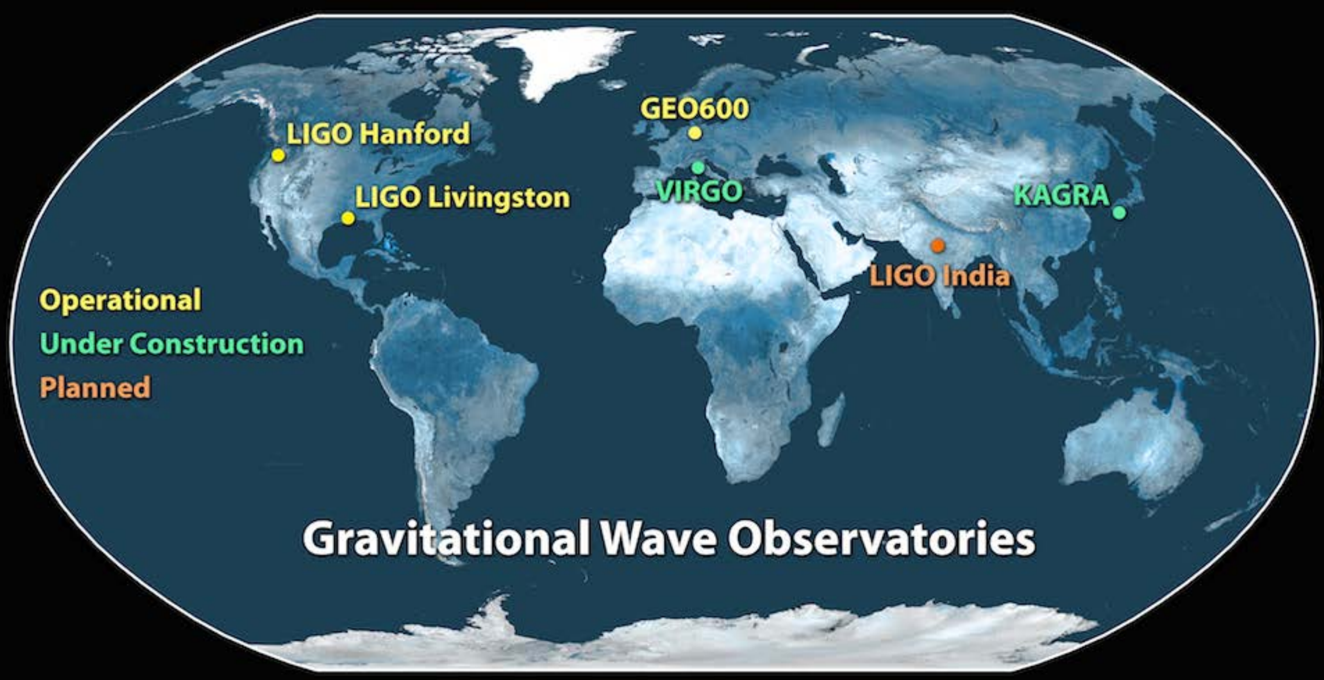

太陽の36倍と29倍のブラックホールが合体して,
太陽の62倍のブラックホールになった.

3倍の質量が消失

$$E = mc^2$$

13億光年先（440 Mpc）

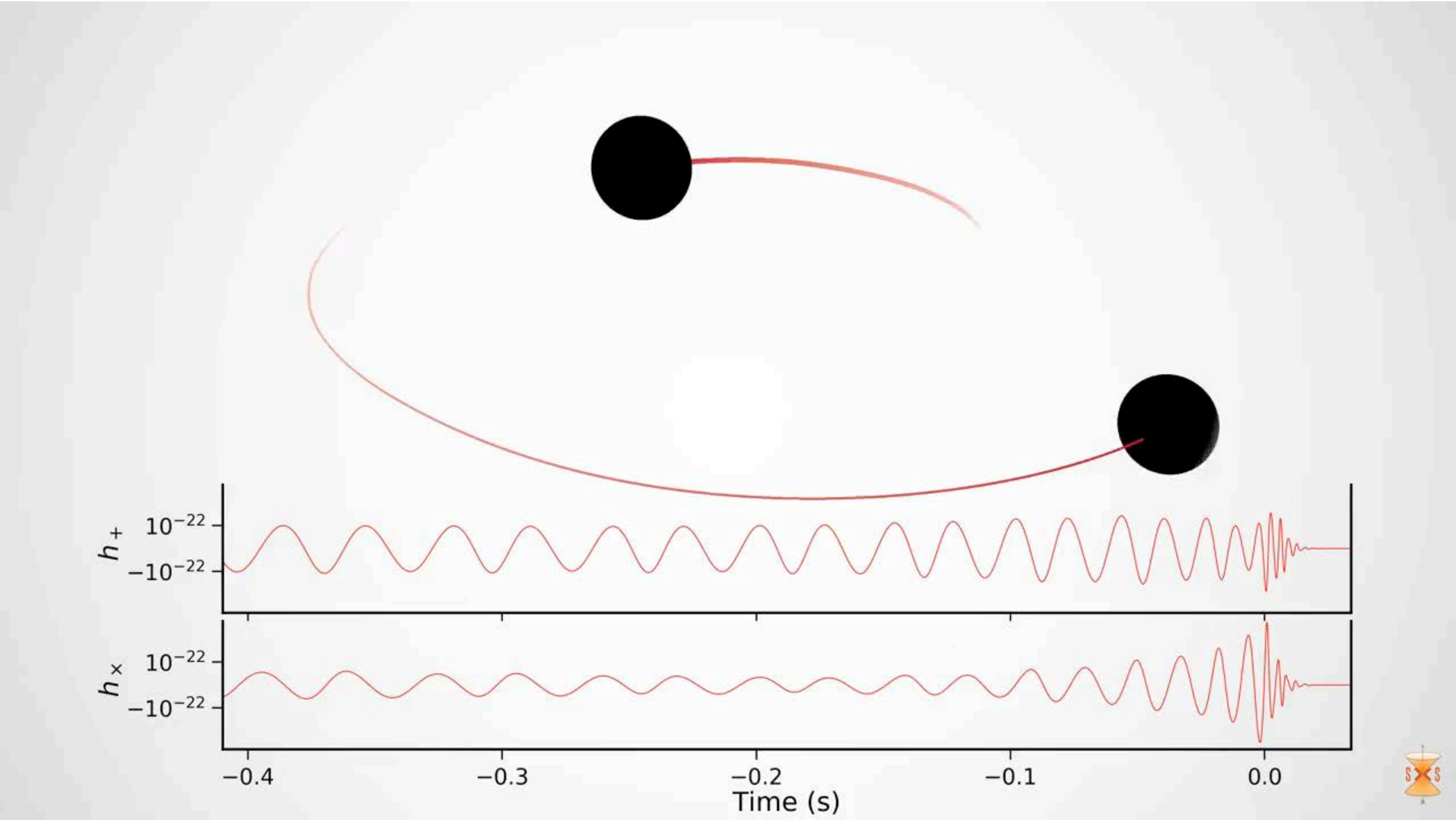

Animation of the inspiral and collision of two black holes consistent with the masses and spins of GW170104. The top part of the movie shows the black hole horizons (surfaces of "no return"). The initial two black holes orbit each other, until they merge and form one larger remnant black hole. The shown black holes are spinning, and angular momentum is exchanged among the two black holes and with the orbit. This results in a quite dramatic change in the orientation of the orbital plane, clearly visible in the movie. Furthermore, the spin-axes of the black holes change, as visible through the colored patch on each black hole horizon, which indicates the north pole.

The lower part of the movie shows the two distinct gravitational waves (called 'polarizations') that the merger is emitting into the direction of the camera. The modulations of the polarizations depend sensitively on the orientation of the orbital plane, and thus encode information about the orientation of the orbital plane and its change during the inspiral. Presently, LIGO can only measure one of the polarizations and therefore obtains only limited information about the orientation of the binary. This disadvantage will be remedied with the advent of additional gravitational wave detectors in Italy, Japan and India.

Finally, the slowed-down replay of the merger at the end of the movie makes it possible to observe the distortion of the newly formed remnant black hole, which decays quickly. Furthermore, the remnant black hole is "kicked" by the emitted gravitational waves, and moves upward. (Credit: A. Babul/H. Pfeiffer/CITA/SXS.) - See more at: http://ligo.org/detections/GW170104.php#sthash.NZPaW2LT.dpuf

http://ligo.org/detections/GW170104.php

What can we learn from gravitational waveform?

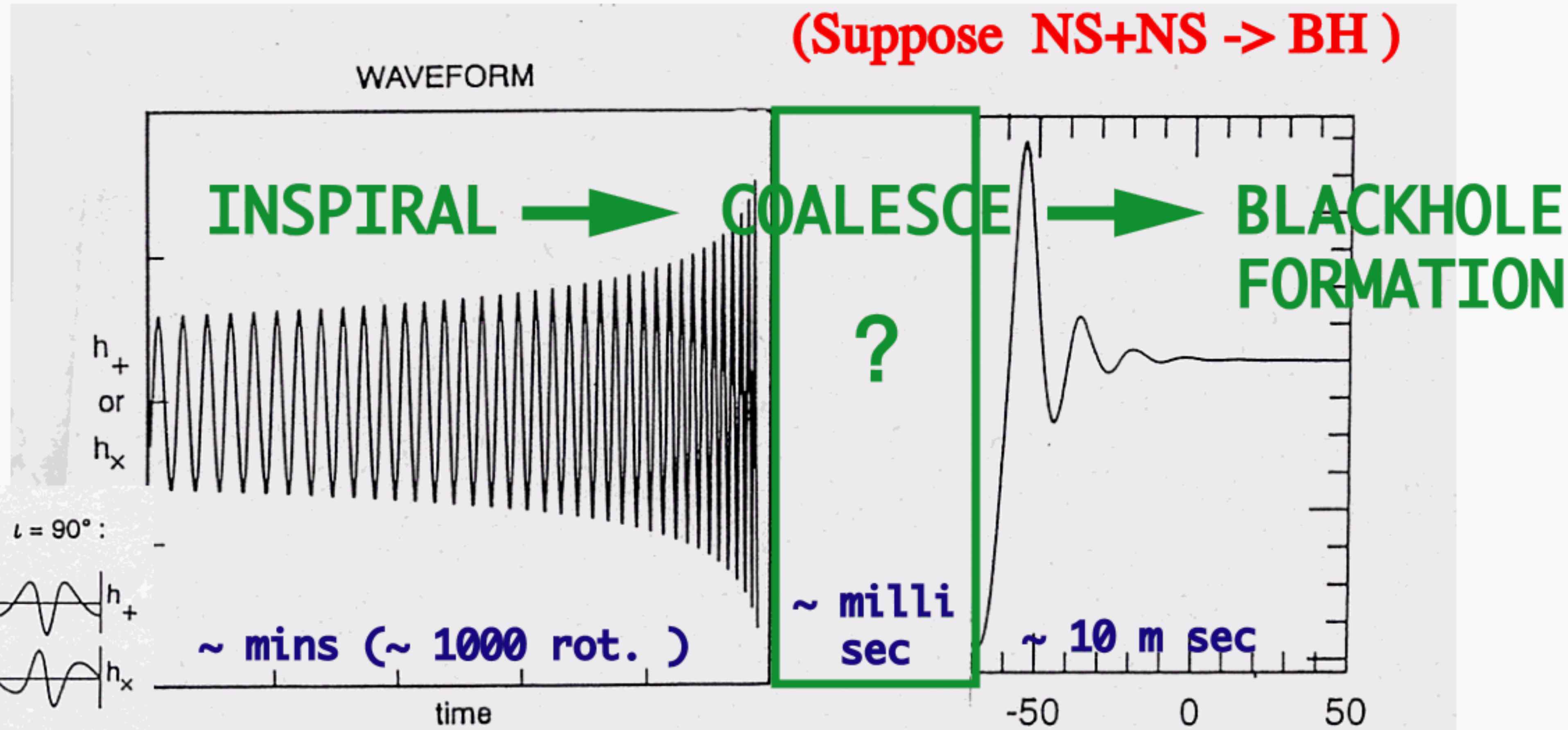

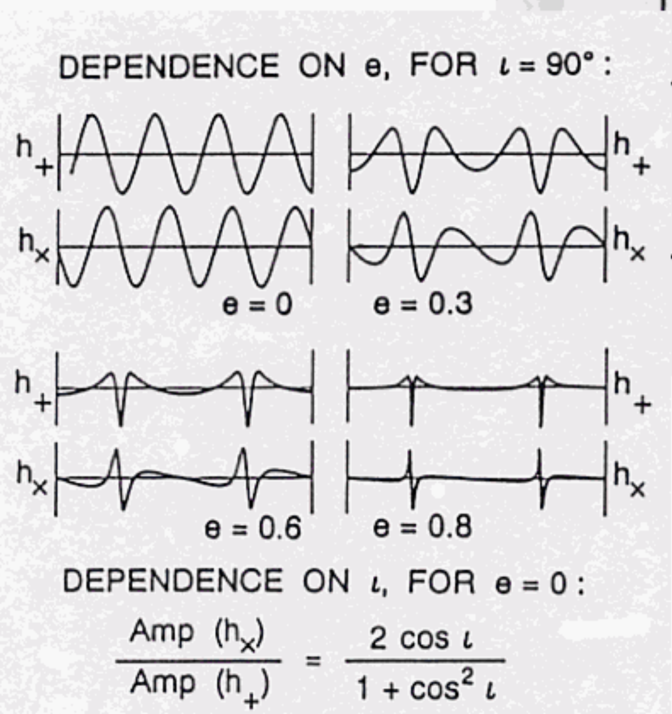

Post Newtonian Approx. | Numerical Relativity | BH. Perturbation

ISCO freq => EoS of NS,
waveform => Formation of BH or NS, BH mass, BH angular momentum,...

"chirps" df/dt => chirp mass, $M_c = (M_1 M_2)^{3/5} / (M_1+M_2)^{1/5}$
amplitude up => M_c, distance
amplitude h+/hx => inclination
waveform => eccentricity
moduration => spin, ...

statistics => cosmological parameters

APPENDIX B: SIMULATION RANKINGS

In this appendix, we enumerate the simulations used in this work, ordered by one measure of their similarity with the data ($\ln L$, in Table III). For nonprecessing binaries, Fig. 6 provides a visual illustration of some trends in $\ln L$ versus mass ratio and the two component spins.

TABLE III. *Peak Marginalized* $\ln L$ *I: Consistency between simulations*: Peak value of the marginalized log likelihood $\ln L$ [Eq. (7)] evaluated using a lower frequency $f_{\rm low} = 30$ Hz and all modes with $l \leq 2$; the simulation key, described in Table II [an asterisk (*) denotes a new simulation motivated by GW150914, and a (+) denotes one of the simulations reported in LVC-detect [1]]; the *initial* spins of the simulation (using – to denote zero, to enhance readability); the initial $\chi_{\rm eff}$; the total (redshifted) mass of the best fit; and the starting frequency (in Hz) of the best fit. Though omitting information accessible to the longest simulations, this choice of low-frequency cutoff eliminates systematic biases associated with simulation duration, which differs across our archive, as seen by the last column.

$\ln L$	Key	q	$\chi_{1,x}$	$\chi_{1,y}$	$\chi_{1,z}$	$\chi_{2,x}$	$\chi_{2,y}$	$\chi_{2,z}$	$\chi_{\rm eff}$	$M_z/M_\odot$	$f_{\rm start}$(Hz)
272.2	SXS:BBH:0310(*)	1.221	⋯	⋯	⋯	⋯	⋯	⋯	0.00	73.0	15.1
272.1	D12_q1.00_a-0.25_0.25_n100(*)	1.0	⋯	⋯	0.250	⋯	⋯	−0.250	−0.00	73.2	20.5
272.1	SXS:BBH:0002[S]	1.0	⋯	⋯	⋯	⋯	⋯	⋯	0.00	73.2	10.0
271.8	D11_q0.75_a0.0_0.0_n100(*)	1.333	⋯	⋯	⋯	⋯	⋯	⋯	−0.00	72.1	23.1
271.8	SXS:BBH:0305(*+)	1.221	⋯	⋯	0.330	⋯	⋯	−0.440	−0.02	74.2	14.8
271.6	SXS:BBH:0218	1.0	⋯	⋯	−0.500	⋯	⋯	0.500	0.00	73.3	10.6
271.6	SXS:BBH:0198	1.202	⋯	⋯	⋯	⋯	⋯	⋯	0.00	73.4	12.7
271.6	SXS:BBH:0307(*)	1.228	⋯	⋯	0.320	⋯	⋯	−0.580	−0.08	70.0	17.0
271.6	GT:BBH:476	1.0	⋯	⋯	−0.200	⋯	⋯	−0.200	−0.20	67.9	24.3
271.6	S0_D10.04_q1.3333_a0.45_-0.80_n100	1.334	⋯	⋯	0.450	⋯	⋯	−0.801	−0.09	71.9	27.9
271.5	D12.00_q0.85_a0.0_0.0_n100(*)	1.176	⋯	⋯	⋯	⋯	⋯	⋯	−0.00	73.0	20.6
271.5	D12.25_q0.82_a-0.44_0.33_n100(*+)	1.22	⋯	⋯	0.330	⋯	⋯	−0.440	−0.02	72.9	20.2
271.5	SXS:BBH:0312(*)	1.203	⋯	⋯	0.390	⋯	⋯	−0.480	−0.00	73.9	14.8
271.4	SXS:BBH:0127	1.34	0.010	−0.077	−0.017	−0.061	−0.065	−0.179	−0.09	71.5	14.3
271.4	SXS:BBH:0115	1.07	0.019	0.013	−0.204	0.243	−0.067	0.291	0.04	74.1	13.8
271.3	SXS:BBH:0213	1.0	⋯	⋯	−0.800	⋯	⋯	0.800	0.00	73.2	11.7
271.3	UD_D10.01_q1.00_a0.4_n100	1.0	⋯	⋯	0.400	⋯	⋯	−0.400	−0.00	73.4	26.7
271.2	D12_q1.00_a-0.25_0.00_n100(*)	1.0	⋯	⋯	⋯	⋯	⋯	−0.250	−0.12	69.4	21.8
271.2	SXS:BBH:0222	1.0	⋯	⋯	−0.300	⋯	⋯	⋯	−0.15	69.1	12.3
271.2	SXS:BBH:0217	1.0	⋯	⋯	−0.600	⋯	⋯	0.600	0.00	73.2	11.9

List of Detected GW events

	ref.	M1+M2=Mf, Mdiff/Mtotal	spin a_final	Mpc z	SNR	deg^2
GW150914	PRL116, 061102 (2016/2/11)	36.2+29.1=**62.3**+3.0 **4.59%**	0.68	410Mpc 0.09	**23.7**	600
LVT151012	(2016/2/11)	23+13=35+1.5 **2.78%**	0.66	1000Mpc 0.20	9.7	
GW151226	PRL116, 241103 (2016/6/15)	14.2+7.5=20.8+0.9 **4.15%**	0.74	440Mpc 0.09	13.0	850
GW170104	PRL118, 221101 (2017/6/1)	31.2+19.4=**48.7**+1.9 **3.75%**	0.64	880Mpc 0.18	**13**	1300
GW170608	ApJ 851, L35 (2017/12/18)	12+7=18.0+1.0 **5.2%**	0.69	340Mpc 0.07	13	520
GW170814	PRL119,141101 (2017/10/6)	30.5+25.3=**53.2**+2.6 **4.66%**	0.70	540Mpc 0.11	**18**	60
GW170817	PRL119, 161101 (2017/10/16)	1.36〜1.60 + 1.17〜1.36 = 2.74 + ?	?	40Mpc	32.4	28

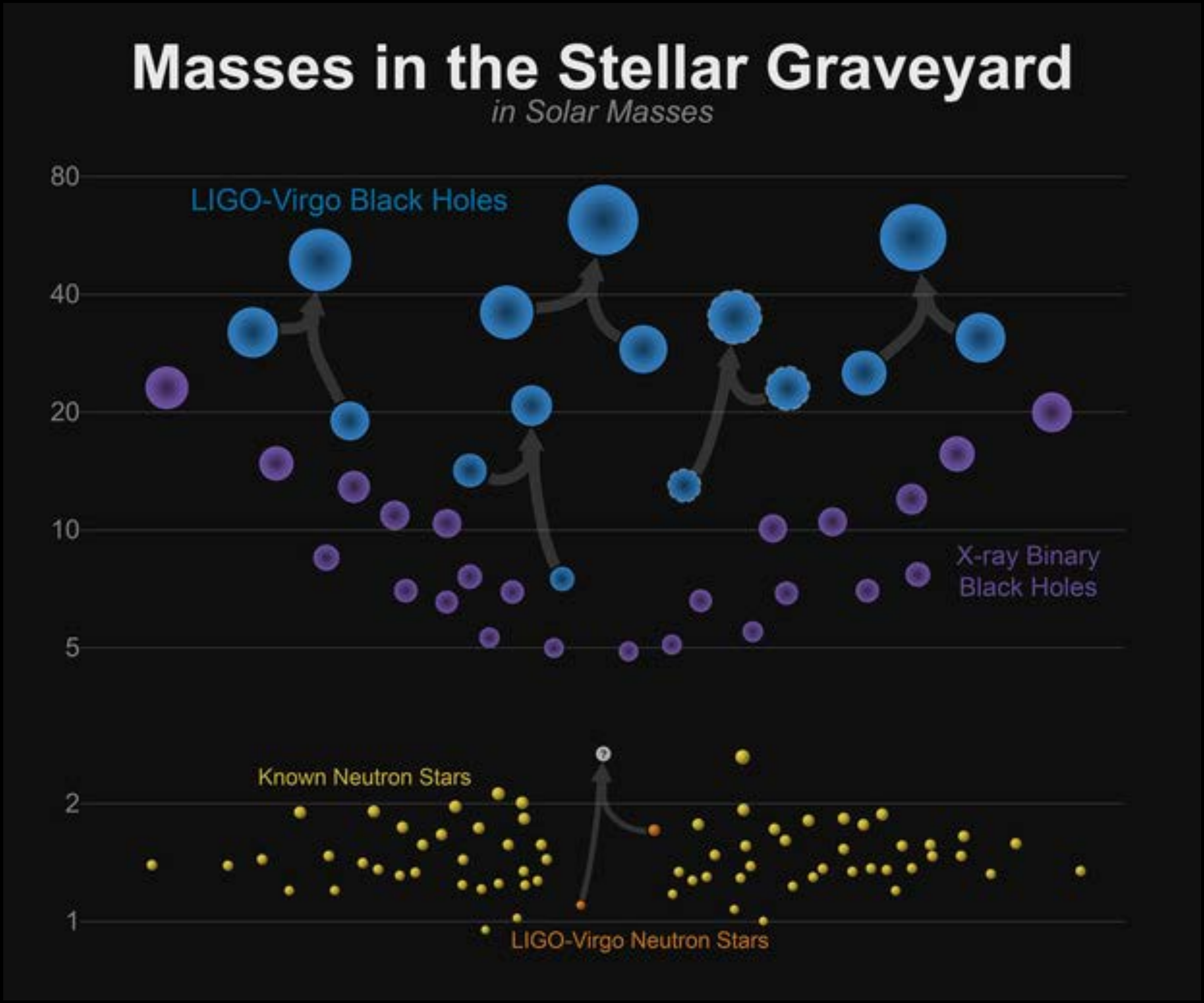

https://www.ligo.caltech.edu/image/ligo20171016a

【宇宙物理】 2017/10/16

連星中性子星合体　重力波検出，多くの天文台が同時観測

GW170817

これまでの
BHBH合体
による重力波

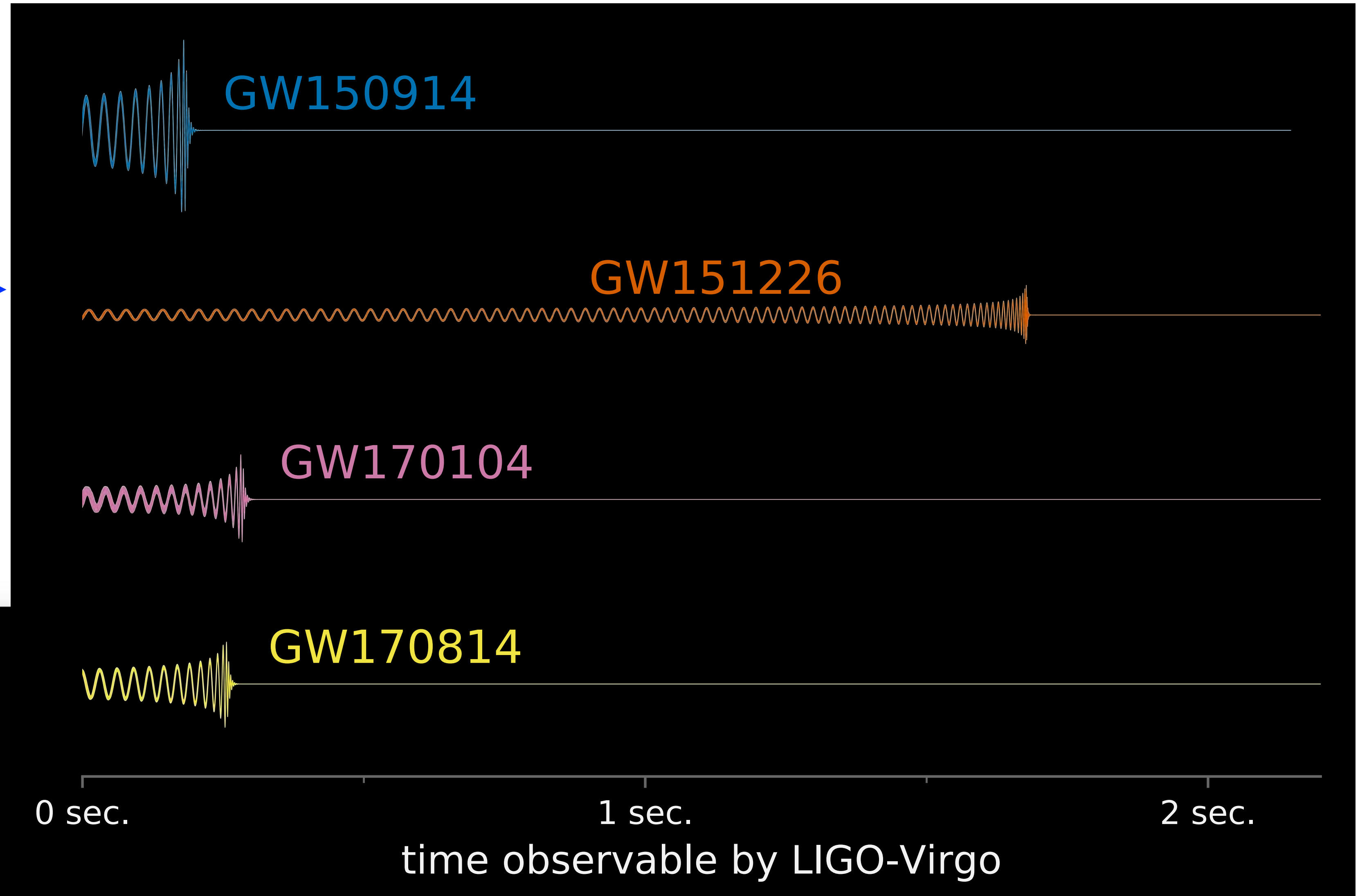

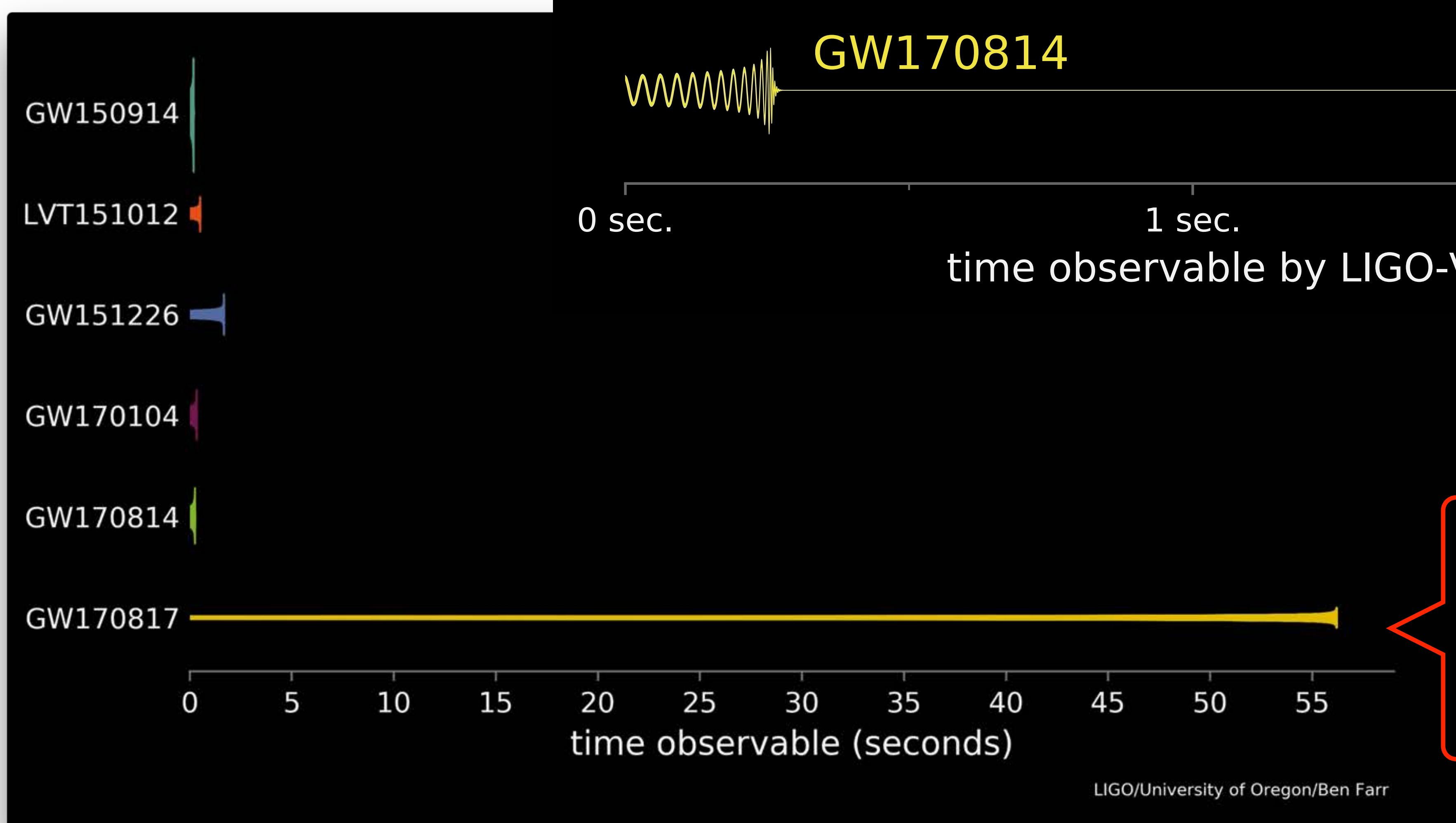

今回のNSNS
合体による重力波

【宇宙物理】 2017/10/16

連星中性子星合体　重力波検出，多くの天文台が同時観測

GW170817

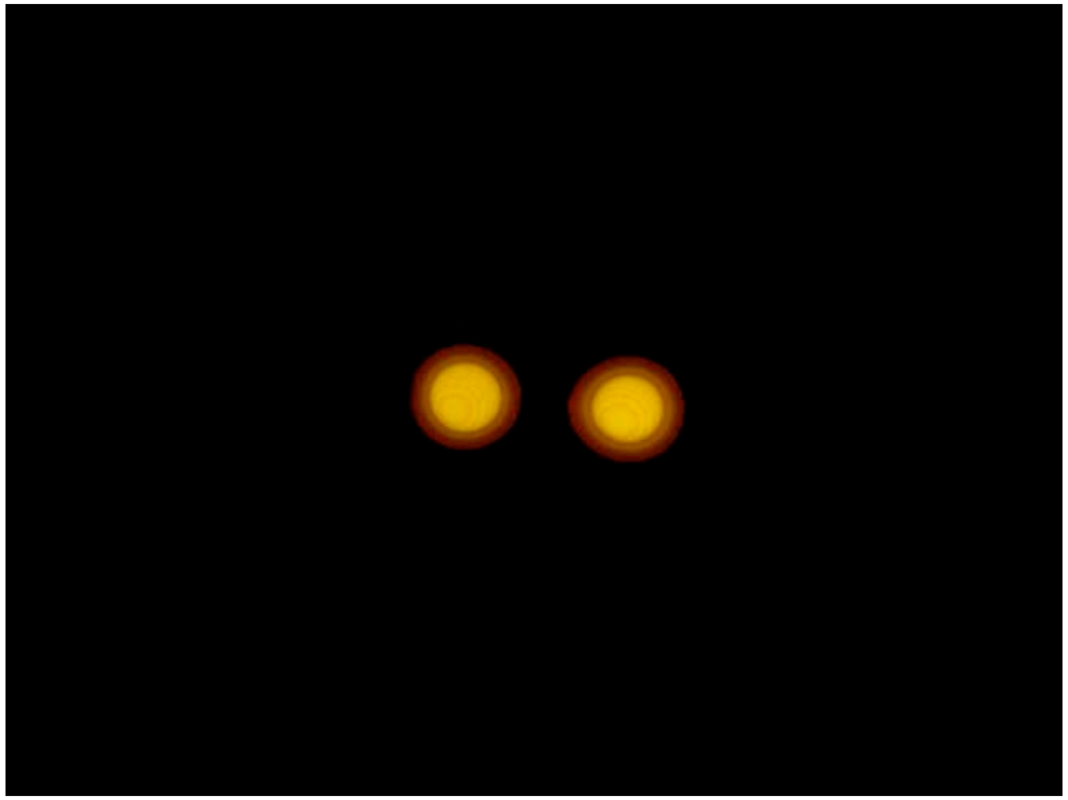

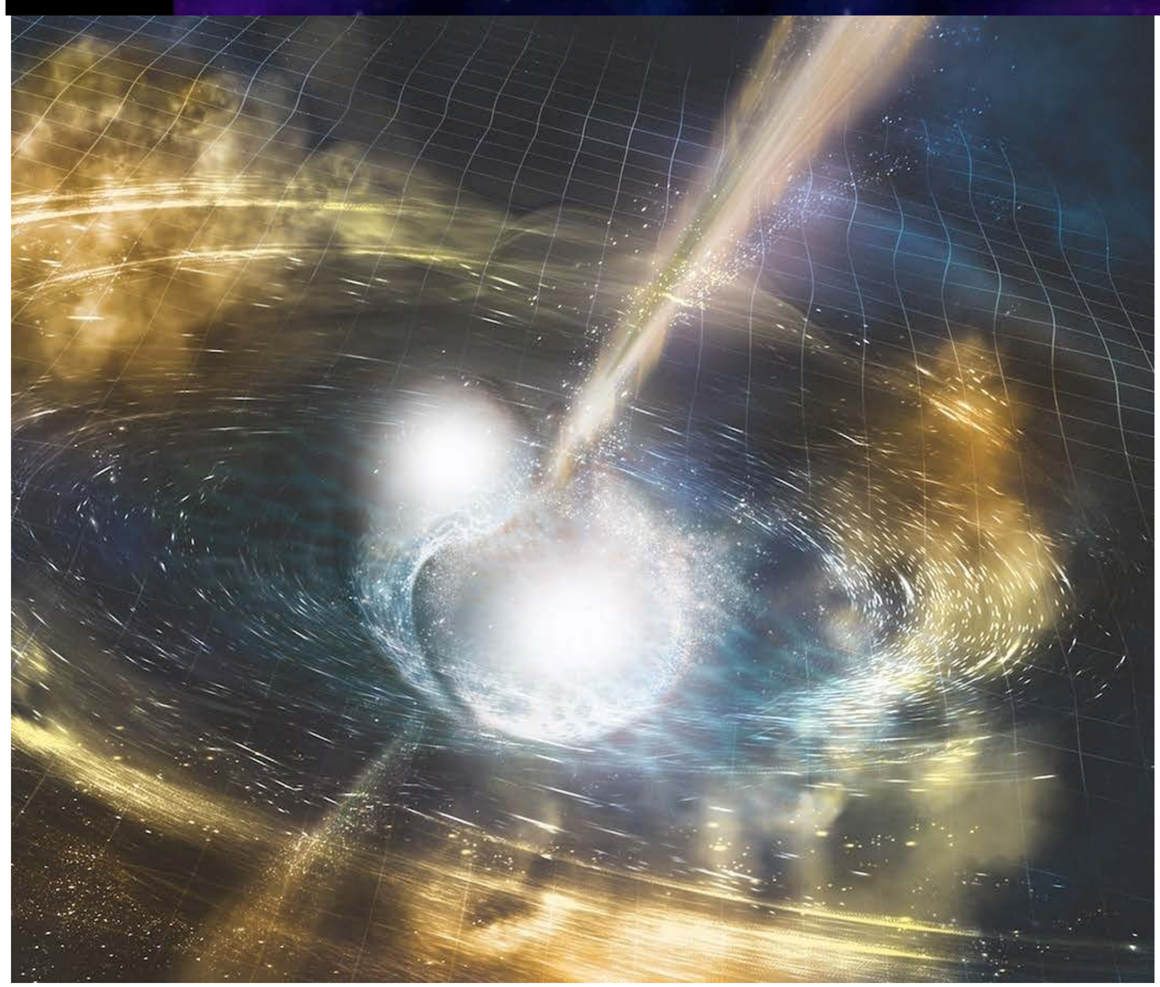

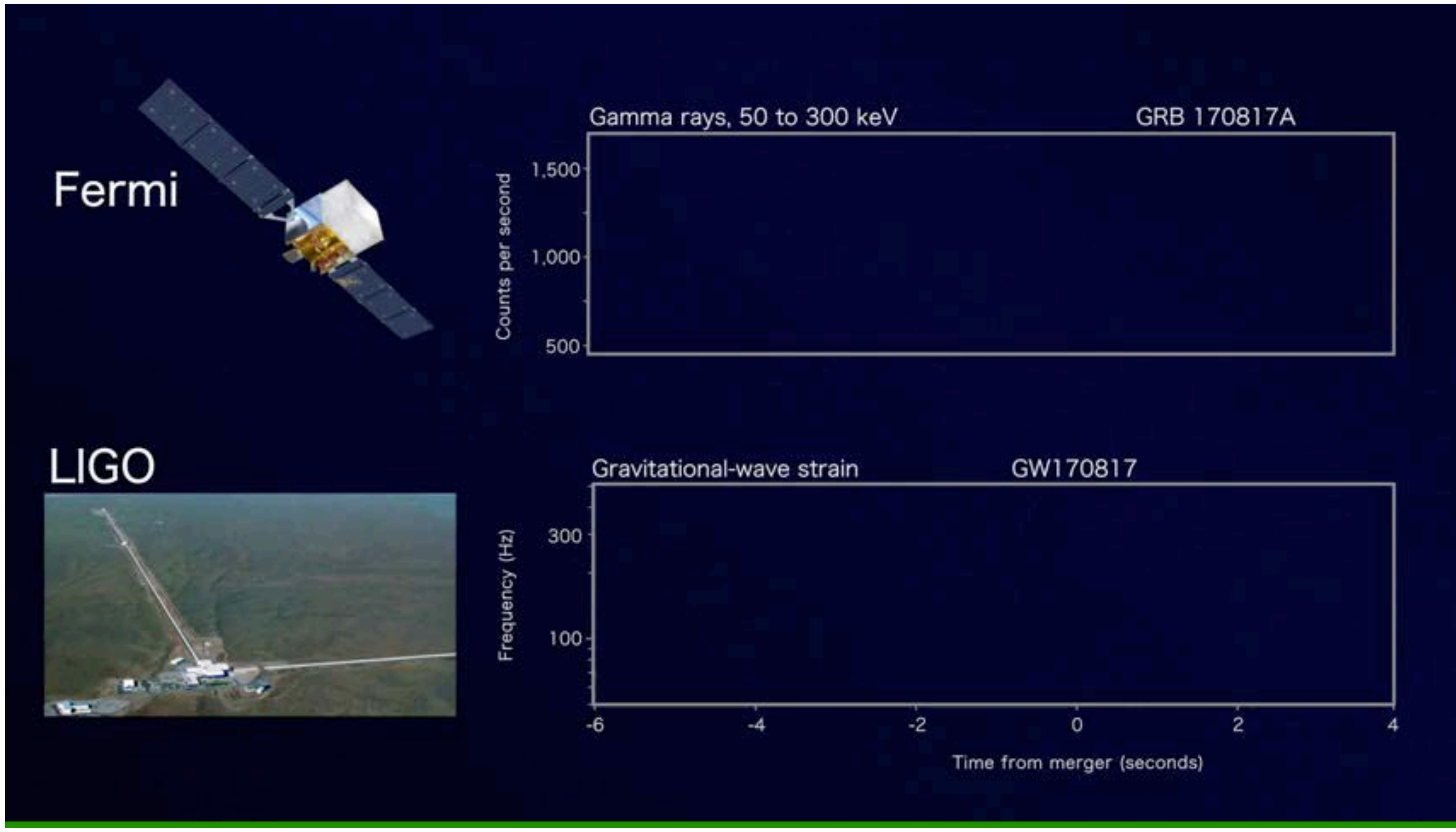

【宇宙物理】 2017/10/16

連星中性子星合体　重力波検出，多くの天文台が同時観測

GW170817

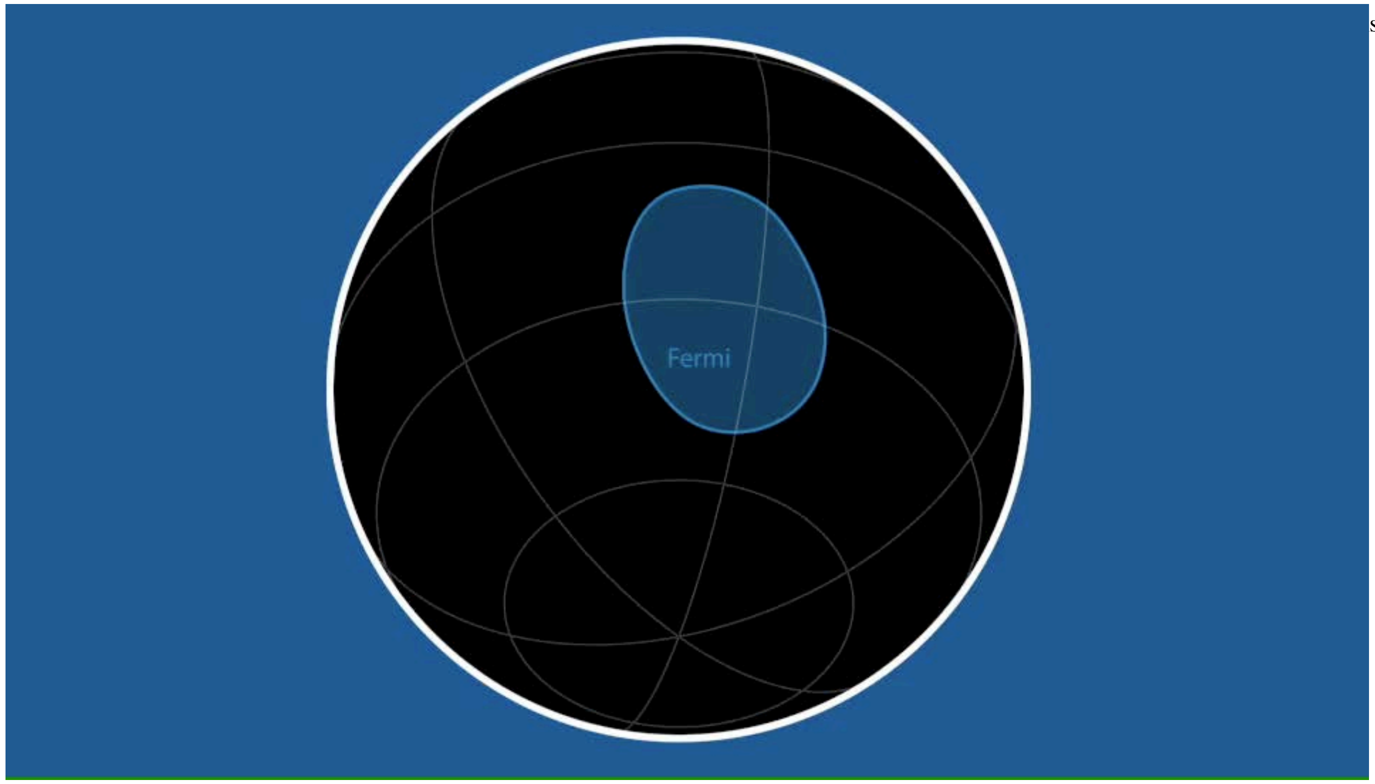

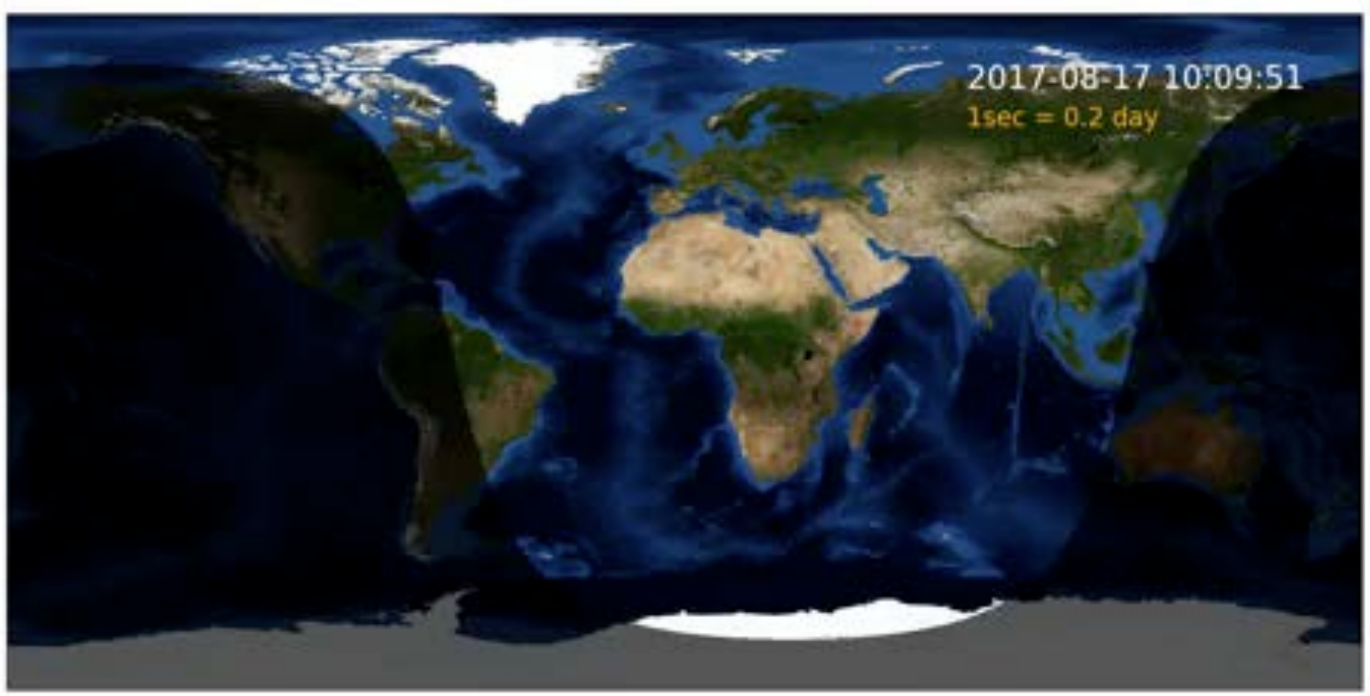

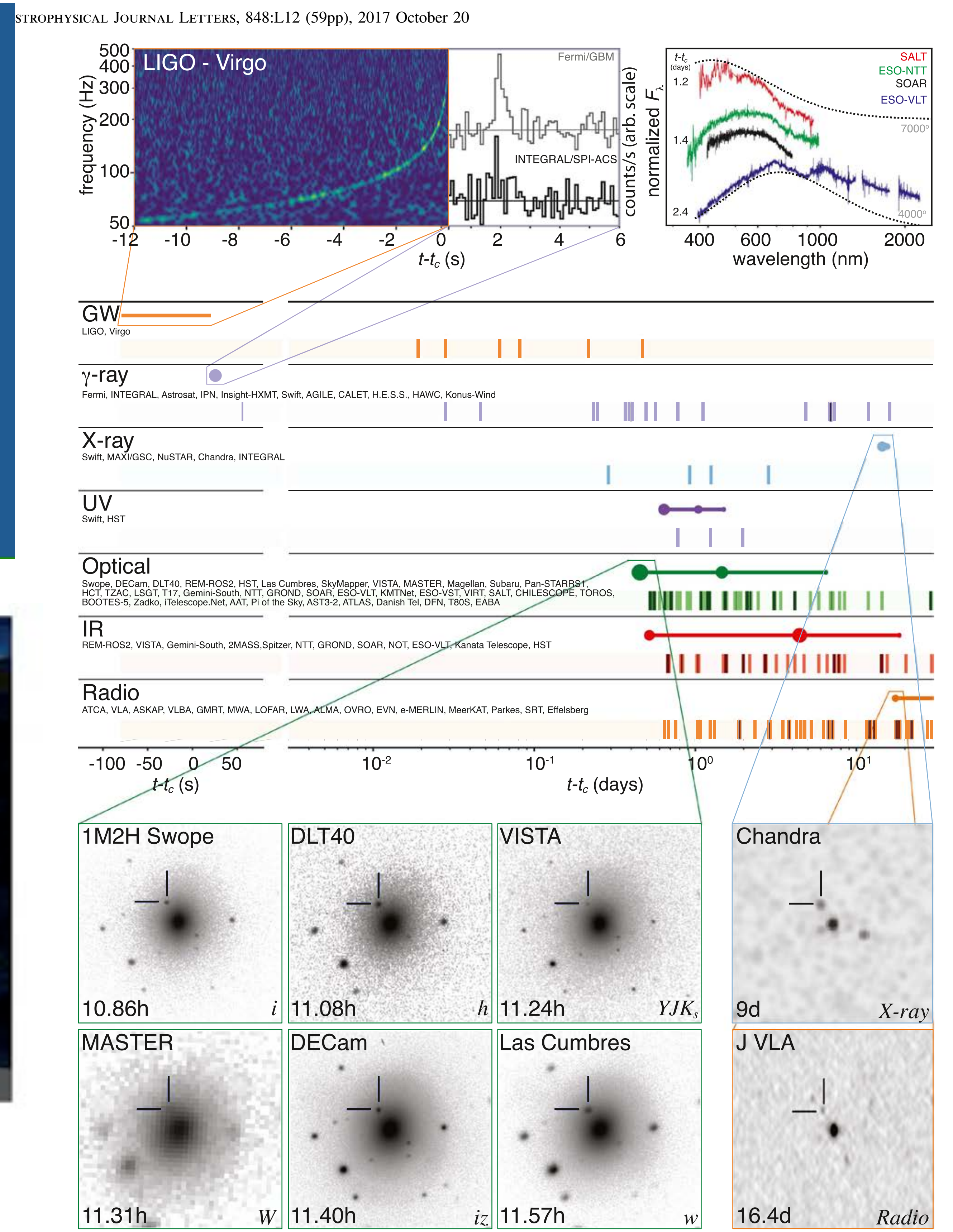

Figure 2. Timeline of the discovery of GW170817, GRB 170817A, SSS17a/AT 2017gfo, and the follow-up observations are shown by messenger and w
relative to the time t_c of the gravitational-wave event. Two types of information are shown for each band/messenger. First, the shaded dashes represent the t

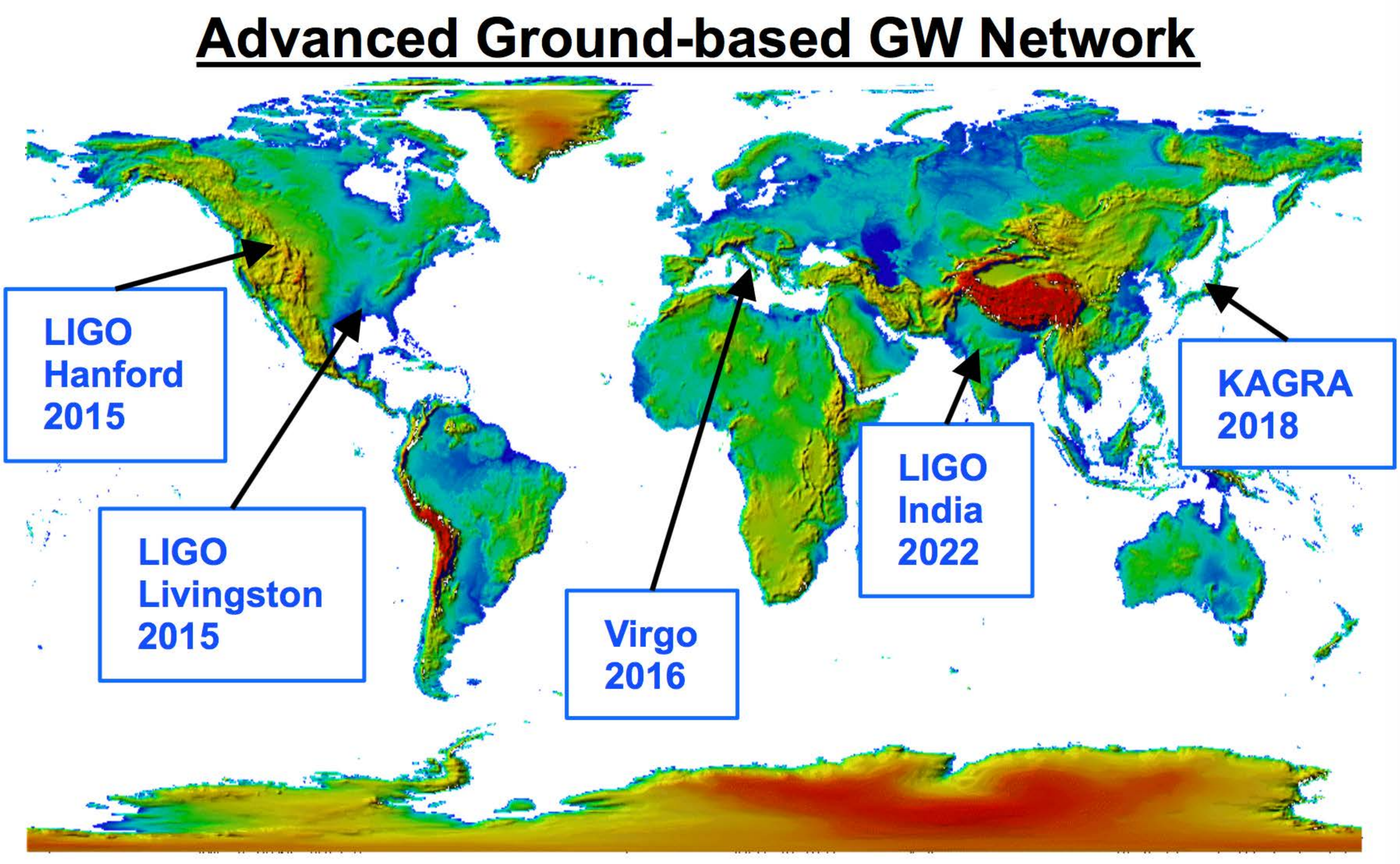
Advanced Ground-based GW Network
LIGO Hanford 2015
LIGO Livingston 2015
Virgo 2016
LIGO India 2022
KAGRA 2018

2. KAGRA 日本の重力波観測

http://gwplotter.com

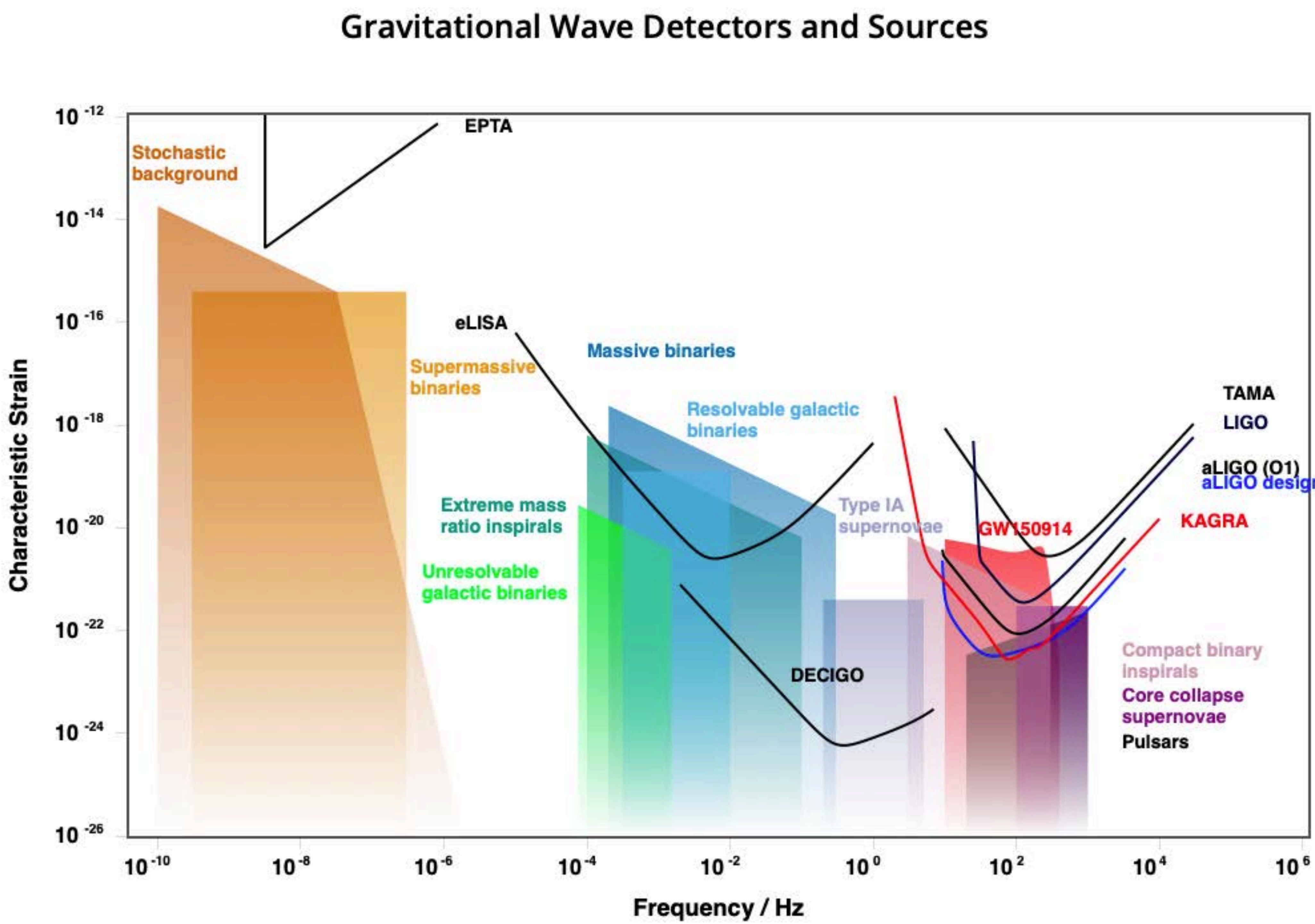

aLIGO, aVirgo & KAGRA： 目標感度曲線

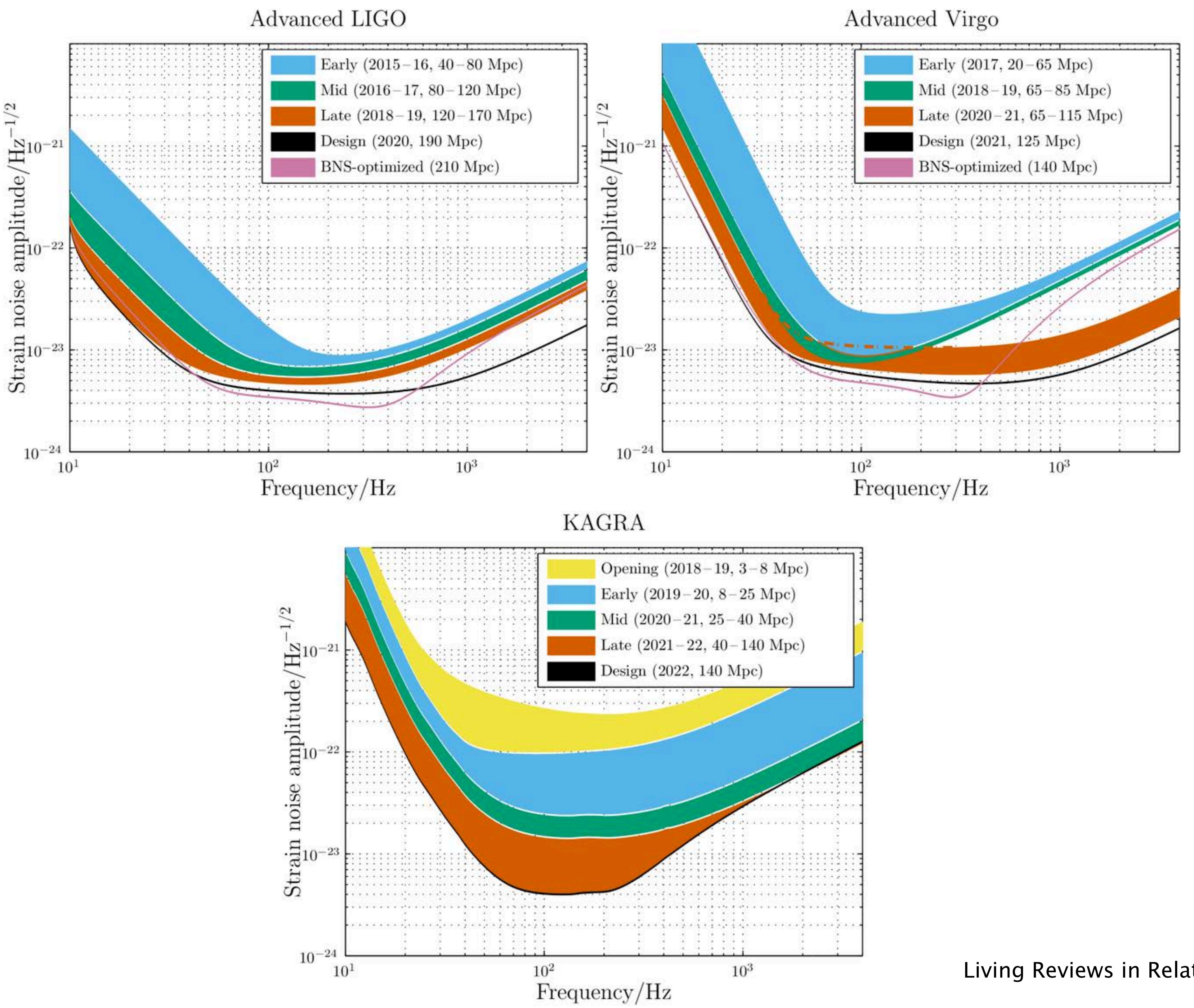

Living Reviews in Relativity; 21:3; 2018

Science 256 (1992) 325

signal = gw + noise

$$s(t) = h(t) + n(t)$$

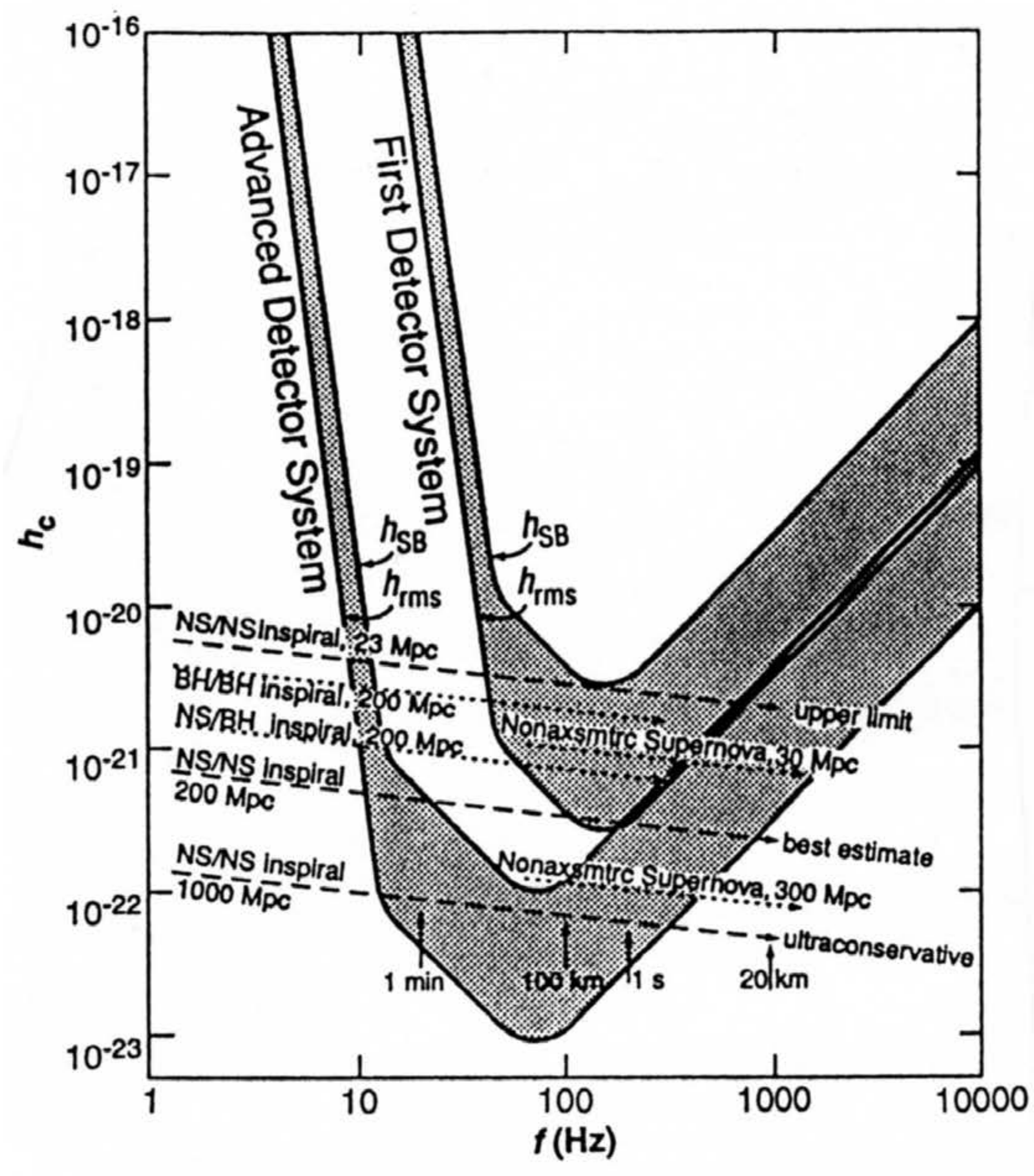

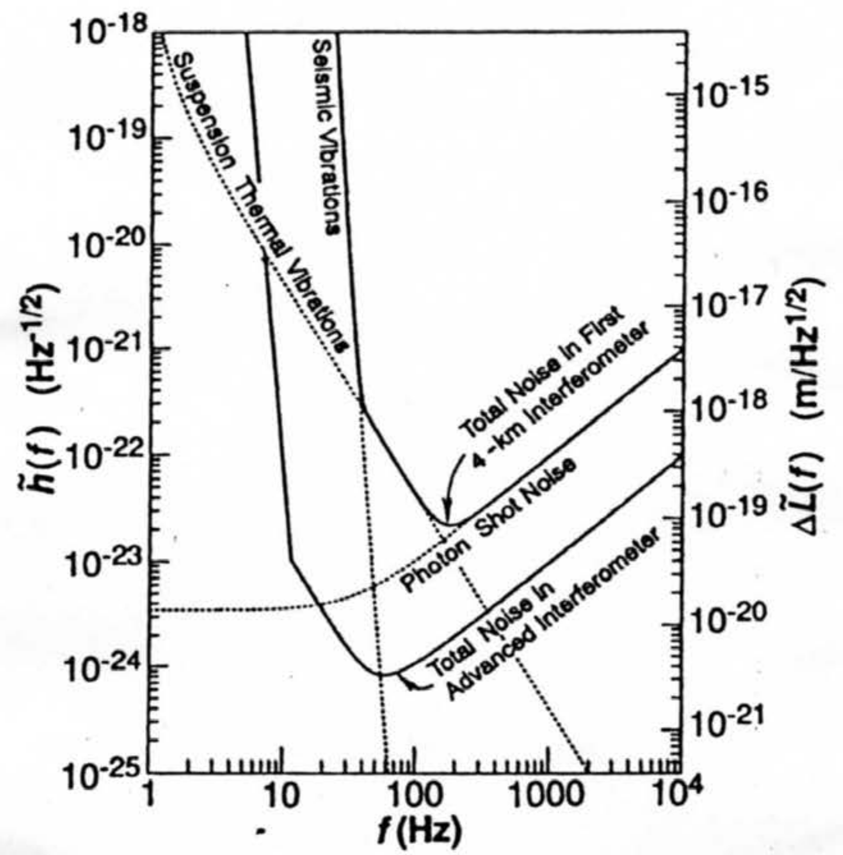

Fig. 7. The expected total noise in each of LIGO's first 4-km interferometers (upper solid curve) and in a more advanced interferometer (lower solid curve). The dashed curves show various contributions to the first interferometer's noise.

spectral density [sec]

$$S_n(f) = 2\int C_n(\tau) e^{i2\pi f\tau} d\tau$$

$$h_n(f) = \sqrt{f S_n(f)}$$

strain noise

$$\sqrt{S_n(f)}$$

$$C_n(\tau) = \overline{n(t)n(t+\tau)}$$

$$\overline{n(t)} = \lim_{T\to\infty} \frac{1}{2T} \int_{-T}^{+T} n(t)\, dt$$

2. 重力波観測計画　（主に KAGRA)

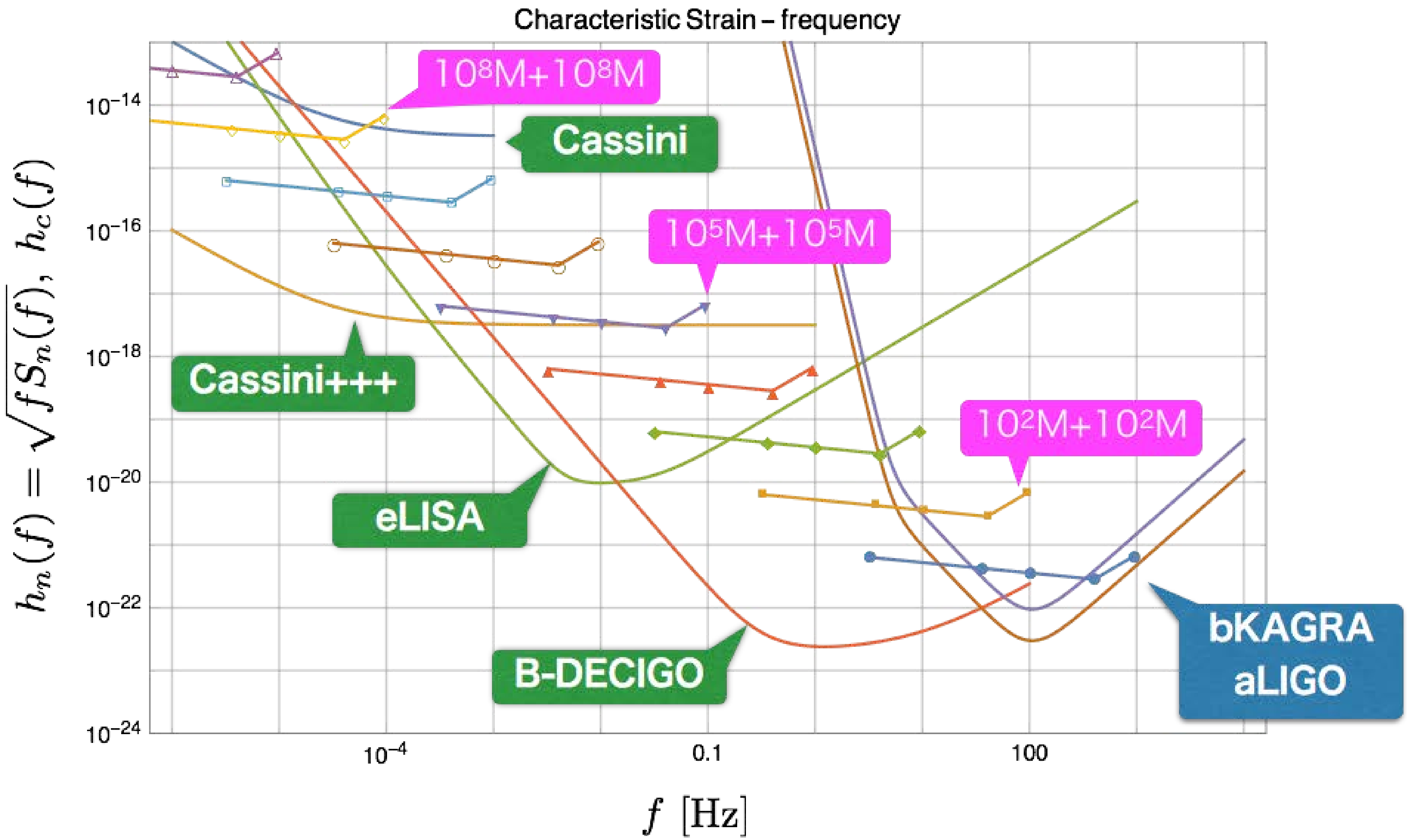

1. Gravitational Wave >> Expected Amplitude

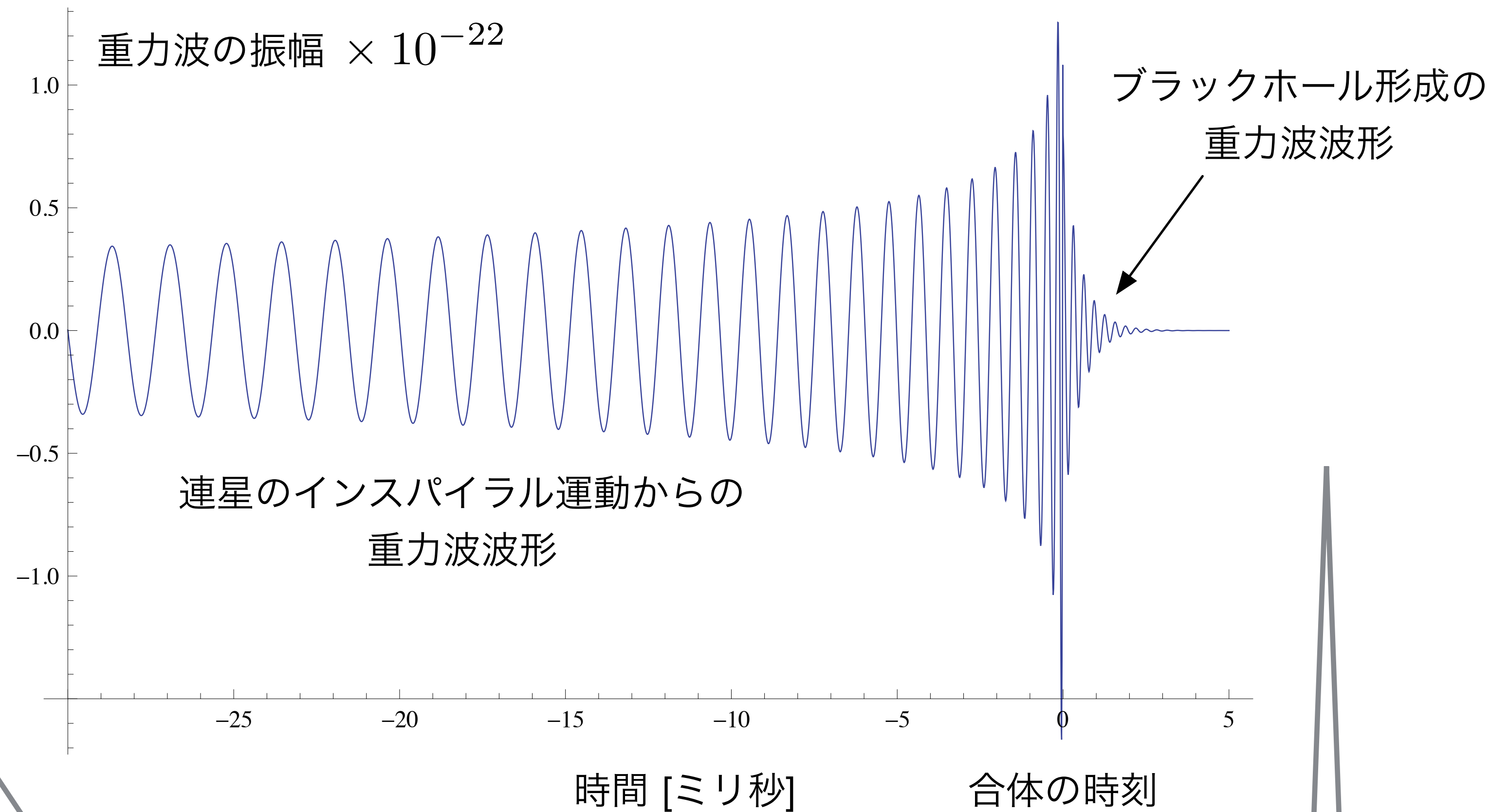

$$f_{\rm insp} = \frac{1}{\pi}\sqrt{\frac{GM_T}{a^3}} \approx 11.4\left(\frac{a}{R_{\rm grav}}\right)^{-3/2}\left(\frac{2\times 10^3\ M_\odot}{M_T}\right)\ \text{Hz},$$

$$h_{\rm insp} = \sqrt{\frac{32}{5}}\pi^{2/3}G^{5/3}c^{-4}M_1M_2M_T^{-1/3}f^{2/3}R^{-1}, \approx 1.49\times 10^{-21}\left(\frac{M_1}{10^3\ M_\odot}\right)\left(\frac{M_2}{10^3\ M_\odot}\right) \times\left(\frac{M_T}{2\times 10^3\ M_\odot}\right)^{-1/3}\left(\frac{f}{1\ \text{Hz}}\right)^{2/3}\left(\frac{R}{4\ \text{Gpc}}\right)^{-1}.$$

$$f_{\rm QNM} \approx \frac{lc^3}{\sqrt{27}GM_T} \sim 39.1\left(\frac{2\times 10^3\ M_\odot}{M_T}\right)\ \text{Hz},$$

$$h_{\rm coal} \approx 5.45\times 10^{-21}\left(\frac{\epsilon}{0.01}\right)^{1/2}\left(\frac{4\ \text{Gpc}}{R}\right)\left(\frac{\mu}{\sqrt{2}\times 10^3\ M_\odot}\right),$$

重力波レーザー干渉計に対する工夫　(1)

干渉計は，大きければ大きいほどよい．

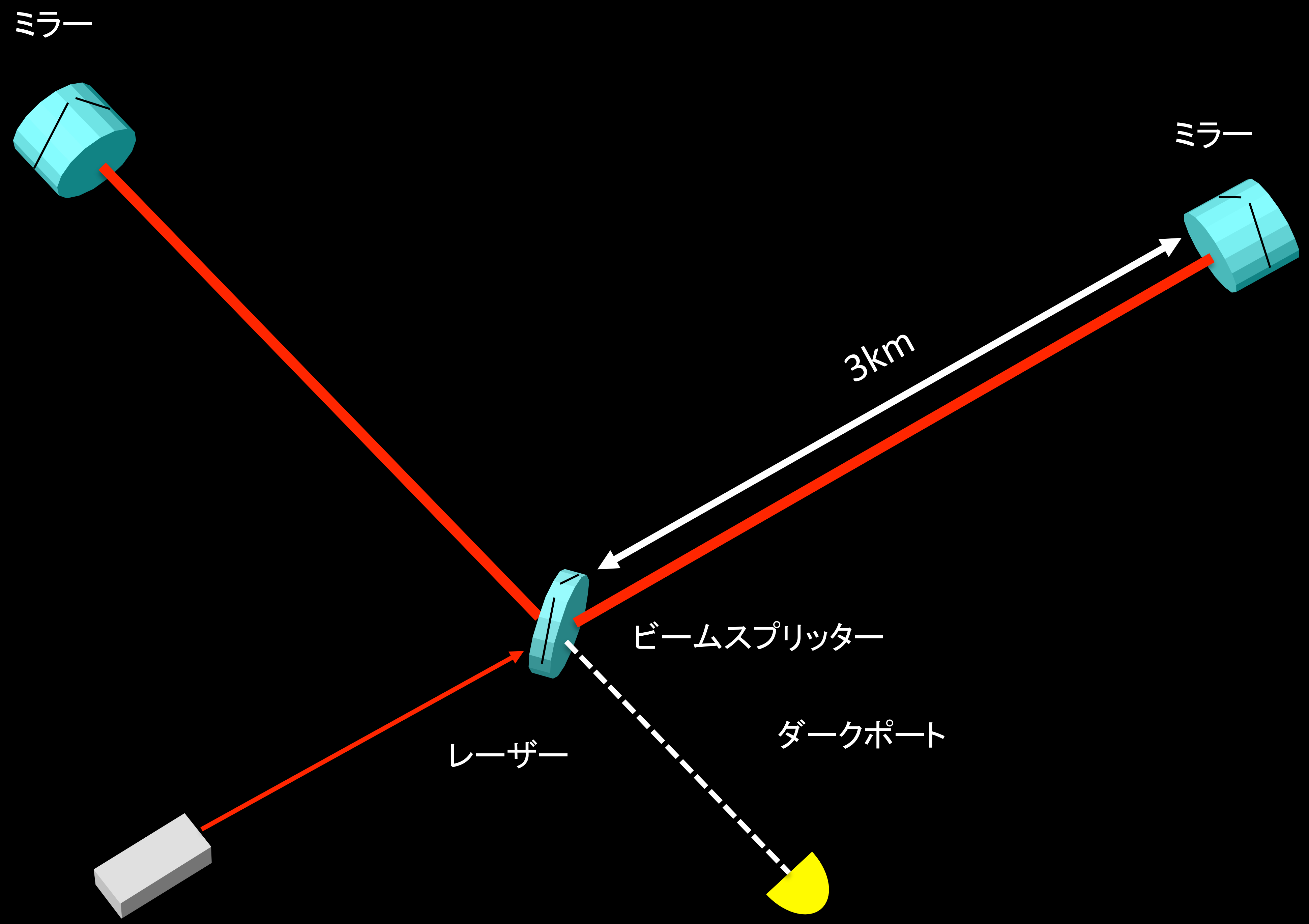

苔山圭似子氏（東京大宇宙線研究所）のスライドから

重力波レーザー干渉計に対する工夫　（2）

さらに，信号を増幅させる

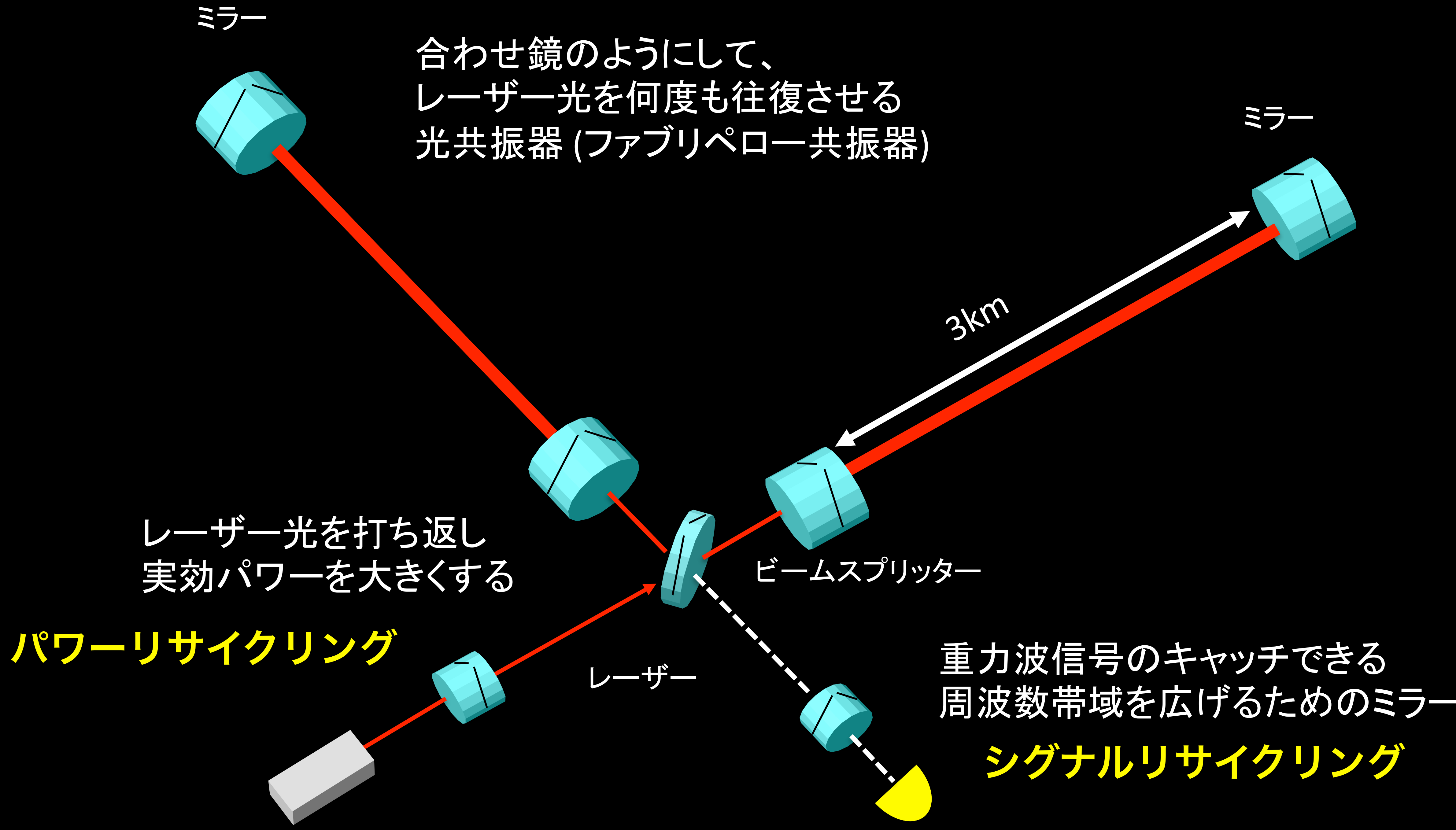

苔山圭似子氏（東京大宇宙線研究所）のスライドから

重力波レーザー干渉計に対する工夫　(3)

さらに，さらに，雑音を減らす

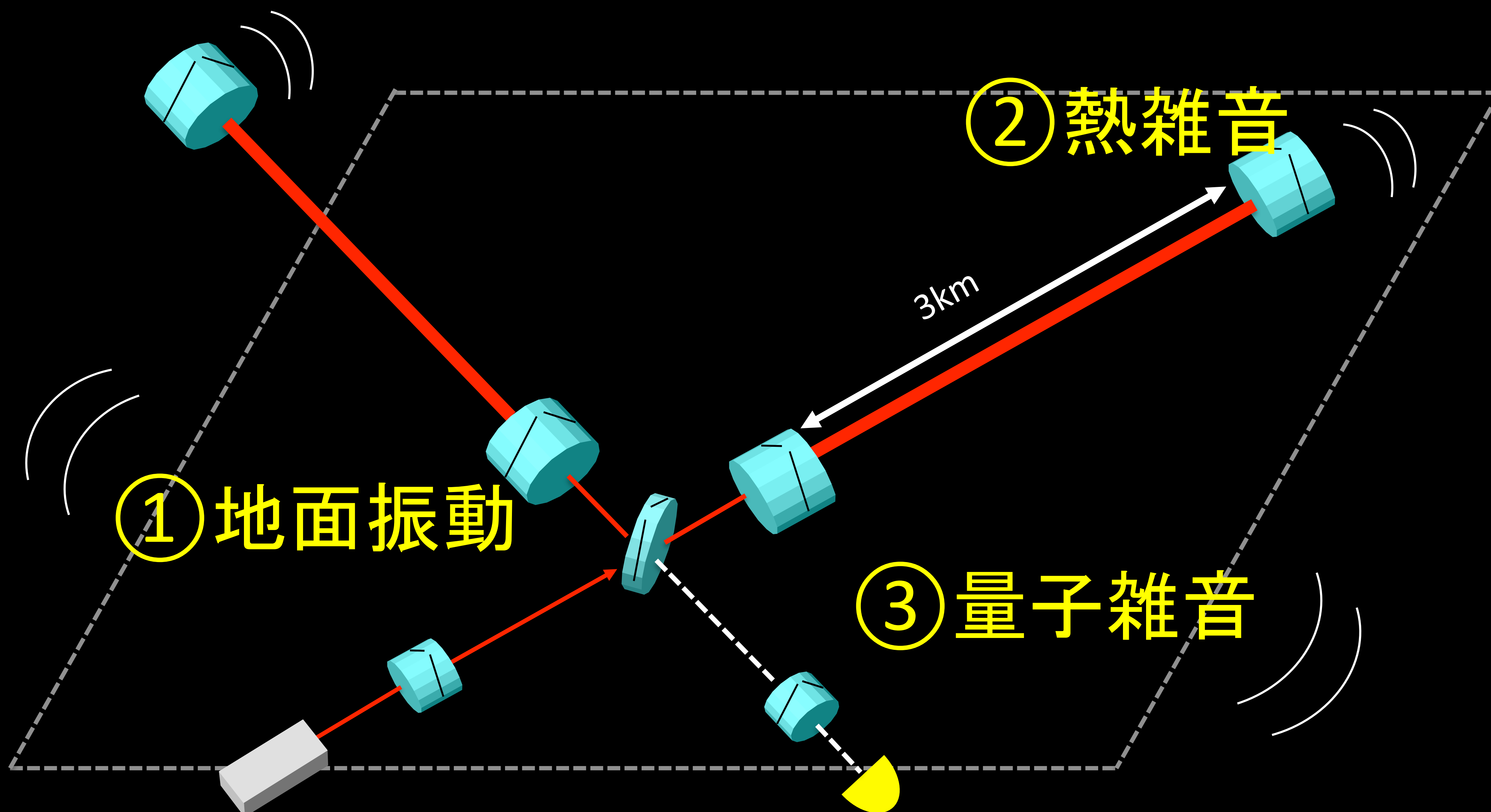

苔山圭以子氏（東京大宇宙線研究所）のスライドから

KAGRAでの雑音対策

①地面振動

- 地下に検出器を設置する
- ミラーを大きな振り子に吊るす

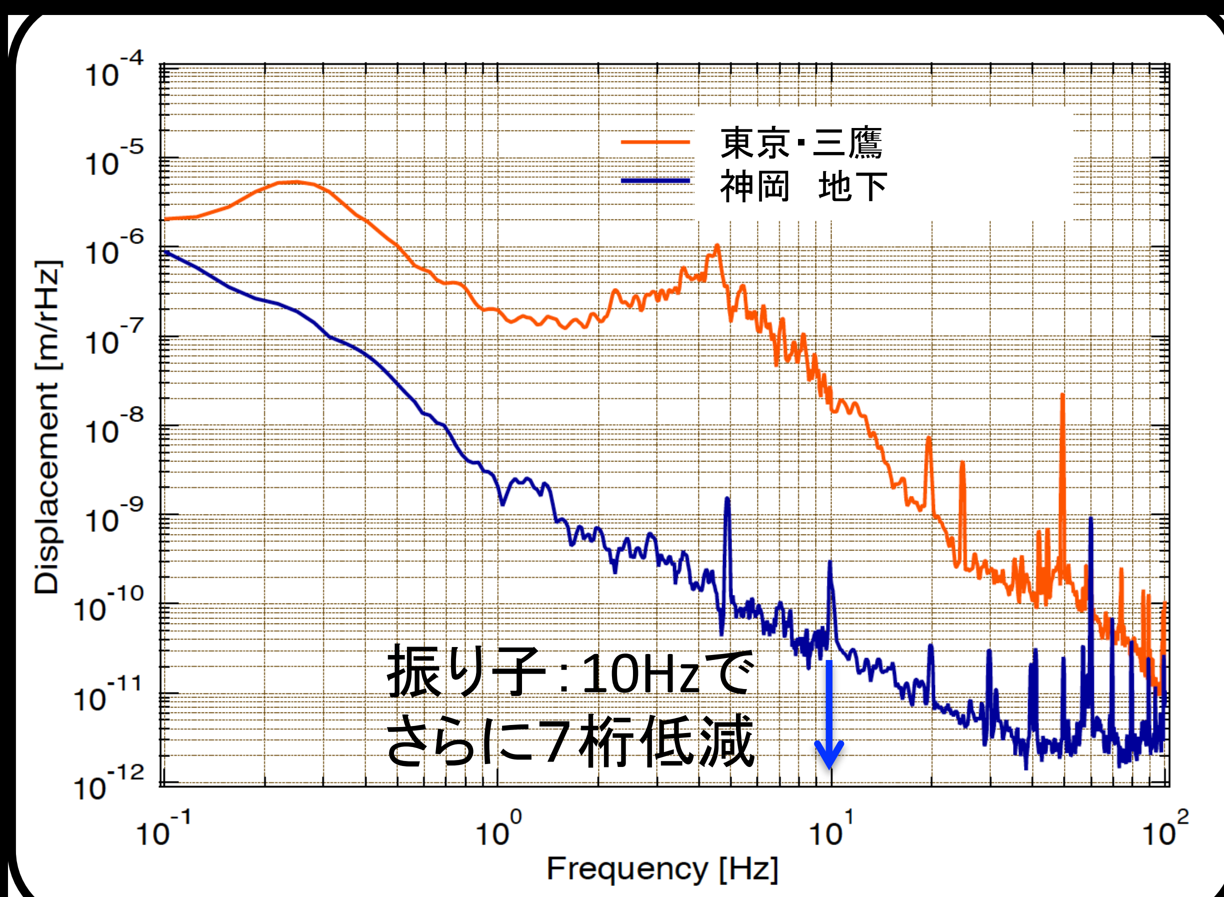

トンネル
２階部分

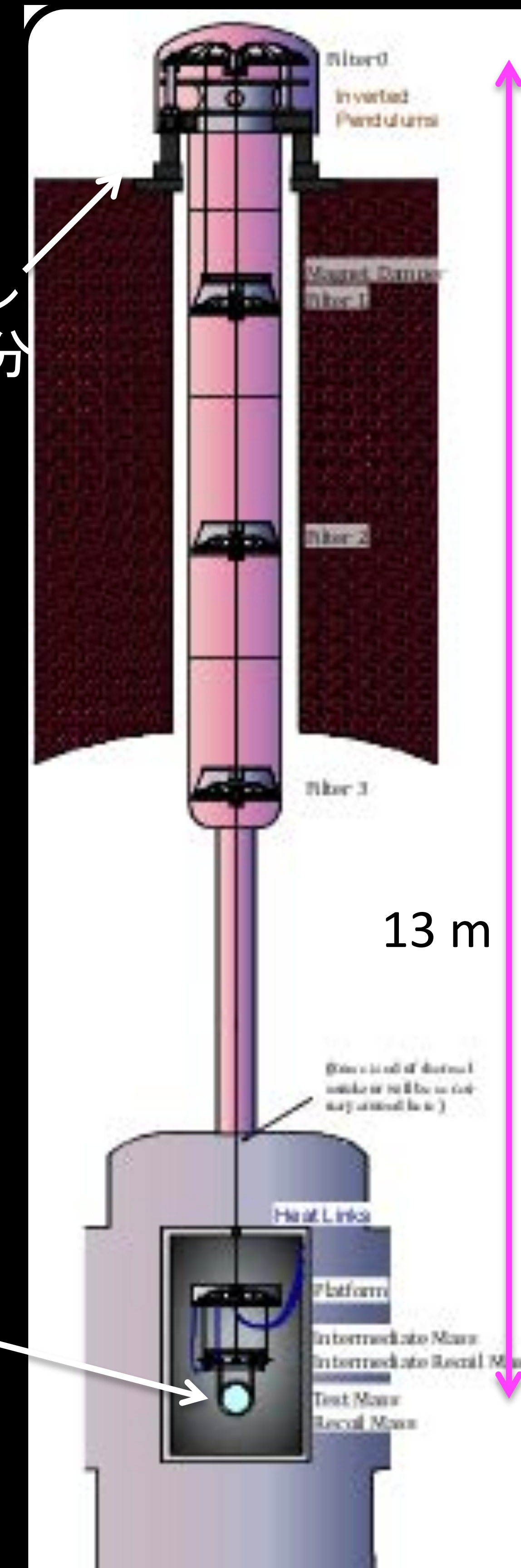

ミラー

苔山圭似子氏（東京大宇宙線研究所）のスライドから

KAGRAでの雑音対策

②熱雑音

鏡の表面の分子や振り子が熱運動して揺れ、
空間の揺らぎと区別がつかずに雑音となる

$$\text{熱雑音} \propto \sqrt{\frac{T}{Q}}$$

- ミラーをマイナス253˚C に冷やす
- サファイアミラーを使う

サファイアミラー

冷却システム

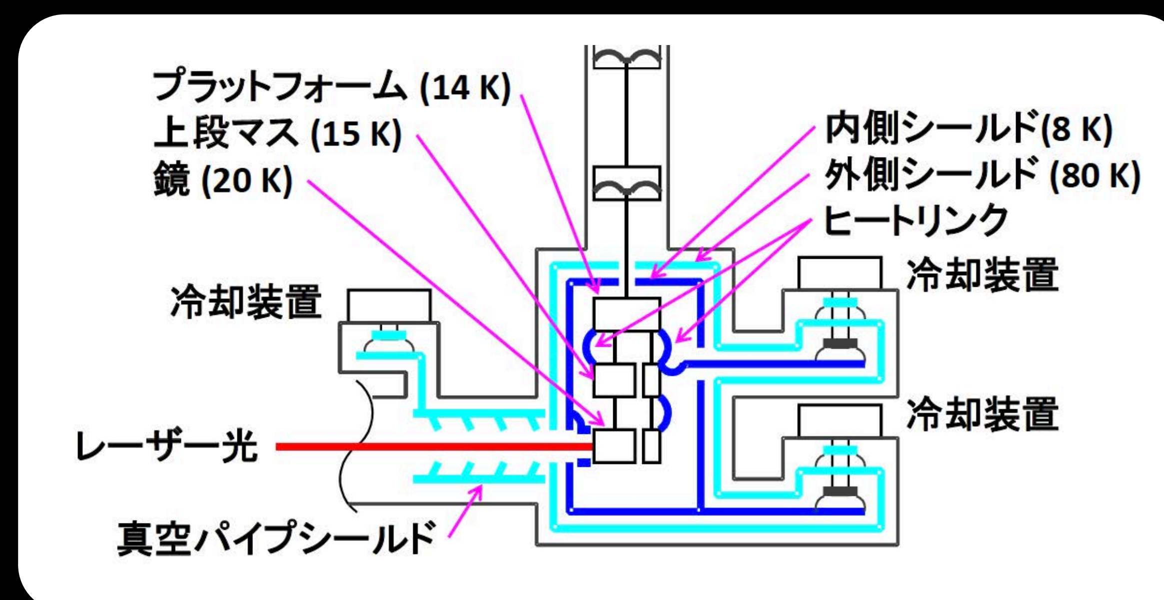

③量子雑音

光子が量子的なふるまいをするせいで起きる雑音

- 180Wのハイパワーレーザーを使う

苔山圭似子氏（東京大宇宙線研究所）のスライドから

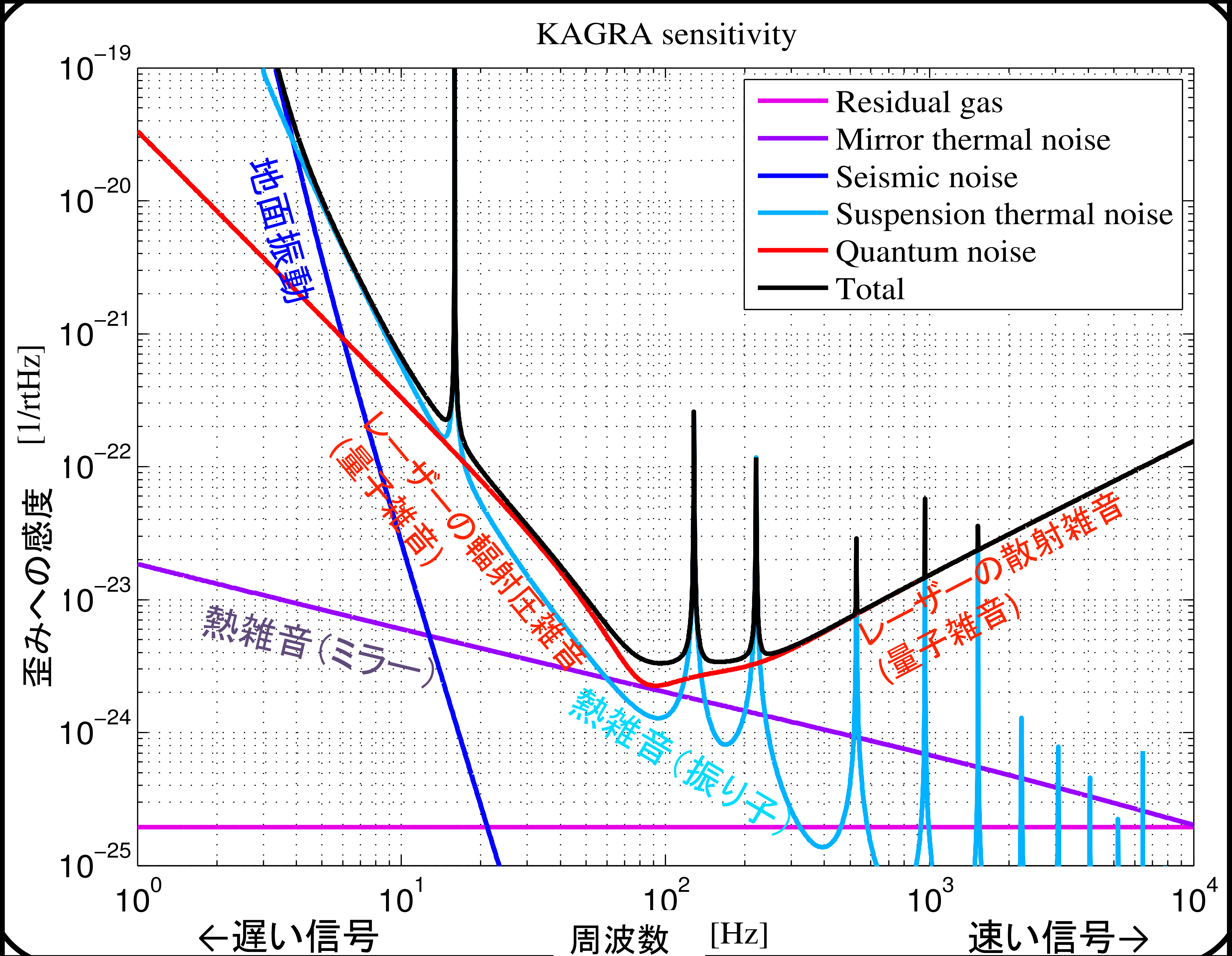

苔山圭似子氏（東京大宇宙線研究所）のスライドから

bKAGRA phase-1 operation (Apr 28 - May 6, 2018)

- All vacuum
- Cooled ETMY (18K for 30 days).
- Duty cycle (88.6% first 5 days; 26.8% May 3 & 4; 59.8% May 5 &6)
- Longest lock was >10 hrs
- Sensitivity 2x10^{-17} / rHz
- PEM injection, hardware injection tests

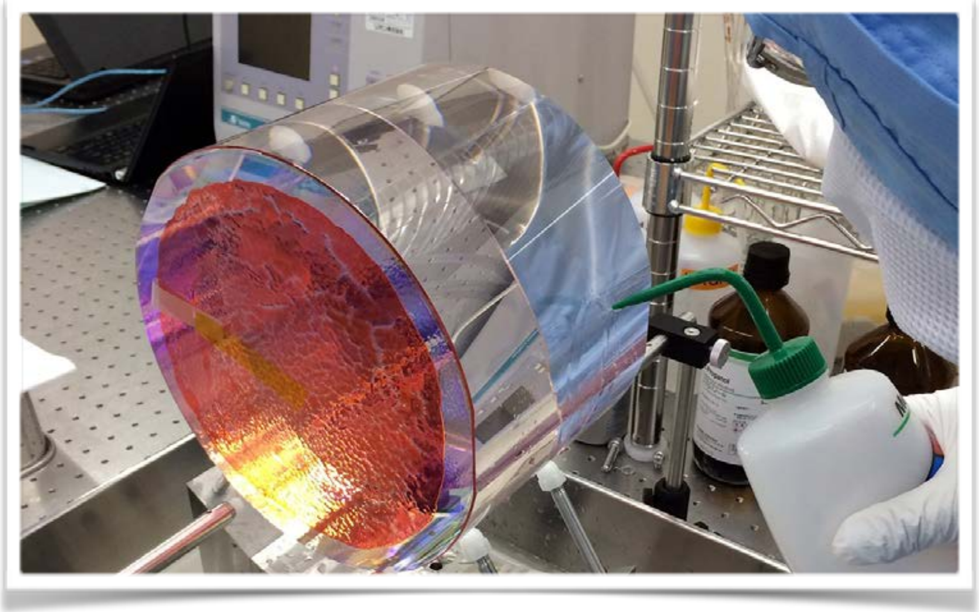

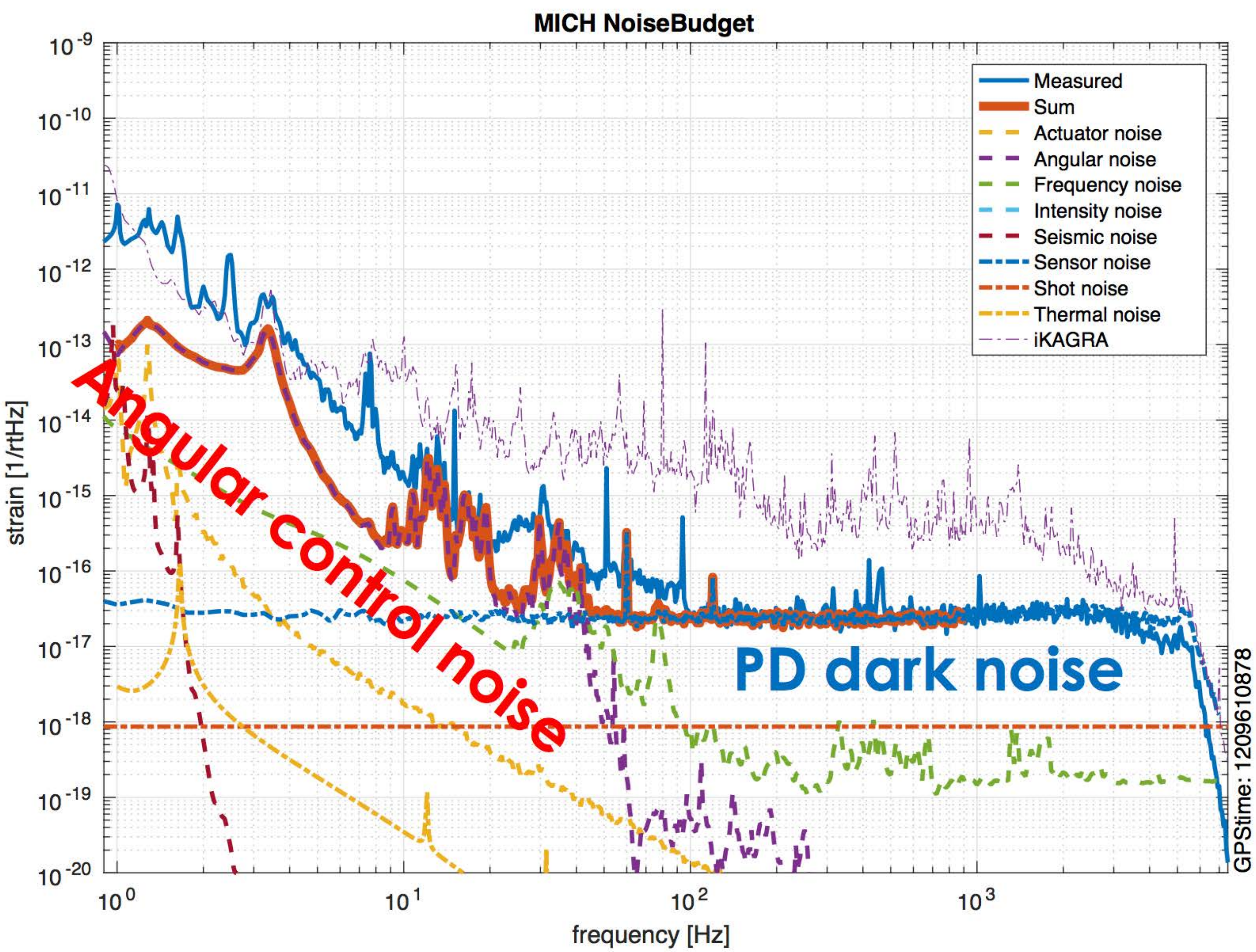

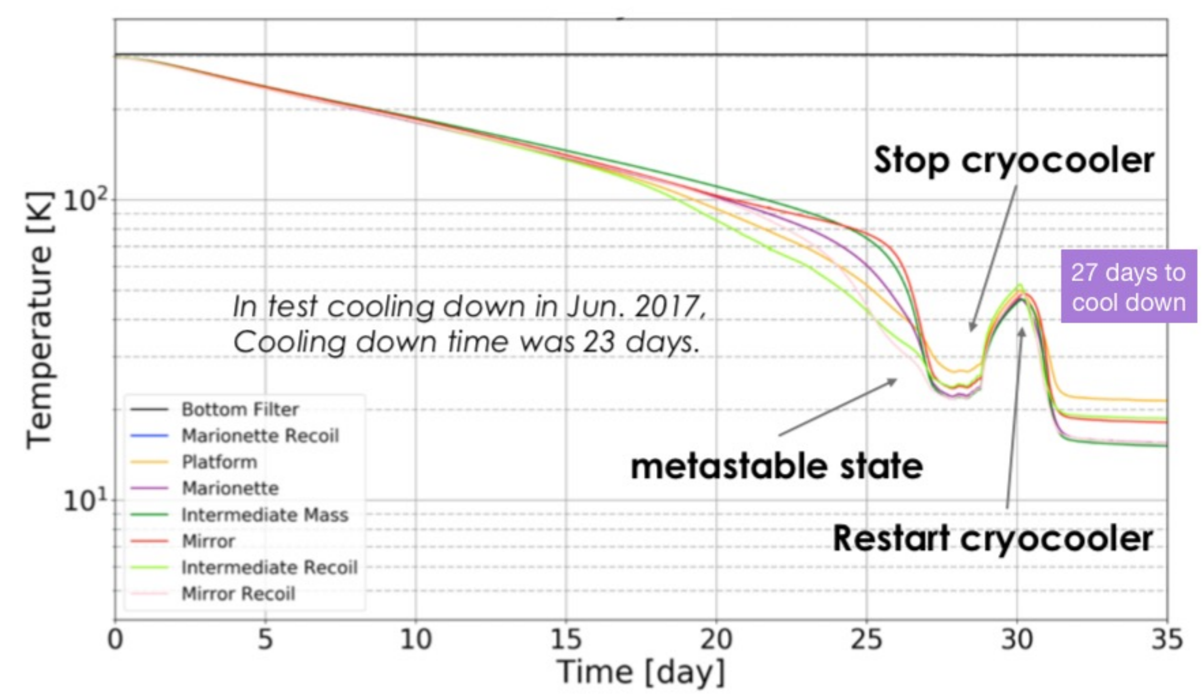

baseline KAGRA 構成図

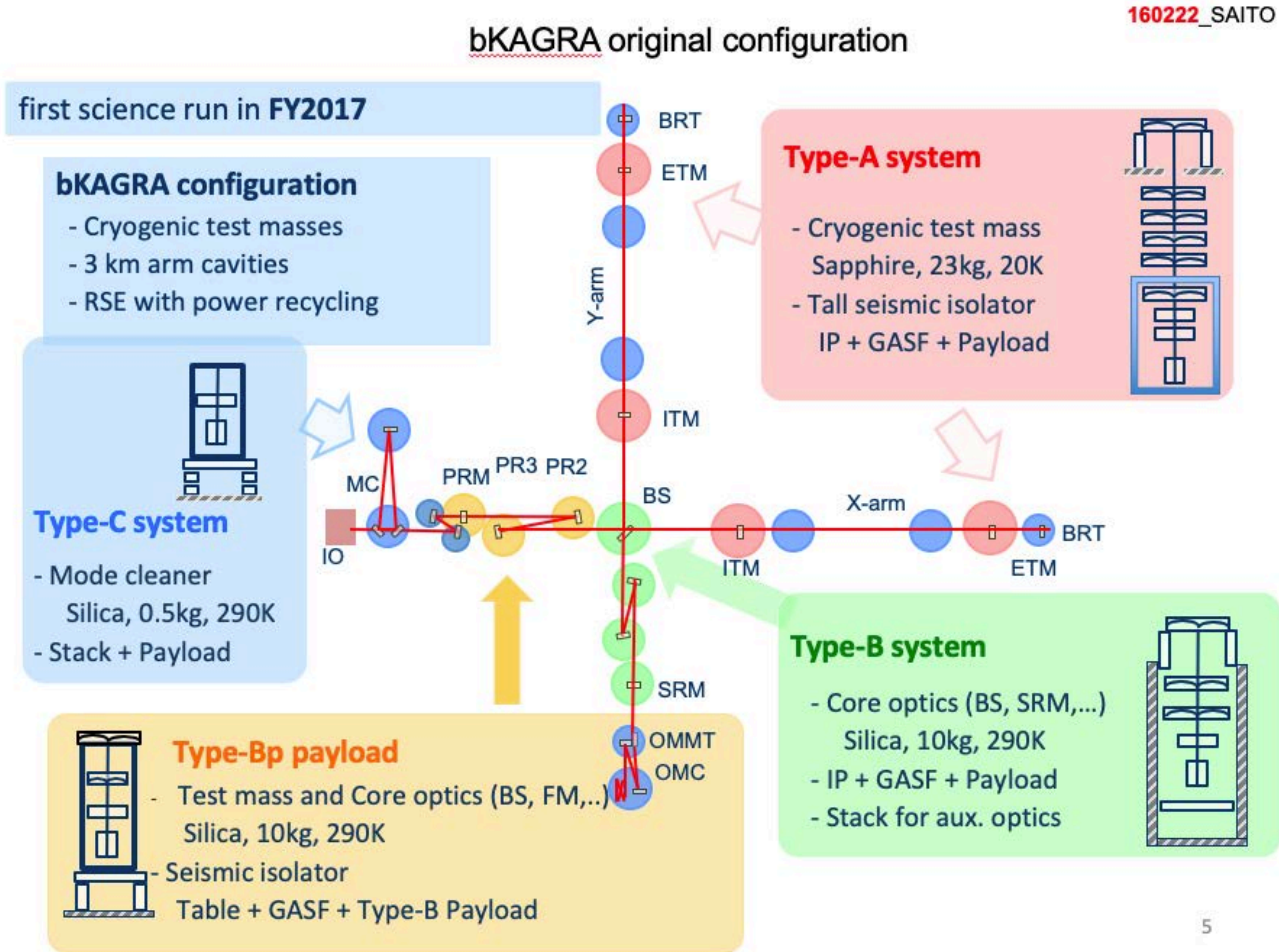

KAGRA Kamioka Gravitational Observatory

former name LCGT = large cryogenic gravitational telescope

named by public naming contest, 神楽（かぐら）dance music in front of Gods

3km Laser Interferometer, Cryogenic

Mozumi control office. (15 min)

Toyama City (60 min)

1000m under the summit of the Mt.

358m above the sea level.

http://gwcenter.icrr.u-tokyo.ac.jp/en/

Schedule (Construction and Operation)

slide from Kajita

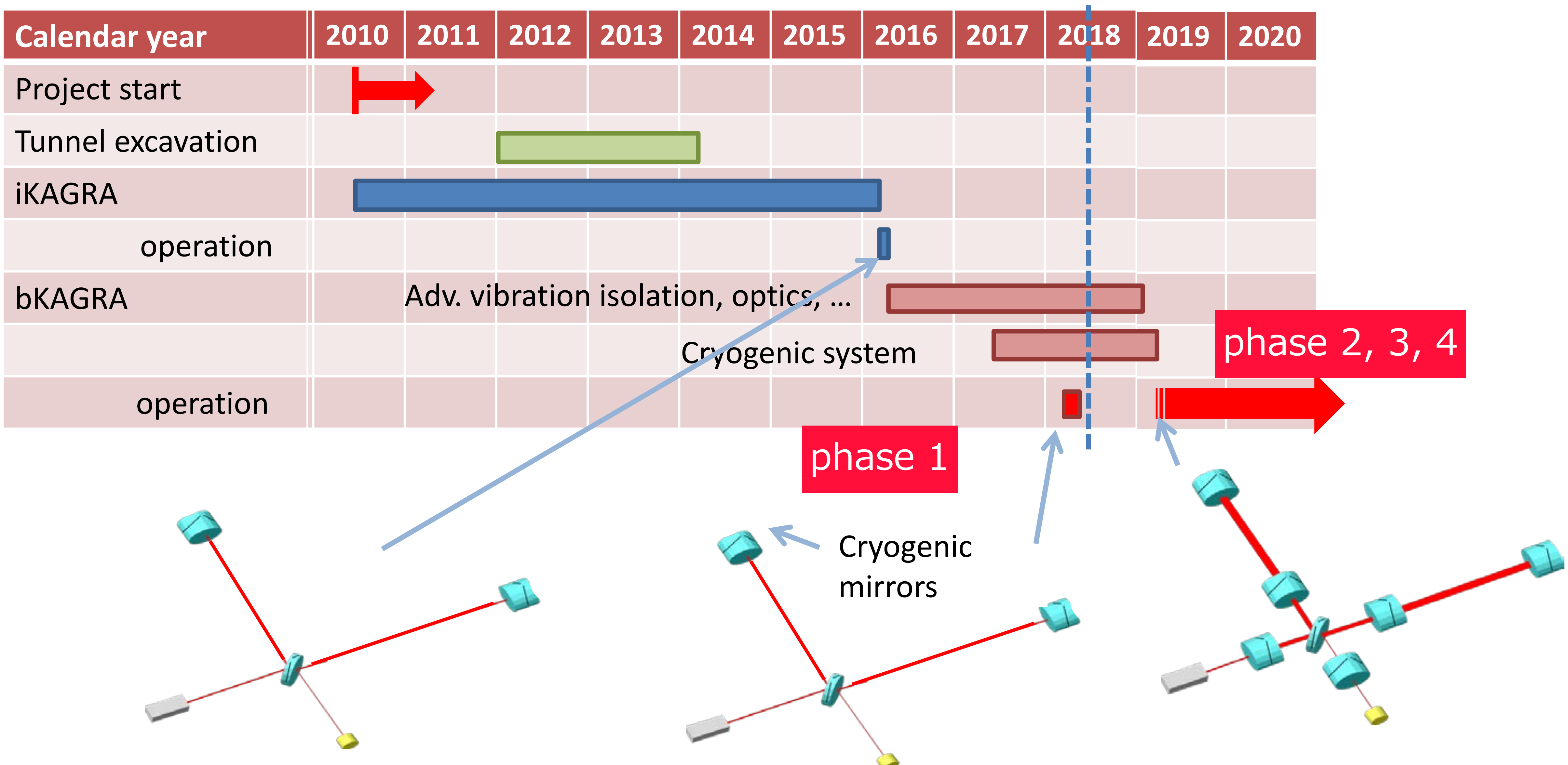

iKAGRA

bKAGRA

(*) The configuration in 2019 is still to be decided referring the milestones.

baseline KAGRA

- Phase-1 operation (Apr 28 — May 6) finished
- Phase-2 starts on May 7.

KAGRA（かぐら：大型低温重力波望遠鏡）

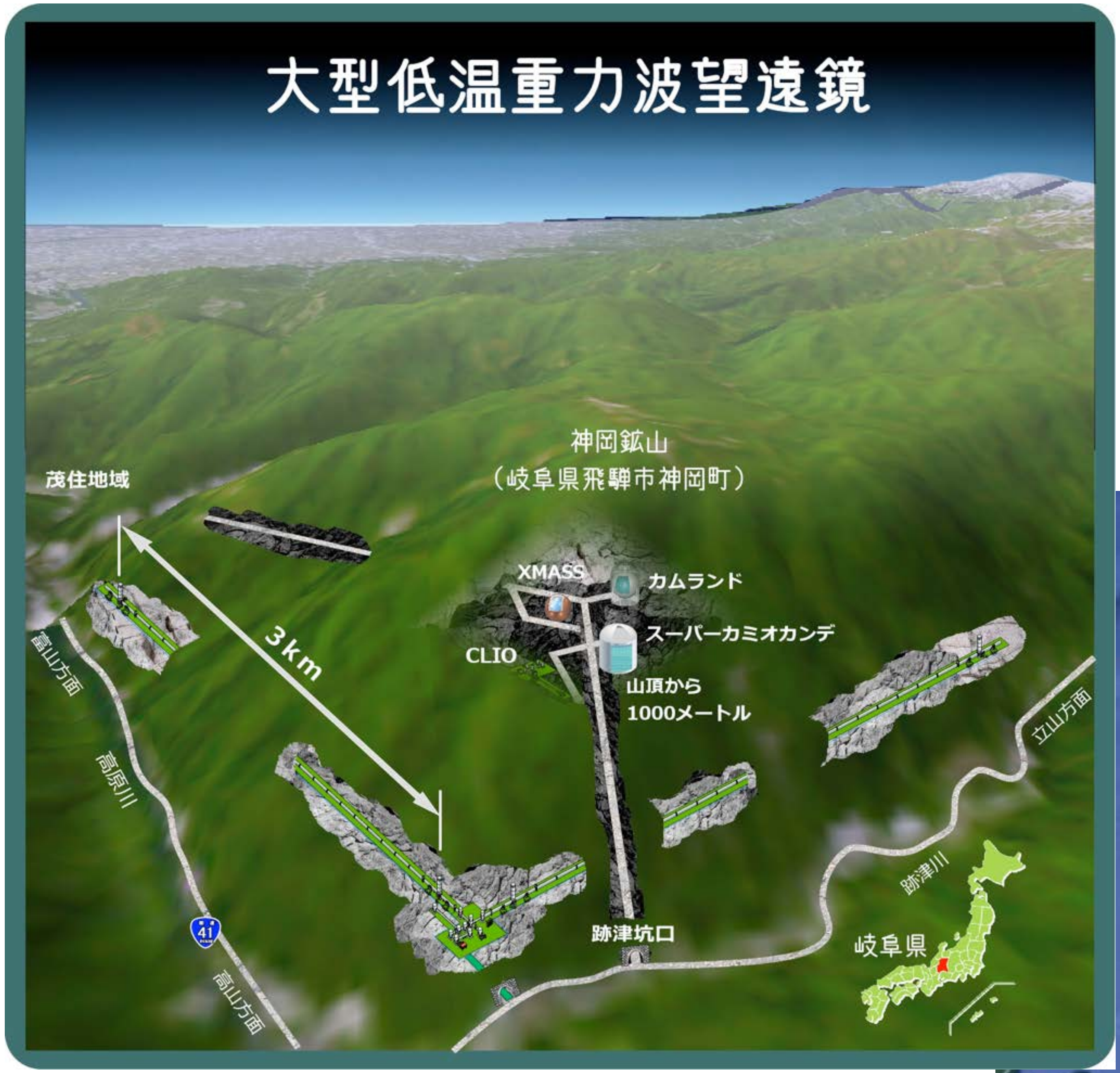

スーパー・カミオカンデ（ニュートリノ観測装置）

Super-Kamiokande　http://www-sk.icrr.u-tokyo.ac.jp/sk/

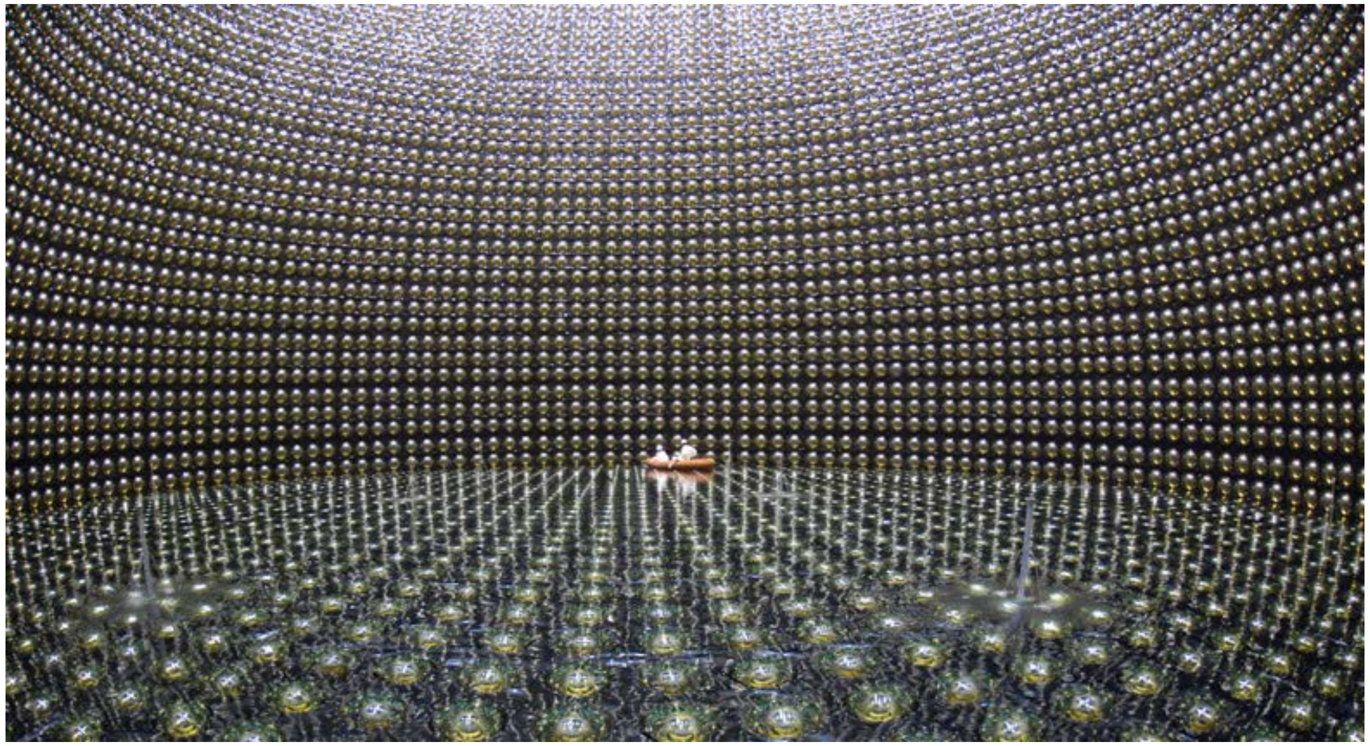

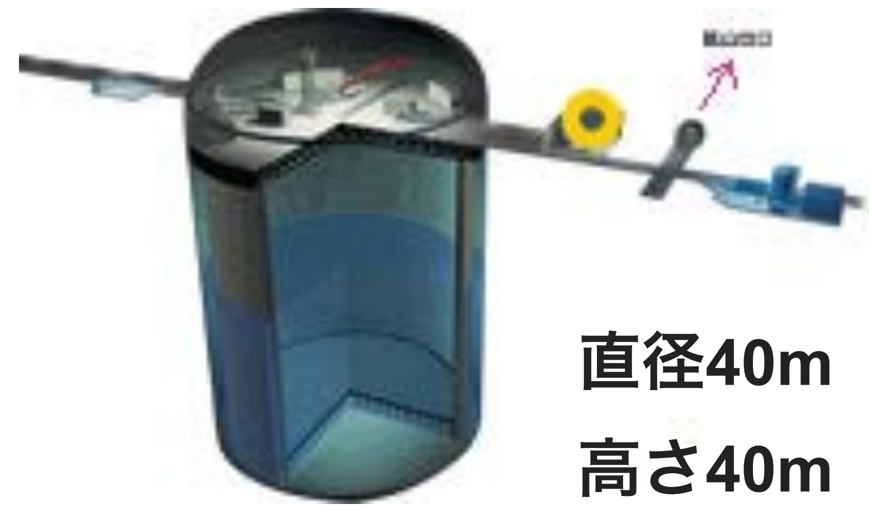

直径40m

高さ40m

岐阜県・神岡の鉱山跡の空洞に巨大な水槽をつくり，
宇宙から飛来するニュートリノを観測する．

ノーベル物理学賞を受賞

小柴昌俊（2002年）

梶田隆章（2015年）

KAGRA（かぐら：大型低温重力波望遠鏡）

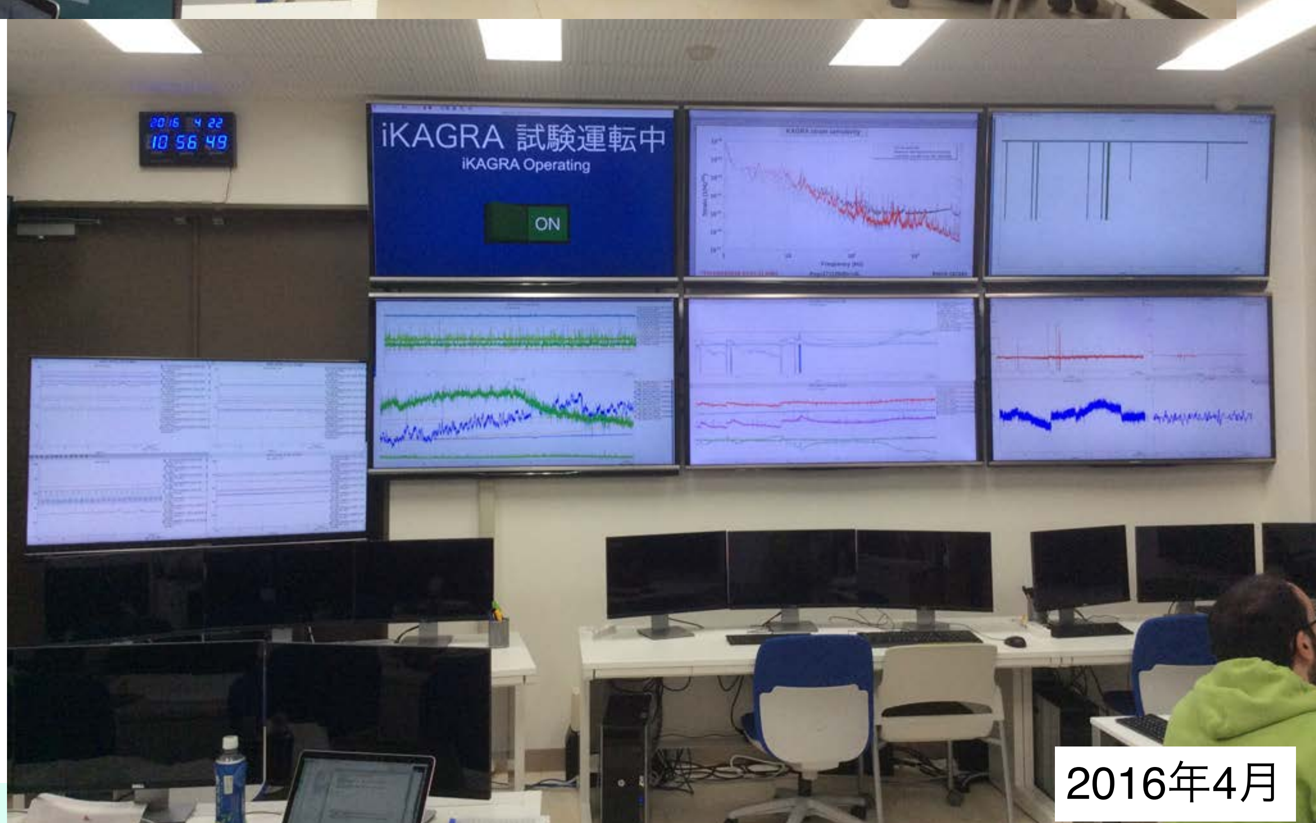

KAGRA（かぐら：大型低温重力波望遠鏡）

Hisaaki Shinkai

Seiji Kawamura Kieran Craig
Martynov Denis

KAGRA（かぐら：大型低温重力波望遠鏡）

天文宇宙検定

受験のご案内 | 公式テキスト | 天文宇宙クイズ

解答速報

2014年度 第４回天文宇宙検定　解答速報

	1級	問題と解答

2014年6月、日本が岐阜県に建設している重力波干渉計KAGRA（かぐら）のトンネルが貫通し、マスコミに公開された。KAGRAは、一辺が3kmもあるレーザー干渉計だが、岐阜県神岡鉱山跡の山中にわざわざ建設した理由は何か。

①近くにはスーパーカミオカンデというニュートリノ観測装置があり、実験装置の調整にニュートリノを使うから
②山の中だと地面の振動が少なく、干渉計装置のゆれを押さえることができるから
③山の中だと温度調整が少なくて済むので、レーザー光源のメンテナンスに都合がよいから
④強力なレーザー光の発生や、真空ポンプの稼働で、騒音が激しいから

KAGRA collaboration: as of June 2018

385 collaborators

(8 B students, 73 M students, 35 D students, 10 PDs)

90 institutes

15 countries

(Australia 5, China 35, France 1, German 1, India 3, Italy 17, Japan 253, Korea 23, The Netherlands 1, Poland 2, Russia 1, Taiwan 34, UK 2, USA 10, Vietnam 2)

PI: Takaaki Kajita

梶田隆章

Face-to-Face meeting
at Osaka City Univ.
May 2018 ⇨

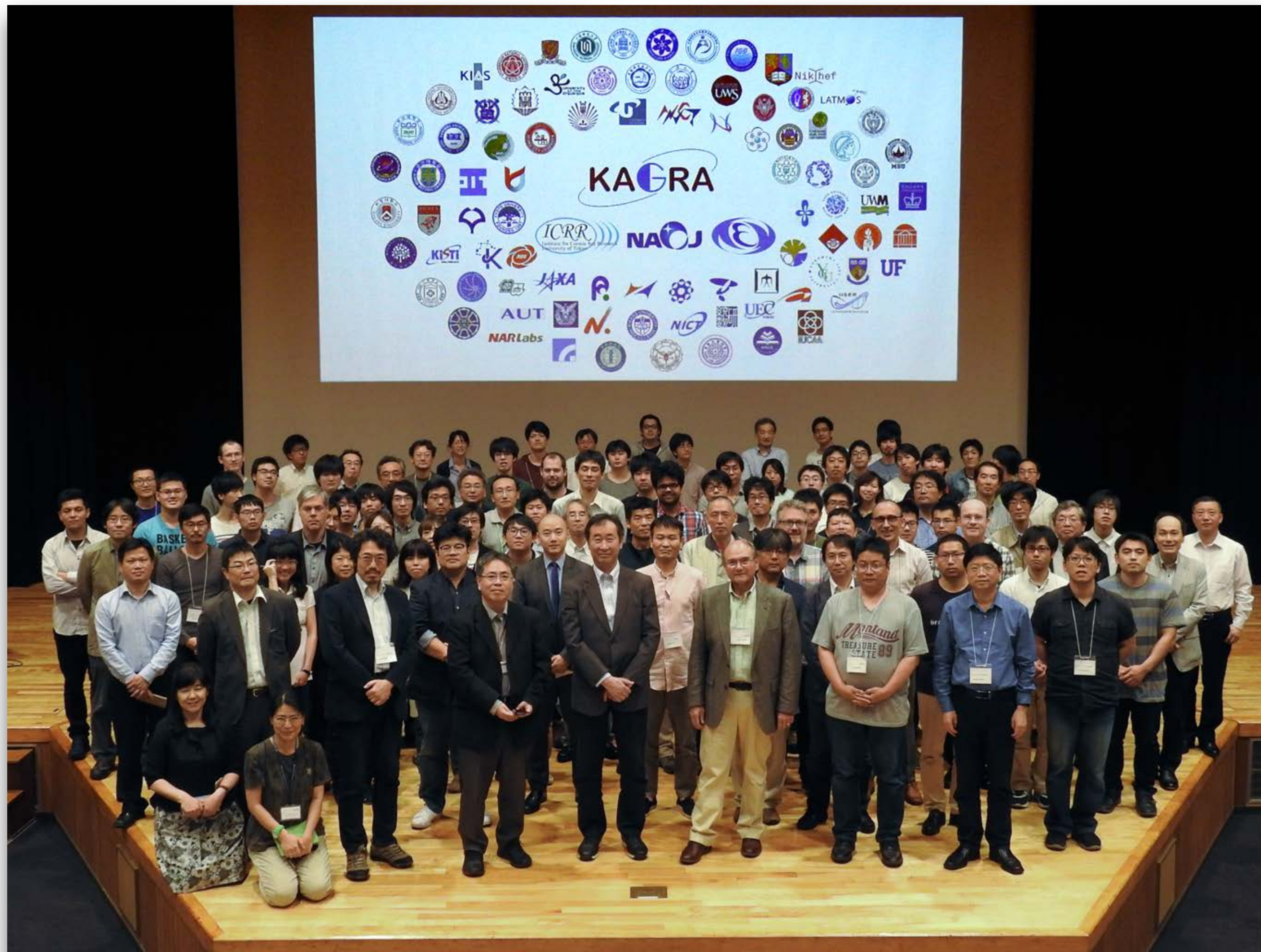

KSC（KAGRA Scientific Congress）

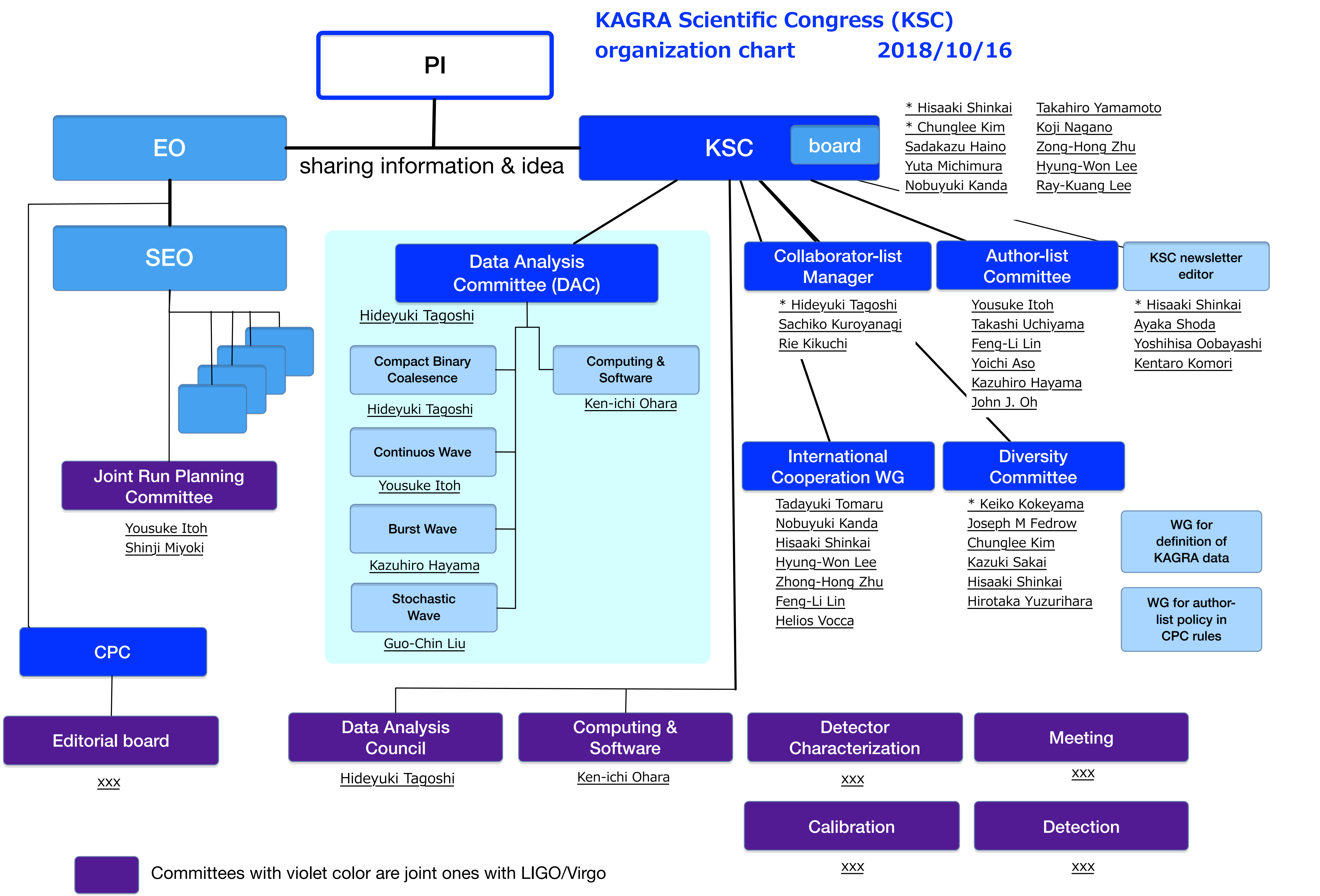

LIGO/Virgo joint observation plans

"Scenario Paper"

Living Rev Relativ (2018) 21:3
https://doi.org/10.1007/s41114-018-0012-9

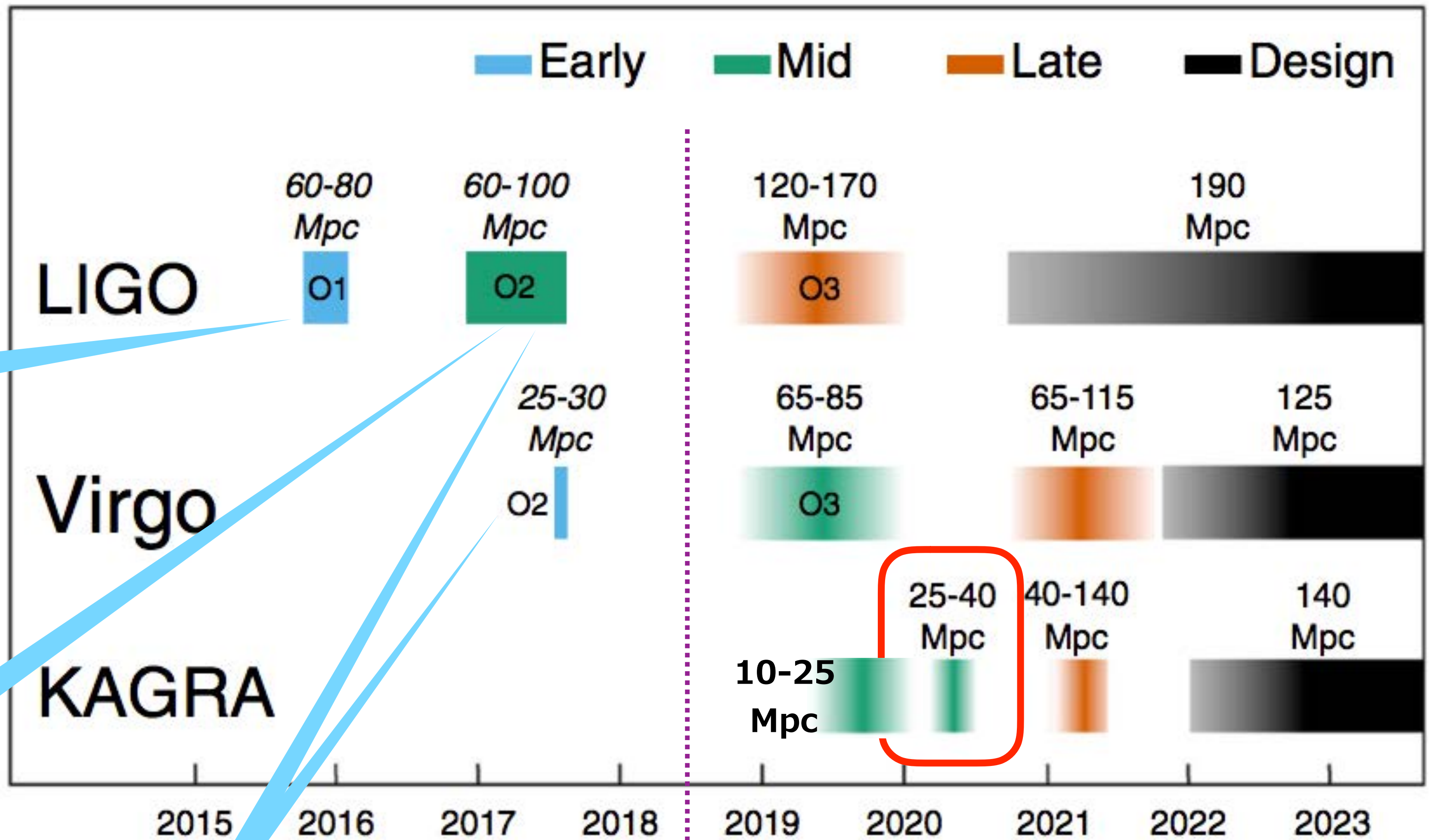

GW150914 BHBH@440Mpc
GW151226 BHBH@440Mpc

GW170104 BHBH@880Mpc
GW170608 BHBH@340Mpc

GW170814 BHBH@540Mpc
GW170817 NSNS@40Mpc

today

"We try to catch up with O3"

Roadmap of bKAGRA phase2 &3, Join LIGO/Virgo O3 run

time limited, we have to compromise

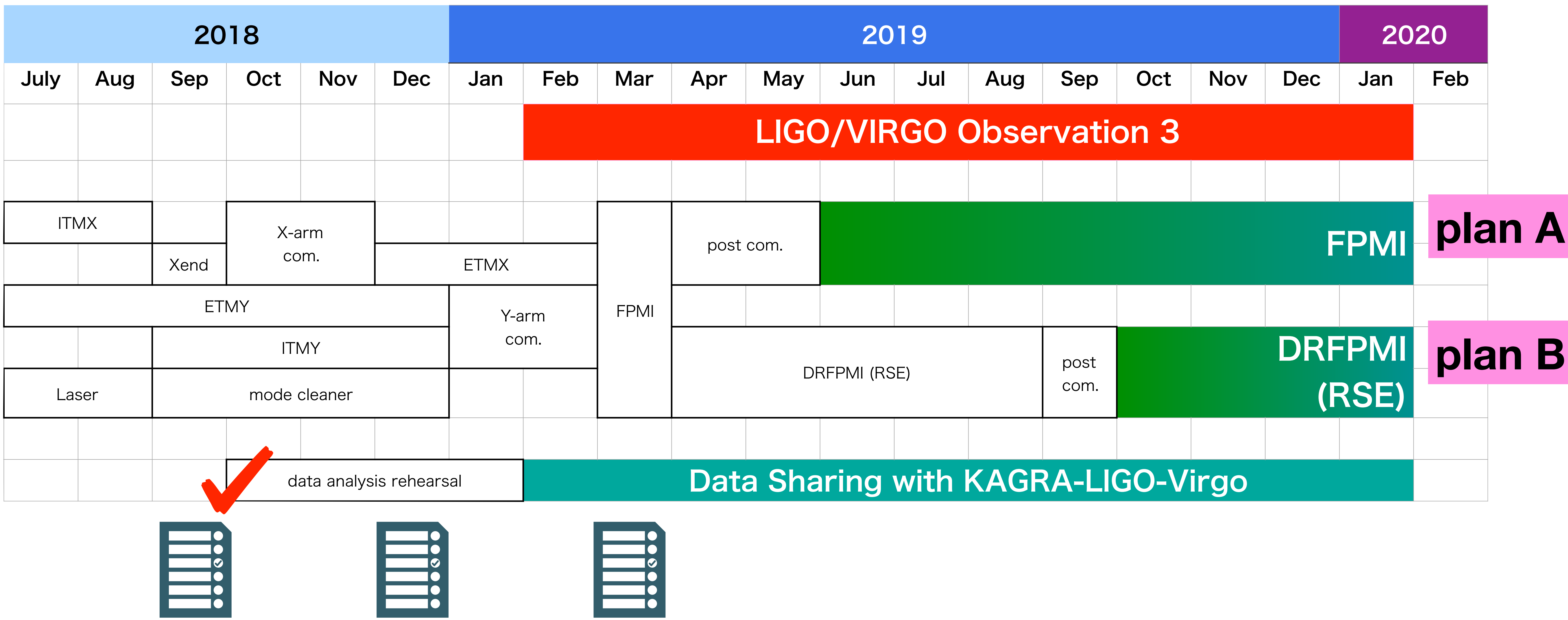

— **either DRFPMI(RSE) (-25Mpc, Oct?) or FPMI (-10Mpc, June?)**
checking points: Sep/2018, Dec/2018 and Mar/2019

Re-organizing KAGRA groups for joint observations

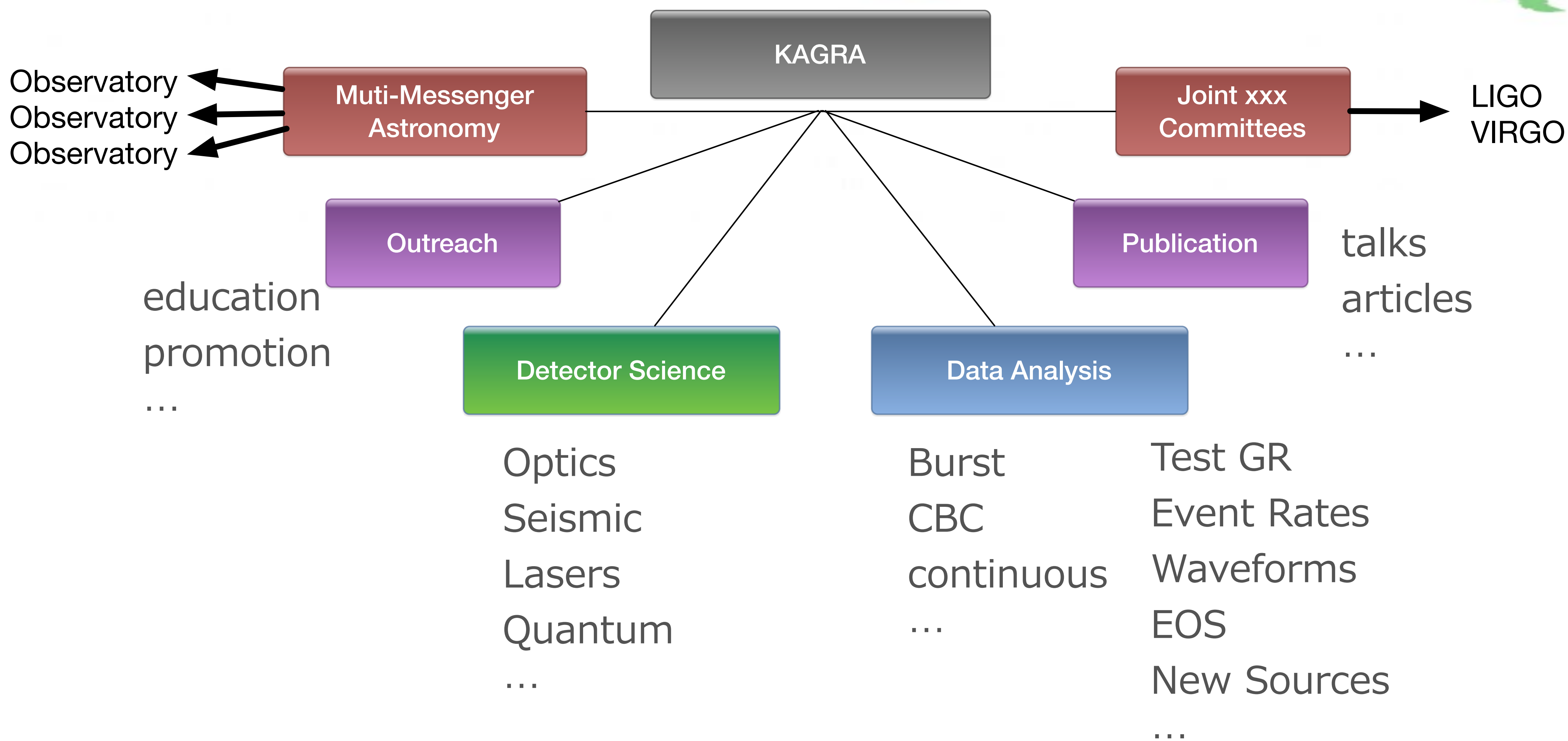

KAGRA SCIENTIFIC CONGRESS: COLLABORATORS' INFORMATION EXCHANGE 2018/08/01

KSC Newsletter

Second Issue

From Phase 1 to Phase 2

Nine-day operation with wild weather & earthquakes

KAGRA now has the world's tallest vibration isolation systems (13.5 m) which help to reduce seismic noise at low frequencies. The volume of the vacuum system is third largest in the world. Two 23-kg sapphire mirrors have been installed at each end, and one of them was kept for 30 days at cryogenic temperature (18K).

A leakage of the vacuum system was found in April 2018, therefore the Phase-1 experimental activity was delayed for 5 days. Despite the difficulties, the phase-1 operation was a success: it lasted from April 28 to May 6, 2018, and during this period many injection tests were performed.

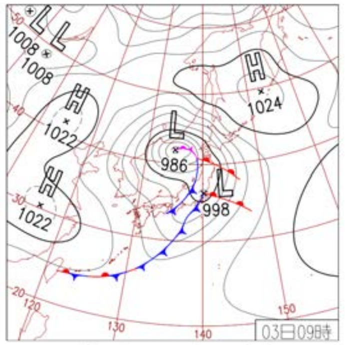

Weather map of May 3, 2018.

The interferometer duty cycle during the Phase-1 operation reached 88.6% between April 28 and May 2, while it dropped to 26.8% on May 3 and 4. Finally it slightly improved to 59.8% over the final days (May 5 & 6). The longest lock was over 10 hours. The low duty cycle on May 3 and on the following days was mainly attributed to the high micro-seismic noise caused by a heavy storm, local earthquakes, volcano eruptions in Hawaii, and visits of theorists.

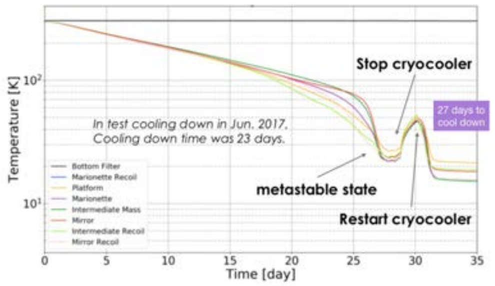

The achieved sensitivity during Phase 1 was still worse than the final sensitivities of TAMA and CLIO, except at the lower frequencies (40 Hz), where KAGRA's sensitivity was better than that of TAMA. KAGRA started Phase 2 from May 7: the final installation work before the real observation run.

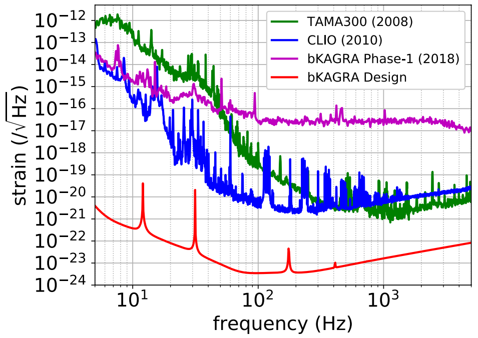

Contents of this issue

KAGRA SCIENTIFIC CONGRESS: COLLABORATORS' INFORMATION EXCHANGE 2018/04/01

KSC NewsLetter

The premiere issue

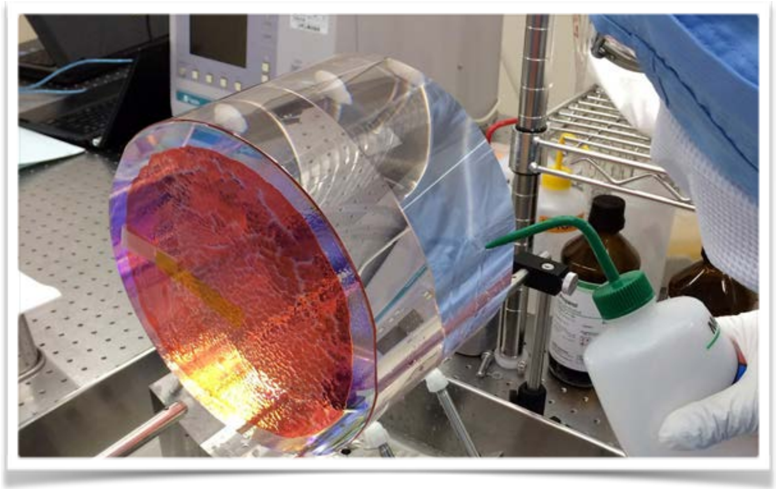

Phase-1 operation starts on April 23

First cryogenic interferometer test will start soon.

After two years from the iKAGRA run, we will start phase-1 operation on April 23 to May 6. Due to the tight schedule for our upcoming real observation, system engineering office (SEO) decided to operate phase-1 with one cryogenic mirror (Y-arm), and the other at normal temperature. We do not know what will be the outcomes. So it might become a sort of fun. A detail list of tests planned during the run is at page-3.

The above photo, taken in a clean room in the University of Toyama, is our 23kg-Sapphire mirror for X-end, which is now under installation. The installation of the cryo-payload at X-end is almost done and the main beam is coming back to the center now 😀.

Three words you should not miss in our conversation.

1 GW
Find GW.
Here GW is not "Gravitational Wave", but "Golden Week".

2 CRYOGENIC
Buy refrigerator, set freezing chamber, feel chilly, but try not to catch a cold.

3 O3
Not an oxygen-allotrope. Not a pathogenic *Vibrio Parahaemolyticus*.

What is this NewsLetter?
Nobody knows if this is the first issue of a series of information letters, or just a April fool's day joke.

O3=Ozone.
We are in a rush for O3 this year. Let's finish looking for O2.

We call for volunteers
We welcome your editorial participation to this journal. It will give you a career update definitely.

http://gwwiki.icrr.u-tokyo.ac.jp/JGWwiki/KAGRA

３．重力波のデータ解析

370　　システム/制御/情報，Vol. 62, No. 9, pp. 370–375, 2018

解　説

重力波の直接検出とデータ解析

真貝　寿明*

一般社団法人
システム制御情報学会
ISCIE
The Institute of Systems, Control and Information Engineers

https://www.iscie.or.jp/pub/journal

http://www.oit.ac.jp/is/~shinkai/

◆◆◆◆ 解説 ◆◆◆◆

重力波の観測とデータ解析

日本物理学会誌　Vol. 72, No. 3, 2017

田 越 秀 行
大阪市立大学大学院理学研究科
tagoshi@sci.osaka-cu.ac.jp

伊 藤 洋 介
東京大学大学院理学系研究科附属ビッグバン宇宙国際研究センター
yousuke_itoh@resceu.s.u-tokyo.ac.jp

端 山 和 大
東京大学宇宙線研究所重力波観測研究施設
hayama@icrr.u-tokyo.ac.jp

428　情報処理 Vol.57 No.5 May 2016

特別解説　応 専

重力波の初検出と情報処理技術
―LIGO と KAGRA で活用されている情報処理技術―

Kipp Cannon [*1]　端山和大 [*1]　伊藤洋介 [*1]　高橋弘毅 [*2]
[*1] 東京大学
[*2] 長岡技術科学大学

重力波のデータ解析

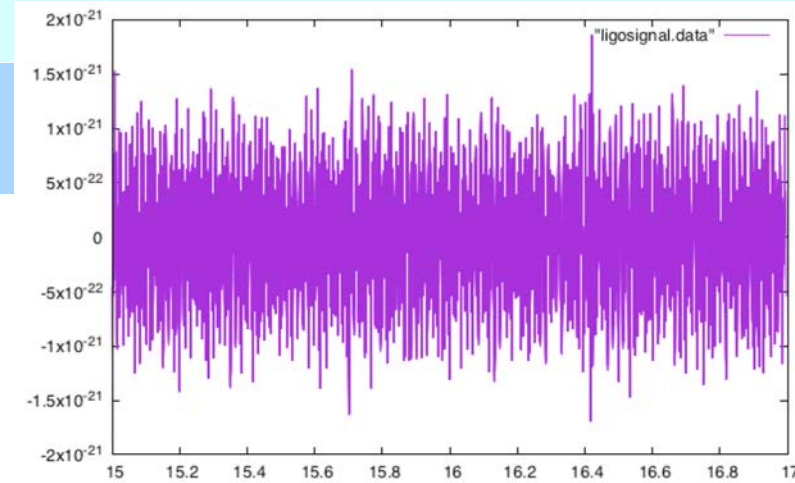

1. **連星合体解析**
   波形が既知．**マッチド・フィルタ解析．**
   `gstlal`, `pycbc`, `lalinference` (MCMC法)
2. **バースト重力波解析**
   超新星爆発・中性子星グリッチ現象
   `cWB` (コヒーレント解析)
3. **連続重力波解析**
   中性子星回転
   `Einstein@Home` (分散型コンピューティング)
4. **バックグラウンド重力波解析**
   宇宙論起源，白色矮星フォアグラウンド

Ideal vs Reality　(Theory vs Data Analysis)

GW150914 (S/N=23.7)

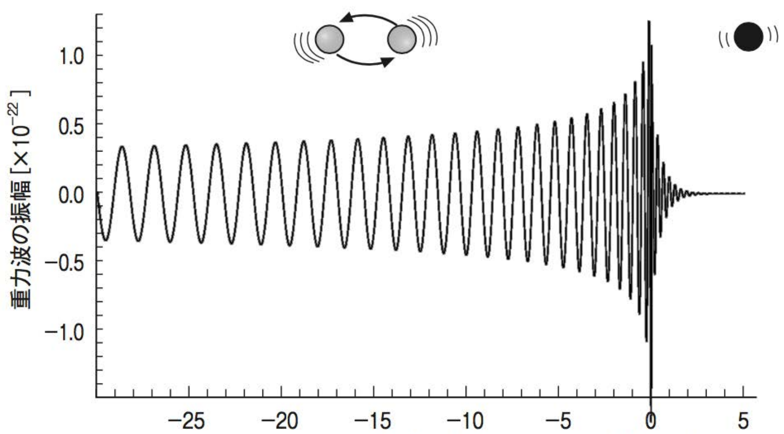

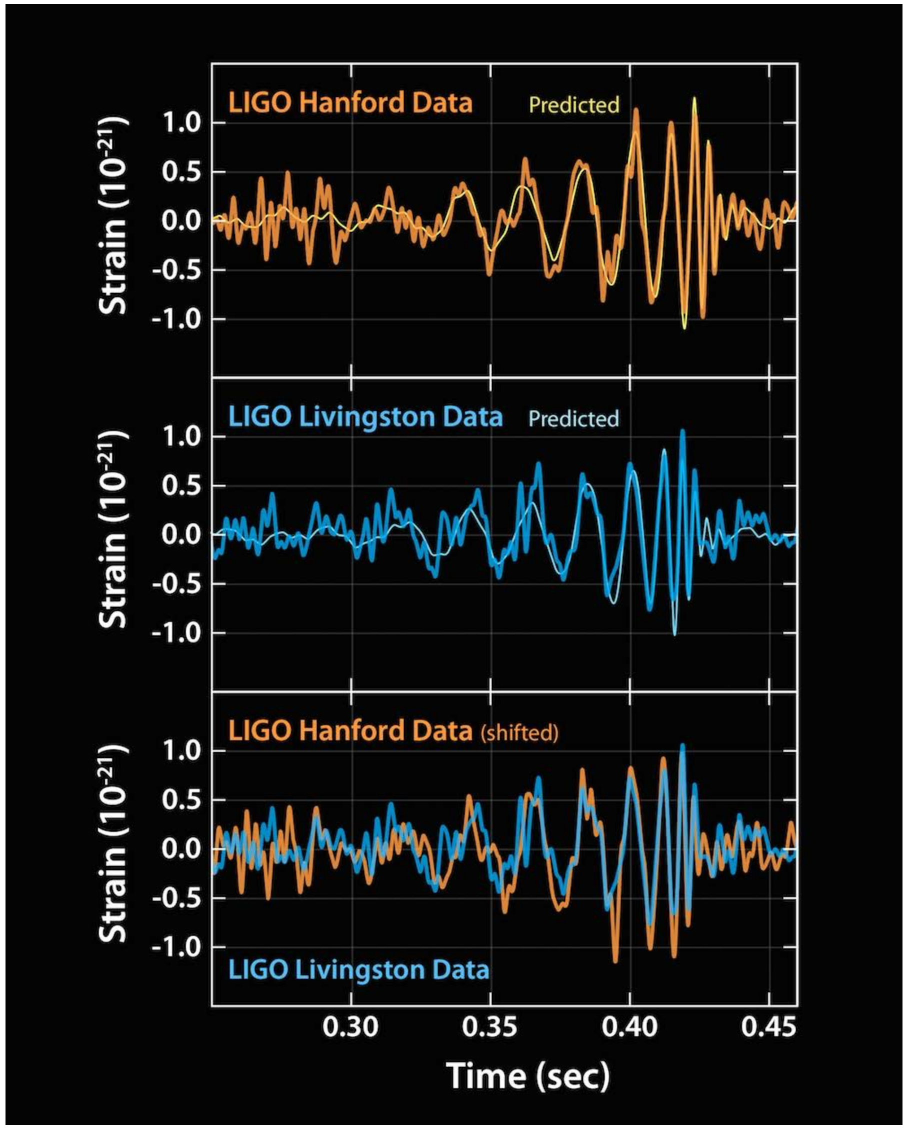

h(t)

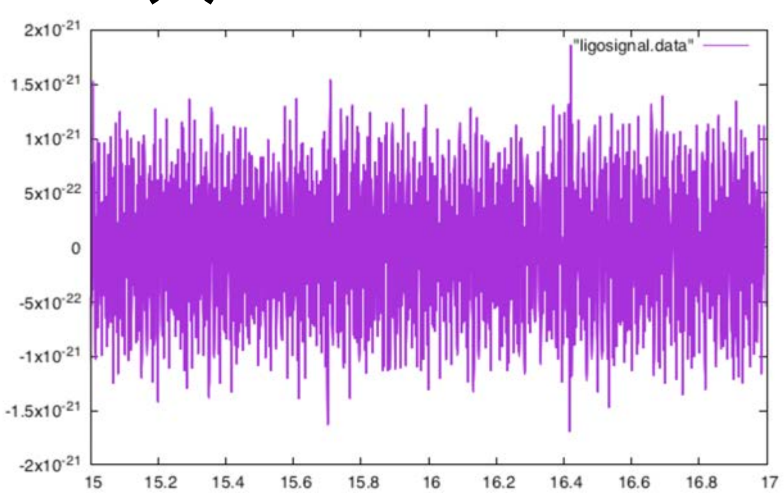

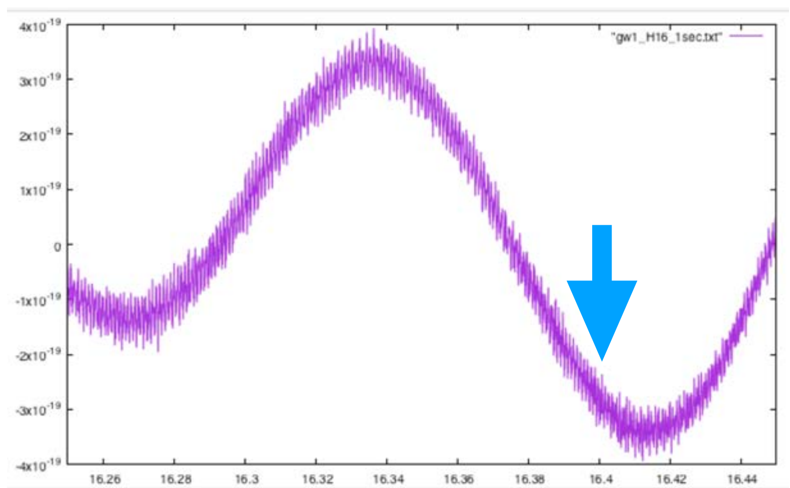

16.25　16.45

challenging for data analysis

GW data is with noise

signal quickly decays

(M=60Msun, a=0.75 —> 300Hz, tau = 3 ms)

Matched Filter 解析

signal = gw + noise

$$s(t) = h(t) + n(t)$$

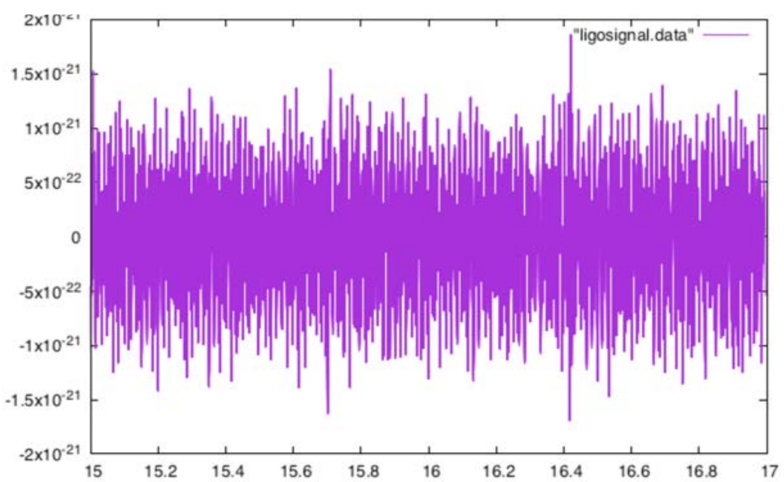

gw template

$$h(t)$$

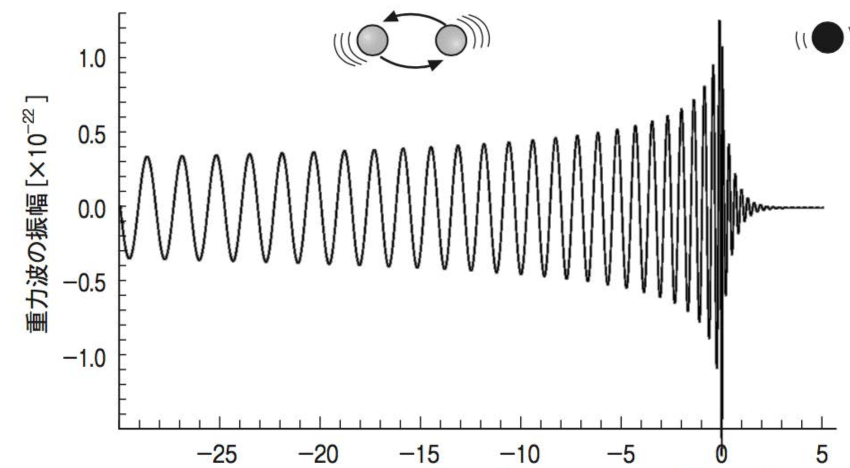

$$\rho = 2\int_{-\infty}^{\infty} \frac{\tilde{s}(f)\tilde{h}^*(f)}{S_h(|h|)} df$$

signal/noise ratio

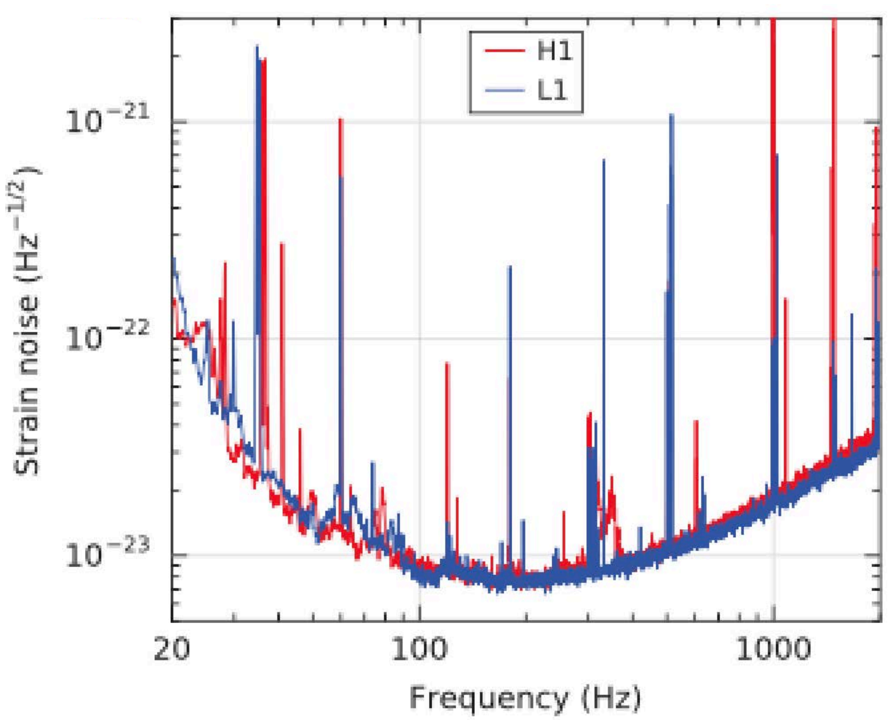

GW151226 (S/N=13.0)

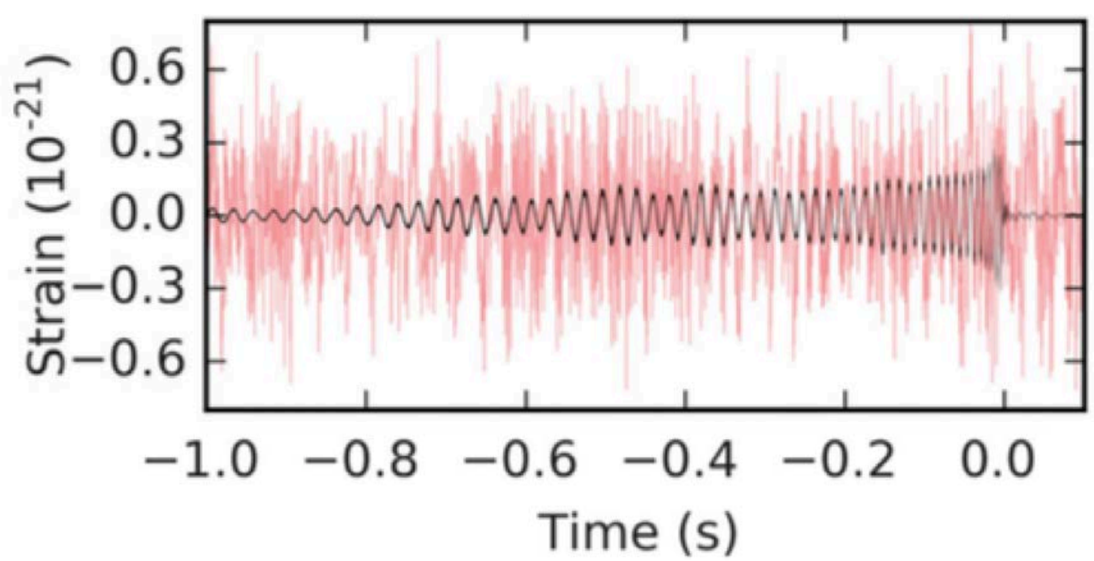

List of Detected GW events

	ref.	M1+M2=Mf, Mdiff/Mtotal	spin a_final	Mpc z	SNR	deg^2
GW150914	PRL116, 061102 (2016/2/11)	36.2+29.1=**62.3**+3.0 **4.59%**	0.68	410Mpc 0.09	**23.7**	600
LVT151012	(2016/2/11)	23+13=35+1.5 **2.78%**	0.66	1000Mpc 0.20	9.7	
GW151226	PRL116, 241103 (2016/6/15)	14.2+7.5=20.8+0.9 **4.15%**	0.74	440Mpc 0.09	13.0	850
GW170104	PRL118, 221101 (2017/6/1)	31.2+19.4=**48.7**+1.9 **3.75%**	0.64	880Mpc 0.18	**13**	1300
GW170608	ApJ 851, L35 (2017/12/18)	12+7=18.0+1.0 **5.2%**	0.69	340Mpc 0.07	13	520
GW170814	PRL119,141101 (2017/10/6)	30.5+25.3=**53.2**+2.6 **4.66%**	0.70	540Mpc 0.11	**18**	60
GW170817	PRL119, 161101 (2017/10/16)	1.36〜1.60 + 1.17〜1.36 = 2.74 + ?	?	40Mpc	32.4	28

LIGO

LIGO Computing Latencies

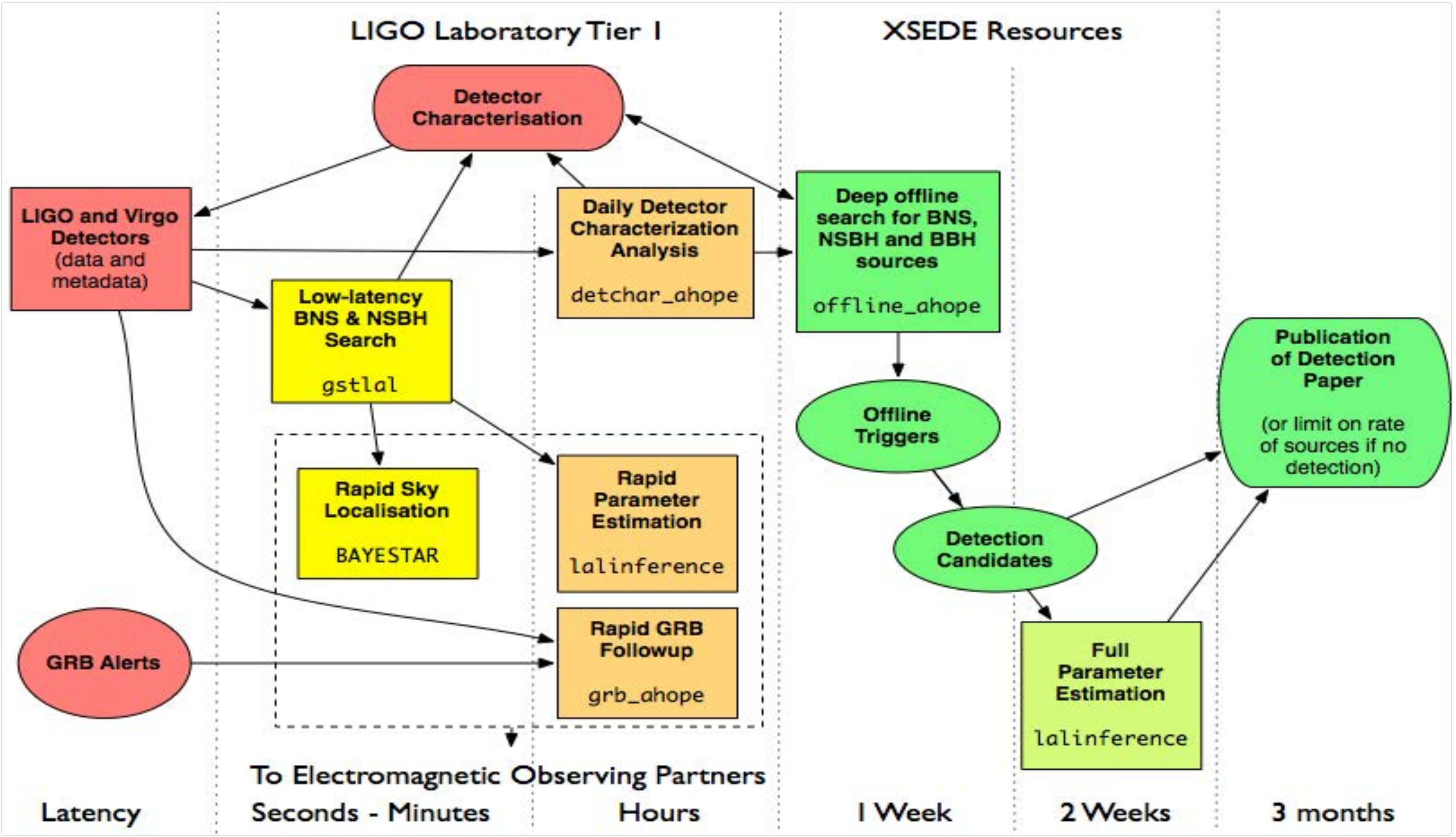

Sharon Brunett, 2015/10

自己回帰モデルを用いた重力波データ解析：ブラックホール合体のリングダウン波形の抽出

真貝寿明，山本峻 元M2（大阪工大）
H. Shinkai, S. Yamamoto (OIT)

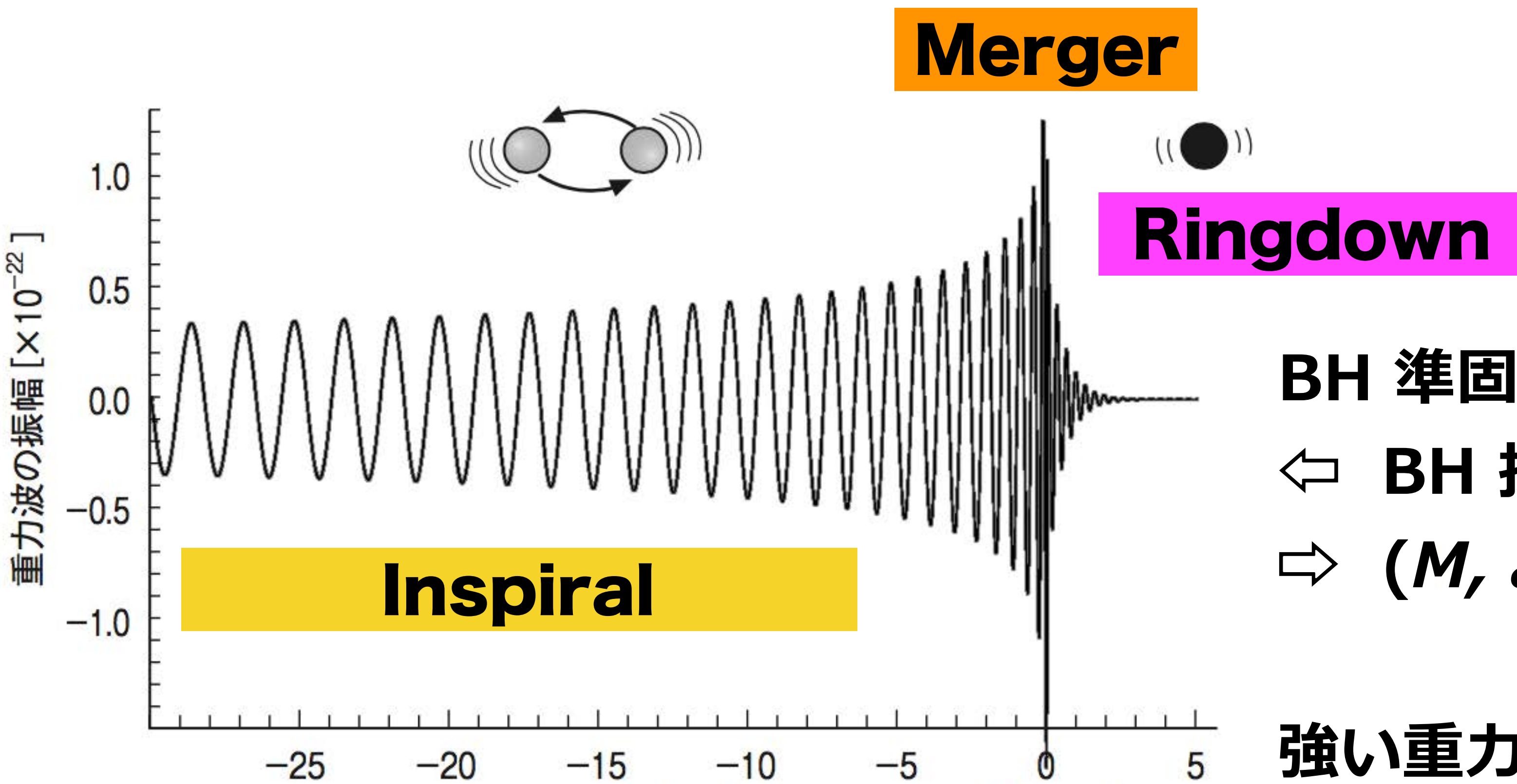

BH 準固有モード(quasi-normal modes)
⇦ BH 摂動理論
⇨ (M, a)

強い重力場の表れ
⇨ 一般相対論の検証ができる

新しい方法を提案．テンプレートを使わず，データから波形を再構築．

2018/9/14 物理学会 @ 信州大学

Mock data example (0) : QNM extraction contest

Mock data challenge for finding ringdown gravitational waves

Hiroyuki Nakano,[1,*] Tatsuya Narikawa,[2,3,†] Ken'ichi Ohara,[4,‡] Kazuki Sakai,[5,§] Hisa-aki Shinkai,[6,¶] Hirotaka Takahashi,[7,8,**] Takahiro Tanaka,[3,††] Nami Uchikata,[2,4,‡‡] Shun Yamamoto,[6] and Takahiro Yamamoto[3,§§]

modified ringdown signals from GR
with LIGO detector's noise

1. Standard Matched-filtering method
2. Improved Matched-filtering method
3. Hilbert-Huang transformation method
4. Auto-Regressive method
5. Neural network method

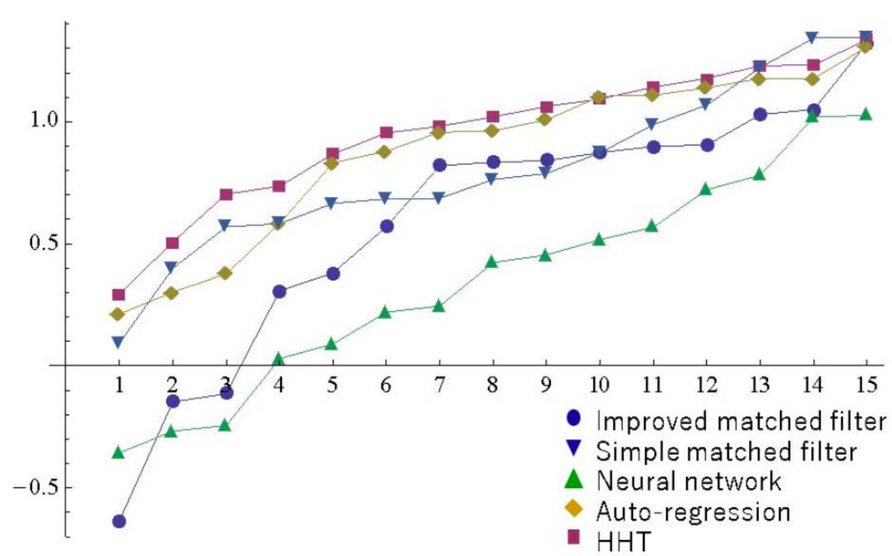

FIG. 1: Real part for Set A

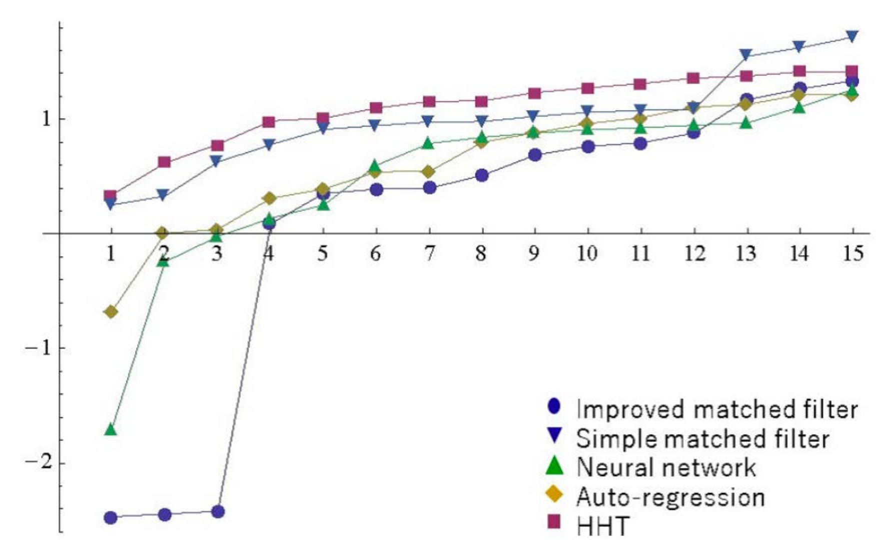

FIG. 3: Imaginary part for Set A

1. Auto-Regressive model (Method, general) I

Fitting data with linear func.

$$
\begin{aligned}
x_n &= a_1 x_{n-1} + a_2 x_{n-2} + \cdots + a_M x_{n-M} + \varepsilon \\
&= \sum_{j=1}^{M} a_j x_{n-j} + \varepsilon
\end{aligned}
$$

e.g. $x_n = Ae^{-rn\Delta t}\cos(\omega n \Delta t)$

$$Z_1 = e^{-(r-j\omega)\Delta t}$$

$$Z_2 = e^{-(r+j\omega)\Delta t}$$

→ $x_n = \frac{A}{2}(Z_1^n + Z_2^n) = (Z_1 + Z_2)x_{n-1} - Z_1 Z_2 x_{n-2}$

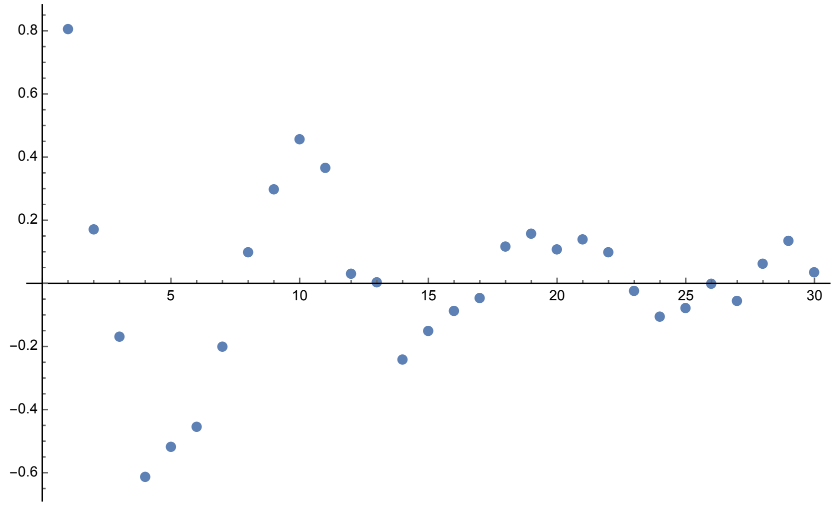

→

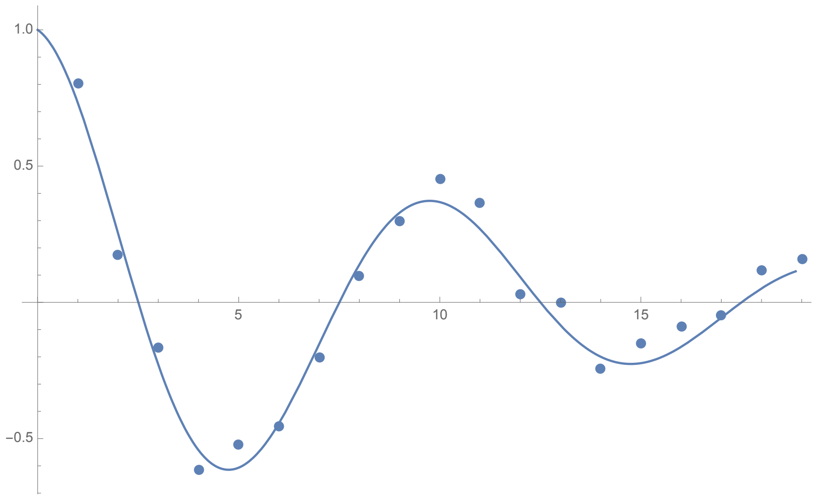

can be applied also to noisy data by adjusting *M*

1. Auto-Regressive model (Method, general) II

Fitting data with linear func.

$$\begin{aligned} x_n &= a_1 x_{n-1} + a_2 x_{n-2} + \cdots + a_M x_{n-M} + \varepsilon \\ &= \sum_{j=1}^{M} a_j x_{n-j} + \varepsilon \end{aligned}$$

- find a_j (Burg method)
- find M (FPE final prediction error method)
- re-construct wave signal from fitted function
- apply FFT with arbitrary precision.

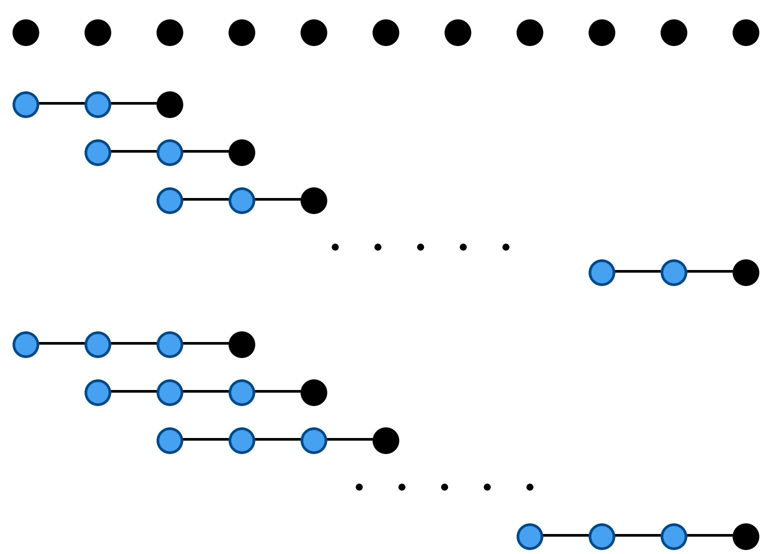

power spectrum

$$p(f) = \frac{\sigma^2}{\left| 1 - \sum_{j=1}^{M} a_j e^{-I 2\pi j f \Delta t} \right|^2}$$

Auto-Regressive model vs Short FFT

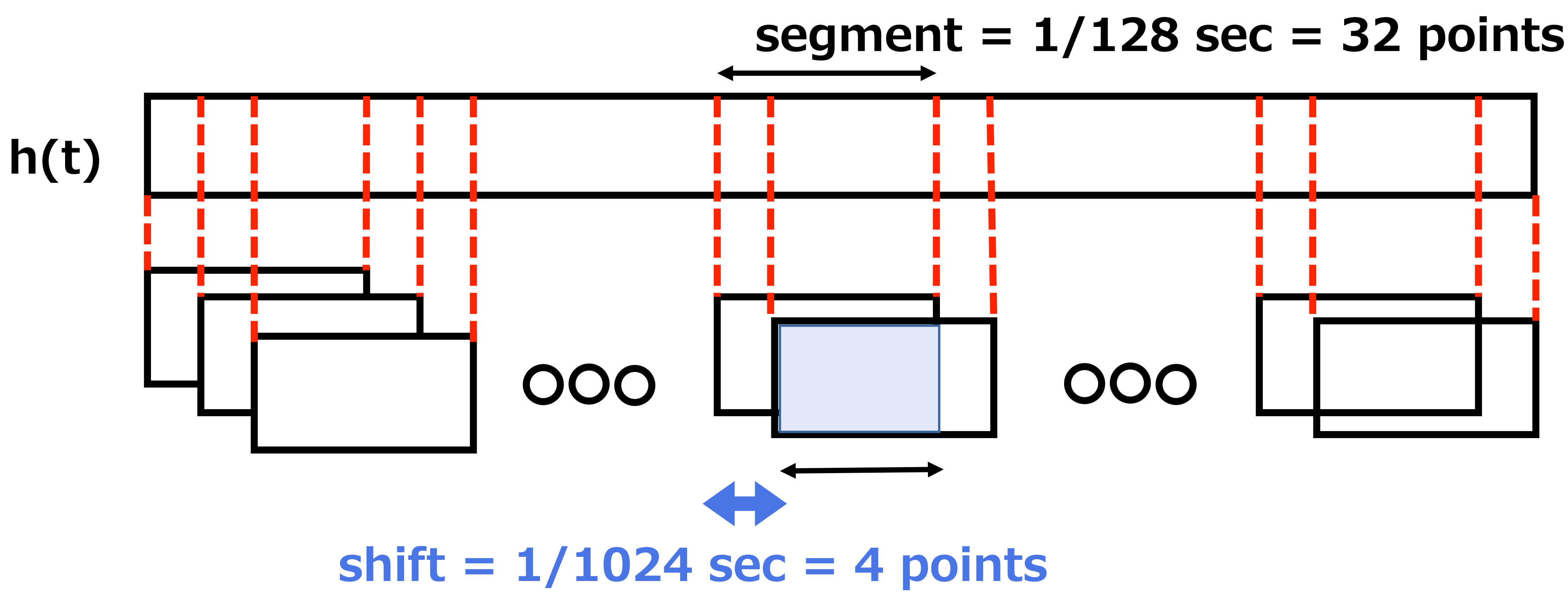

P(f)

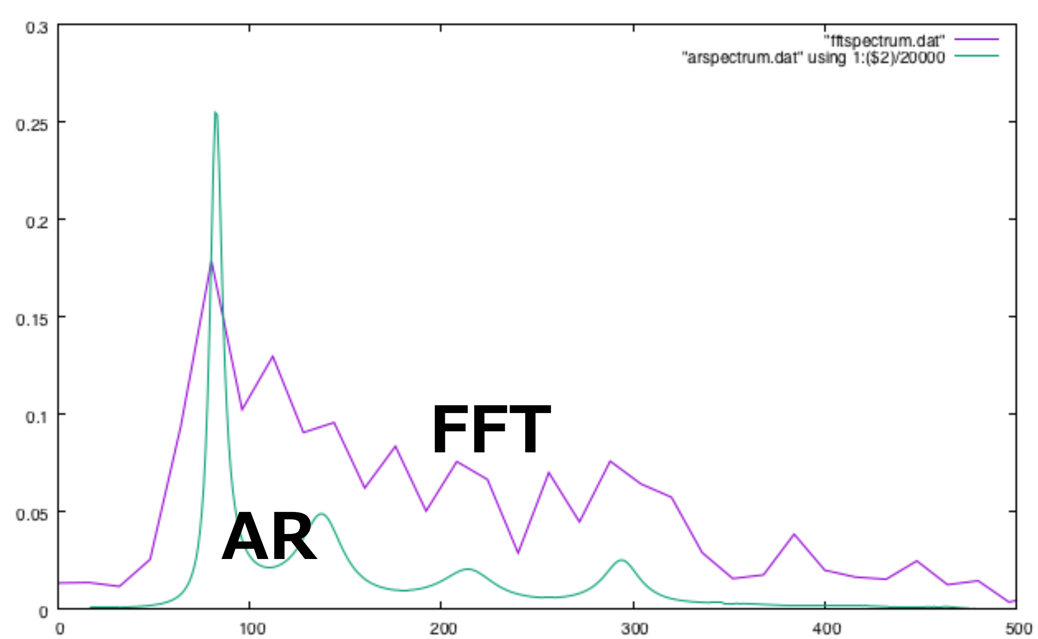

freq. [mock data, SNR=40, inspiral part]

The order *M* can be fixed at 2〜8.

Even for short segment, AR model shows precise power-spectrum.

1. Auto-Regressive model (Method, general) III

Fitting data with linear func.

$$x_n = a_1 x_{n-1} + a_2 x_{n-2} + \cdots + a_M x_{n-M} + \varepsilon$$
$$= \sum_{j=1}^{M} a_j x_{n-j} + \varepsilon$$

- find a_j (Burg method)
- find M (FPE final prediction error method)
- re-construct wave signal from fitted function
- apply FFT with arbitrary precision.

power spectrum

$$p(f) = \frac{\sigma^2}{\left| 1 - \sum_{j=1}^{M} a_j e^{-I 2\pi j f \Delta t} \right|^2}$$

characteristic eq.

$$f(z) = 1 - \sum_{j=1}^{M} a_j z^j = 0$$

$|z_k|$ says amplitude,
$\arg(z_k)$ says frequency.

Mock data example (1) fitting well

Mock Data (Nakano02 p)

spectrogram

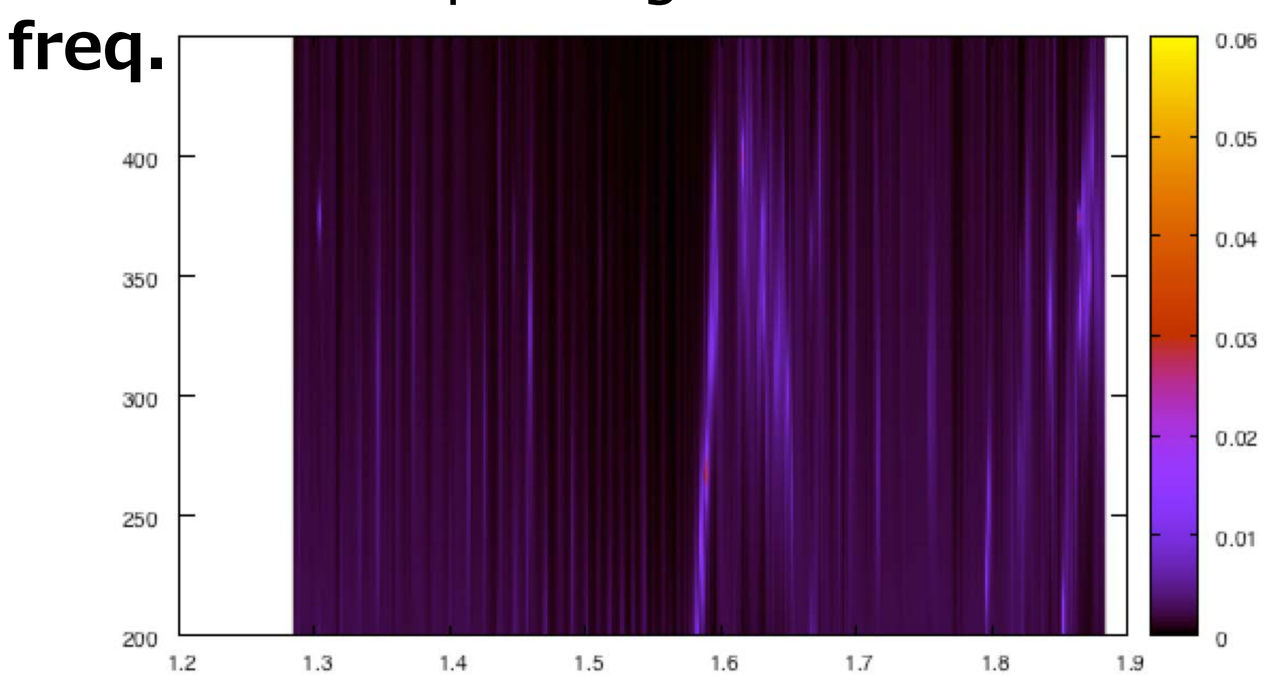

h(t) x original data, — fitted

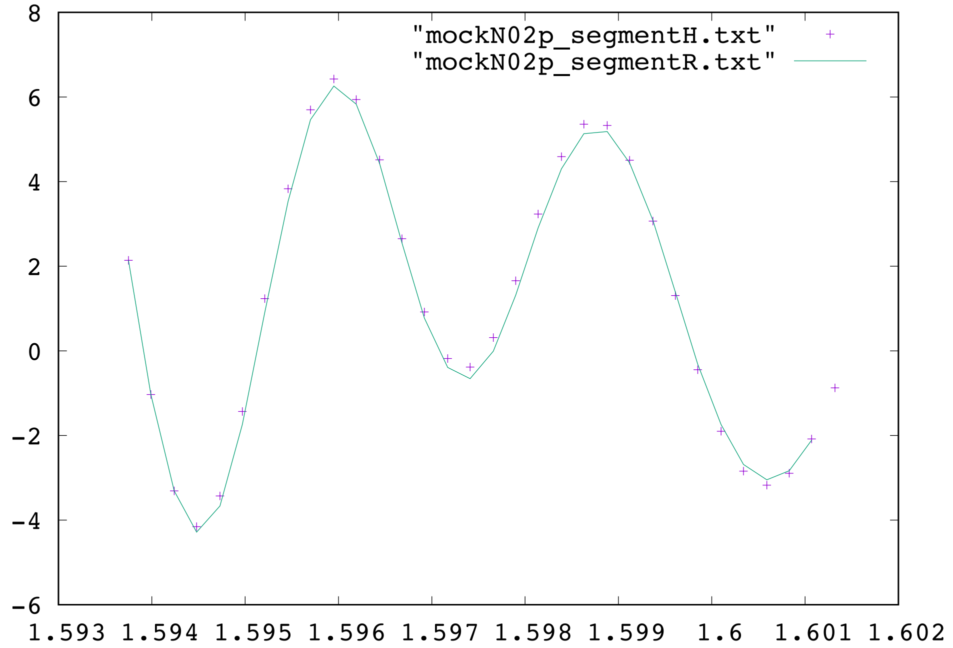

Fitting data with linear func.

$$x_n = a_1 x_{n-1} + a_2 x_{n-2} + \cdots + a_M x_{n-M} + \varepsilon$$
$$= \sum_{j=1}^{M} a_j x_{n-j} + \varepsilon$$

```
a.1  = -2.235e+00
a.2  =  1.869e+00
a.3  = -5.545e-01
```

Mock data example (2) spectrogram

Mock Data (Nakano02 p)

spectrogram

freq.

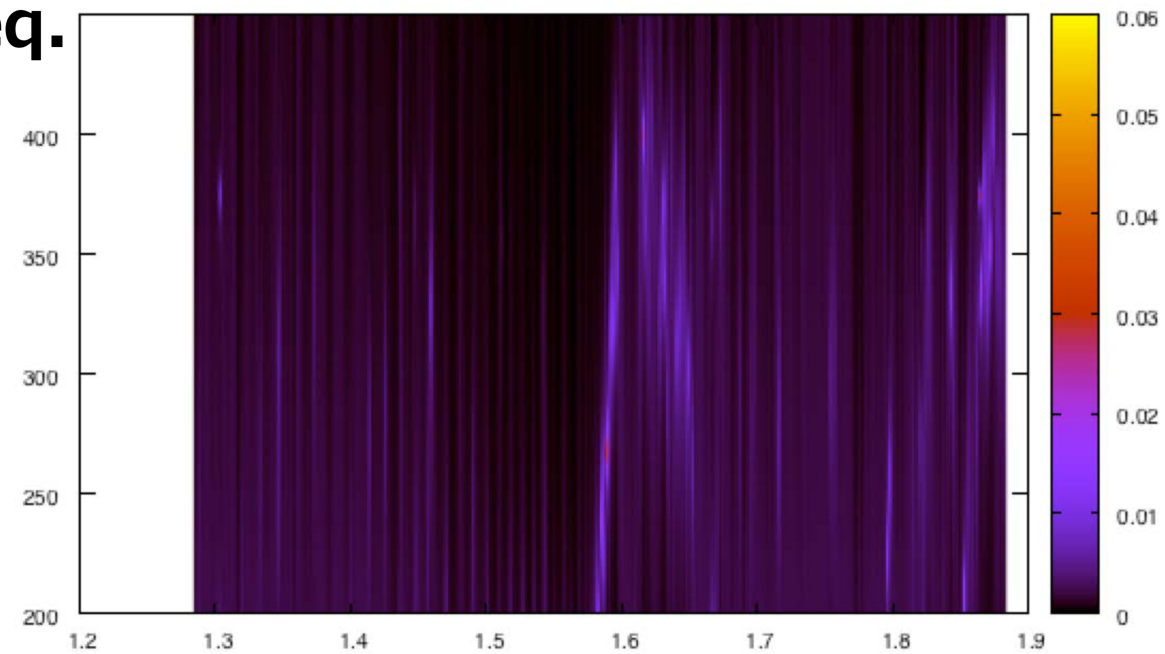

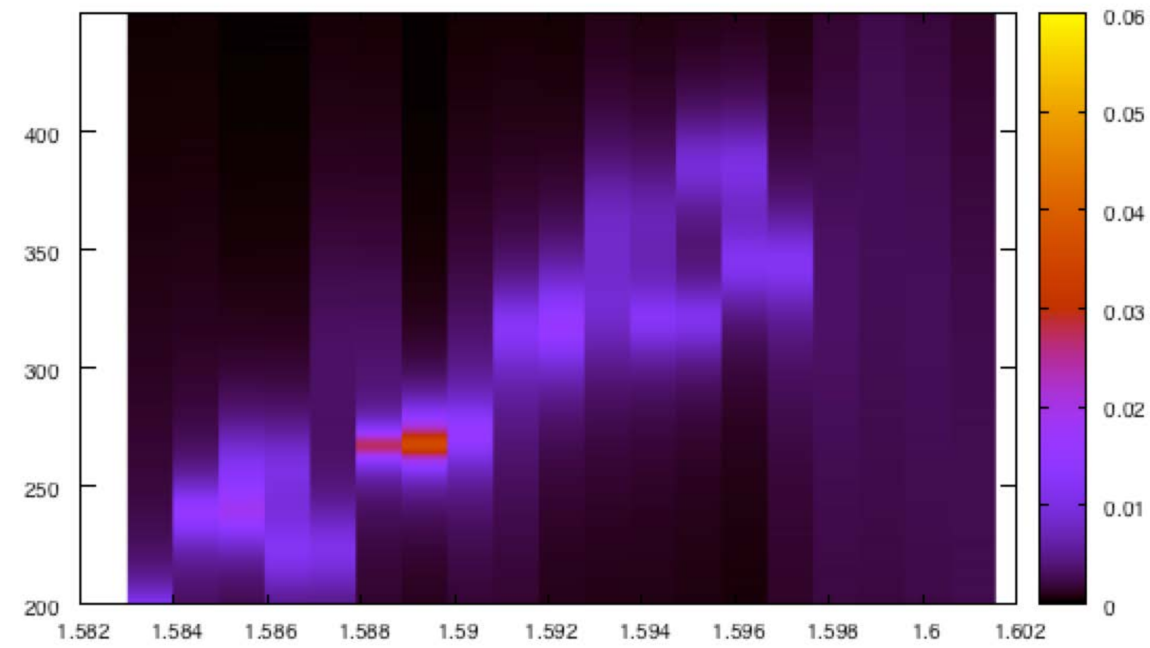

power spectrum

$$p(f) = \frac{\sigma^2}{\left|1 - \sum_{j=1}^{M} a_j e^{-I 2\pi j f \Delta t}\right|^2}$$

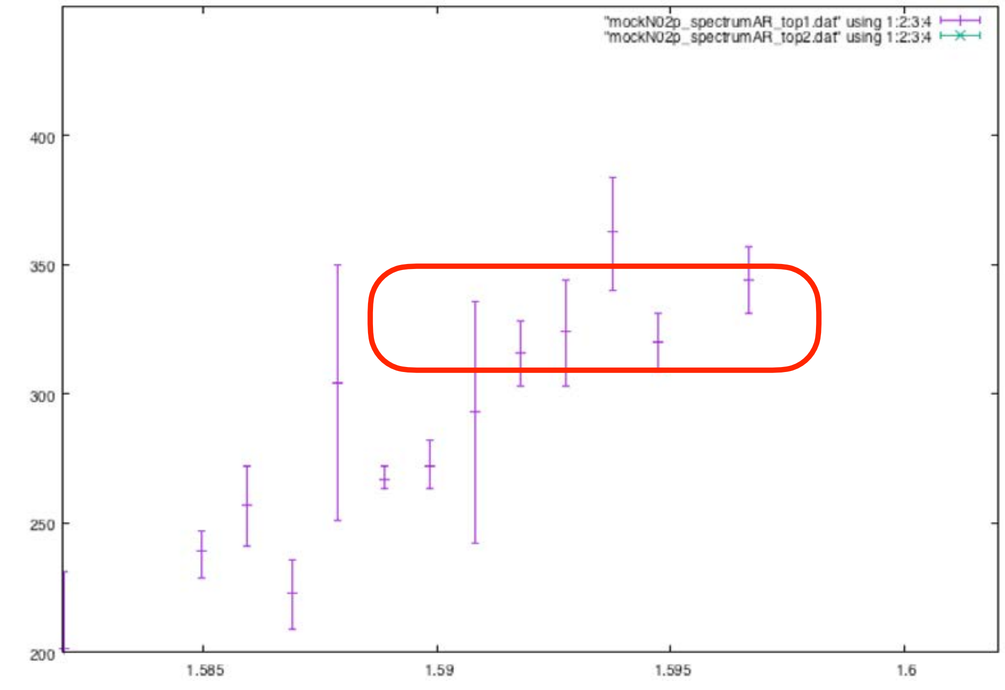

Mock data example (3) characteristic eq.

Mock Data (Nakano02 p)

Fitting data with linear func.

$$x_n = a_1 x_{n-1} + a_2 x_{n-2} + \cdots + a_M x_{n-M} + \varepsilon$$
$$= \sum_{j=1}^{M} a_j x_{n-j} + \varepsilon$$

```
a.1   = -2.235e+00
a.2   =  1.869e+00
a.3   = -5.545e-01
```

characteristic eq.

$$f(z) = 1 - \sum_{j=1}^{M} a_j z^j = 0$$

$$x_{n-1} = z x_n$$

$$z = \exp[-2\pi i f \Delta t]$$

$|z_k|$ says amplitude,
$\arg(z_k)$ says frequency.

	x.r	x.i	f_R[Hz]	|x|	f_I[Hz]
1	0.962	0.566	346.800	8.025e-01	71.721
2	0.962	-0.566	-346.800	8.025e-01	71.721
3	1.447	0.000	0.000	4.775e-01	240.931

Mock data example (4) identify ring-down freq.

Mock Data (Nakano02 p)

characterestic eq.

$$f(z) = 1 - \sum_{j=1}^{M} a_j z^j = 0$$

$$x_{n-1} = z x_n$$

$$z = \exp[-2\pi i f \Delta t]$$

$|z_k|$ says amplitude,
$\arg(z_k)$ says frequency.

	x.r	x.i	f_R[Hz]	|x|	f_I[Hz]
1	0.962	0.566	346.800	8.025e-01	71.721
2	0.962	-0.566	-346.800	8.025e-01	71.721
3	1.447	0.000	0.000	4.775e-01	240.931

t	f_R (z_plane)	f_I (z_plane)	f_Rh(spectr)	f_Rmax(spectr)	f_Rh(spectr)
0.159375E+01	0.363837E+03	0.280414E+02	0.340000E+03	0.363000E+03	0.384000E+03
0.159668E+01	0.344258E+03	0.166608E+02	0.331000E+03	0.344000E+03	0.357000E+03
0.159766E+01	0.346800E+03	0.717212E+02	0.240000E+03	0.329000E+03	0.382000E+03
0.161230E+01	0.357677E+03	0.122067E+03	0.213000E+03	0.338000E+03	0.431000E+03
0.161328E+01	0.361098E+03	0.948919E+02	0.261000E+03	0.350000E+03	0.422000E+03
0.161523E+01	0.379918E+03	0.772796E+02	0.304000E+03	0.373000E+03	0.432000E+03

```
 average & variance zfr =    0.359E+03    0.118E+02   fr(sp) =    0.350E+03   0.148E+02
 average & variance zfi =    0.684E+02    0.365E+02
```

Application to the LIGO/Virgo data

List of Detected GW events

	ref.	M1+M2=Mf, Mdiff/Mtotal	spin a_final	Mpc z	SNR	deg^2
GW150914	PRL116, 061102 (2016/2/11)	36.2+29.1=62.3+3.0 **4.59%**	0.68	410Mpc 0.09	**23.7**	600
LVT151012	(2016/2/11)	23+13=35+1.5 **2.78%**	0.66	1000Mpc 0.20	9.7	
GW151226	PRL116, 241103 (2016/6/15)	14.2+7.5=20.8+0.9 **4.15%**	0.74	440Mpc 0.09	13.0	850
GW170104	PRL118, 221101 (2017/6/1)	31.2+19.4=48.7+1.9 **3.75%**	0.64	880Mpc 0.18	**13**	1300
GW170608	ApJ 851, L35 (2017/12/18)	12+7=18.0+1.0 **5.2%**	0.69	340Mpc 0.07	13	520
GW170814	PRL119,141101 (2017/10/6)	30.5+25.3=53.2+2.6 **4.66%**	0.70	540Mpc 0.11	**18**	60
GW170817	PRL119, 161101 (2017/10/16)	1.36〜1.60 + 1.17〜1.36 = 2.74 + ?	?	40Mpc	32.4	28

Ringdown wave of GW150914

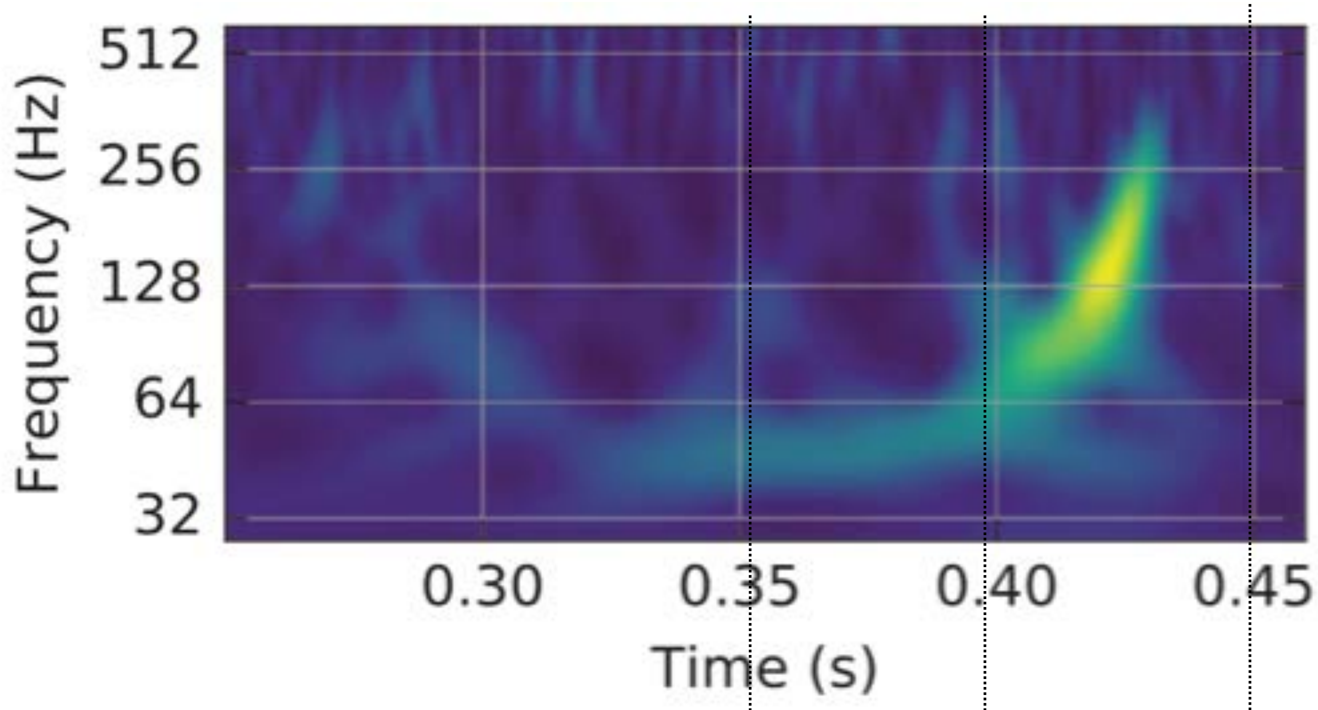

LIGO paper

4096 sampling rate

100-400 Hz filter

1 segment = 1/64 sec= 64 points

1 shift = 1/512 sec = 8 points

AR model

Hanford

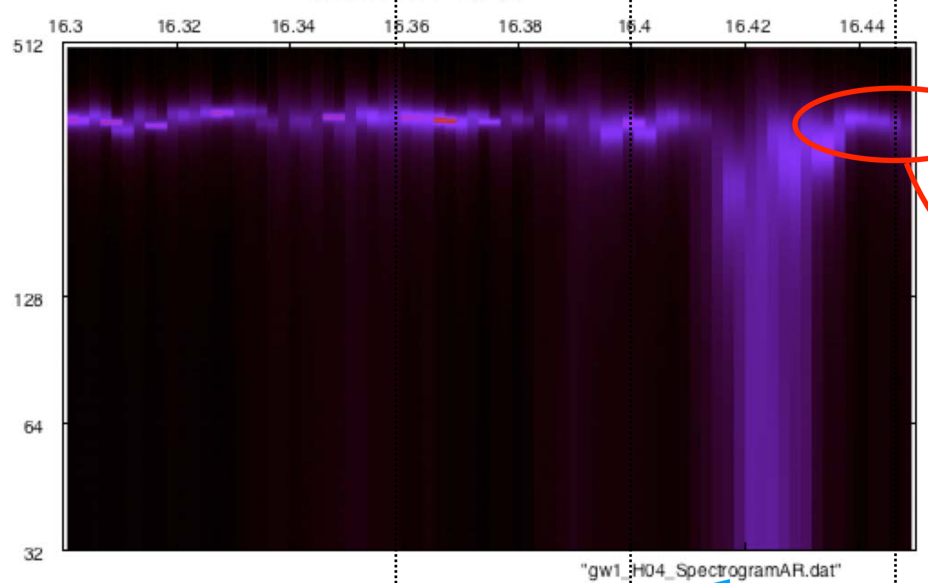

max M = 3

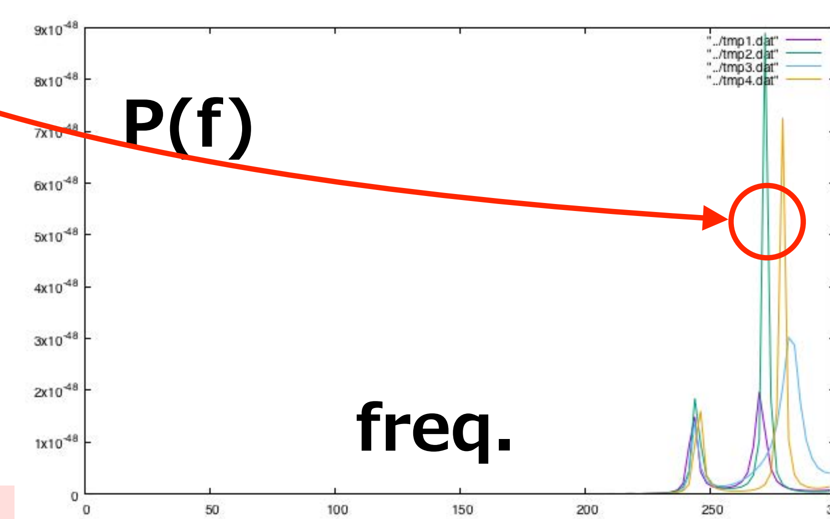

Ringdown wave of GW150914

AR model Hanford

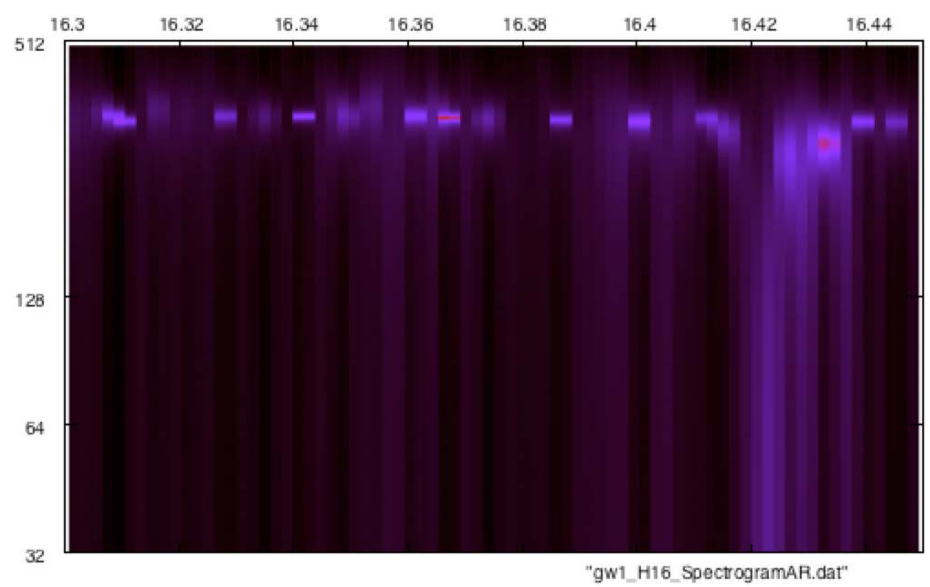

16384 sampling rate

AR model Hanford

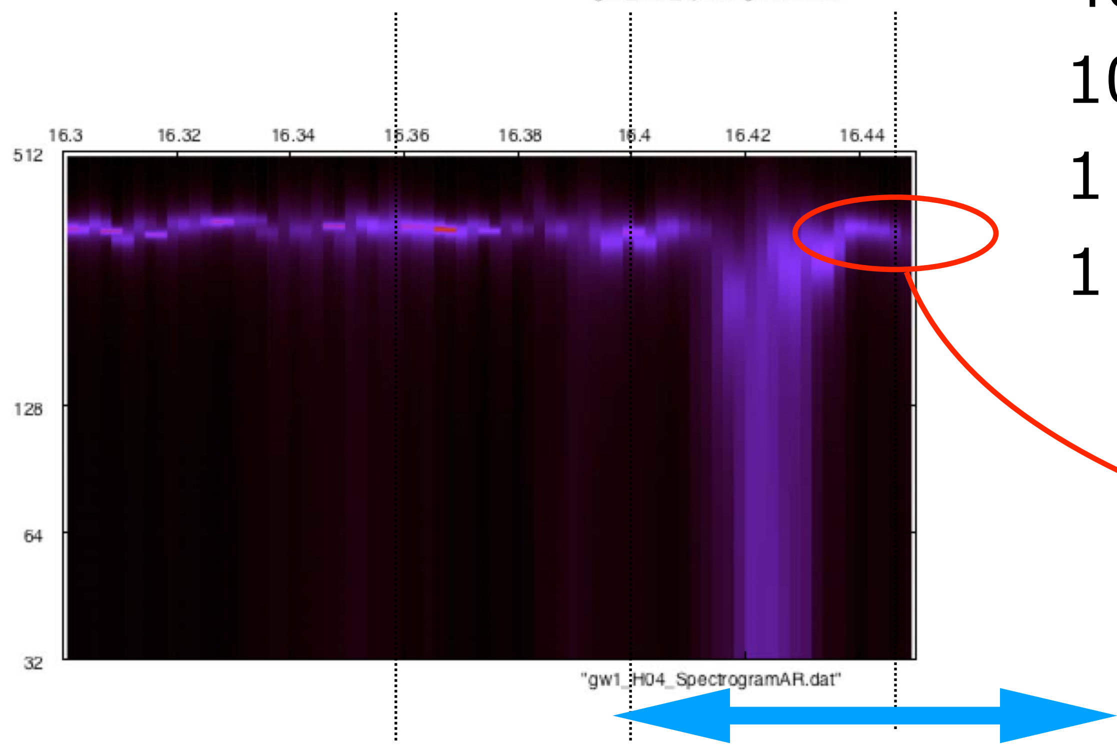

4096 sampling rate
100-400 Hz filter
1 segment = 1/64 sec= 64 points
1 shift = 1/512 sec = 8 points

max M = 3

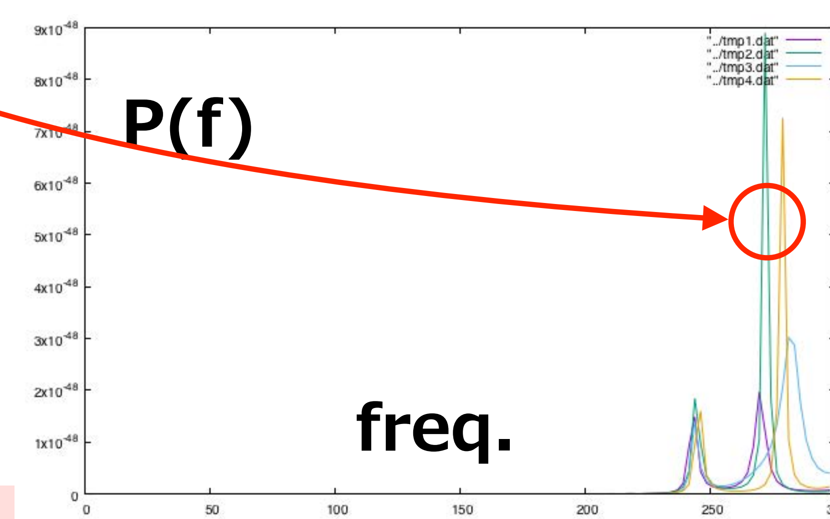

Ringdown wave of GW150914

AR model
Hanford

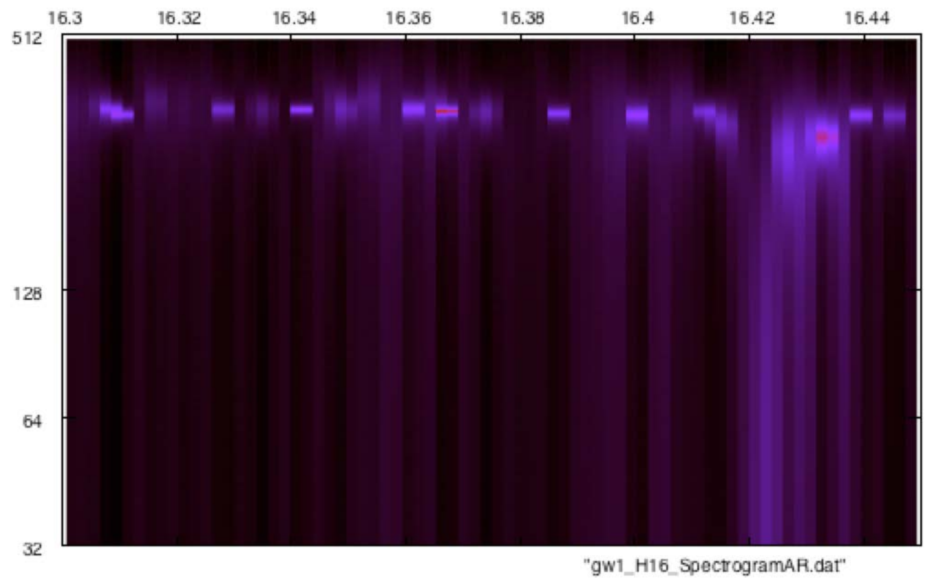

16384 sampling rate

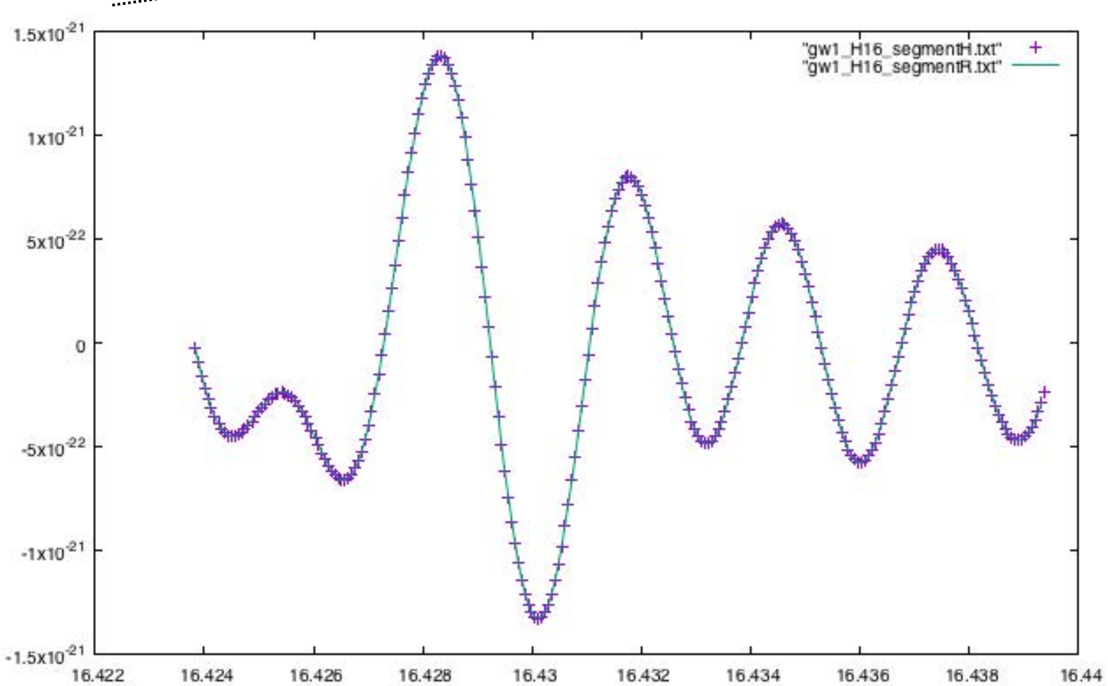

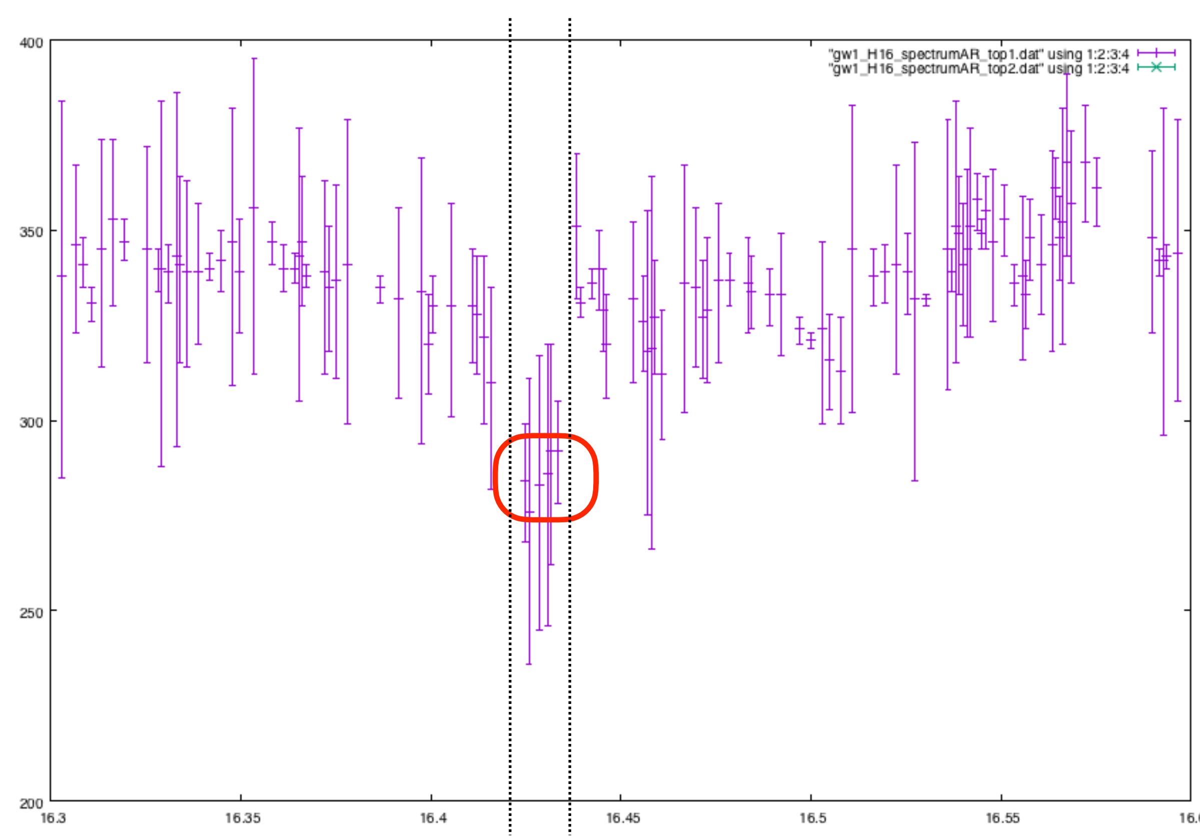

Ringdown wave of GW150914

t			f real	f imag			
4486	1	0.164258E+02	0.313508E+03	0.432791E+02	0.259000E+03	0.305000E+03	0.337000E+03
4488xx	2	0.164297E+02	0.300353E+03	0.578188E+02	0.218000E+03	0.287000E+03	0.330000E+03
4489	1	0.164316E+02	0.317507E+03	0.382182E+02	0.274000E+03	0.311000E+03	0.339000E+03
4498	1	0.164492E+02	0.314336E+03	0.538556E+02	0.261000E+03	0.309000E+03	0.349000E+03
4501	1	0.164551E+02	0.317640E+03	0.349751E+02	0.282000E+03	0.314000E+03	0.340000E+03
4505	1	0.164629E+02	0.316355E+03	0.429281E+02	0.277000E+03	0.314000E+03	0.346000E+03
4508	1	0.164688E+02	0.311752E+03	0.297619E+02	0.285000E+03	0.310000E+03	0.332000E+03

```
data points =      7
average & variance zfr =     0.313E+03    0.556E+01   fr(sp) =     0.307E+03    0.871E+01
average & variance zfi =     0.430E+02    0.926E+01
```

We see QNM at 300Hz, 0.003s after the merger.

$$f_R = f_1 + f_2(1-a)^{f_3}$$
$$Q \equiv \frac{f_R}{2f_I} = q_1 + q_2(1-a)^{q_3}$$

$$f_{\rm qnm}[{\rm Hz}] = \frac{c^3}{2\pi GM} f_R \sim 32314.1 \left(\frac{M_\odot}{M}\right) f_R.$$

$$a = 1 - \left(\frac{Q-q_1}{q_2}\right)^{1/q_3}$$
$$M[M_\odot] = 32314.1 \times \frac{f_1 + f_2(1-a)^{f_3}}{f_{\rm qnm}[{\rm Hz}]}$$

Berti, Cardoso & Will PRD 73, 064030 (2006).

Table 1. Results of frequency and damping rate of ring-down gravitational wave of GW150914.

data	$f_{\rm real}$[Hz]	$f_{\rm imag}$[Hz]	mass $(M/M_\odot)$	Kerr parameter a/M
Hanford	$305.94^{+18.68}_{-27.82}$	$43.55^{+13.00}_{-17.99}$	$58.74^{+16.03}_{-9.37}$	$0.75^{+0.18}_{-0.27}$
Livingston	$300.02^{+17.49}_{-27.21}$	$44.94^{+12.88}_{-18.30}$	$58.15^{+16.49}_{-9.53}$	$0.71^{+0.20}_{-0.30}$

LIGO says (GW150914): $M = 62.2^{+3.7}_{-3.4}$ $a = 0.68^{+0.05}_{-0.06}$

Ringdown wave of GW150914, GW170814, GW170104

Table 1. Results of frequency and damping rate of ring-down gravitational wave of GW150914.

data	$f_{\rm real}$[Hz]	$f_{\rm imag}$[Hz]	mass ($M/M_\odot$)	Kerr parameter a/M
Hanford	$305.94^{+18.68}_{-27.82}$	$43.55^{+13.00}_{-17.99}$	$58.74^{+16.03}_{-9.37}$	$0.75^{+0.18}_{-0.27}$
Livingston	$300.02^{+17.49}_{-27.21}$	$44.94^{+12.88}_{-18.30}$	$58.15^{+16.49}_{-9.53}$	$0.71^{+0.20}_{-0.30}$

LIGO says (GW150914): $M = 62.2^{+3.7}_{-3.4}$ $a = 0.68^{+0.05}_{-0.06}$

Table 2. Results of frequency and damping rate of ring-down gravitational wave of GW170814.

data	$f_{\rm real}$[Hz]	$f_{\rm imag}$[Hz]	mass ($M/M_\odot$)	Kerr parameter a/M
Hanford	$308.67^{+11.66}_{-8.59}$	$39.39^{+10.89}_{-17.85}$	$61.70^{+16.04}_{-8.15}$	$0.81^{+0.15}_{-0.16}$
Livingston	$287.54^{+102.77}_{-74.88}$	$47.17^{+11.66}_{-16.39}$	$57.29^{+14.32}_{-11.62}$	$0.64^{+0.21}_{-0.50}$

LIGO says (GW170814): $M = 53.2^{+3.2}_{-2.5}$ $a = 0.70^{+0.07}_{-0.05}$

Table 3. Results of frequency and damping rate of ring-down gravitational wave of GW170104.

data	$f_{\rm real}$[Hz]	$f_{\rm imag}$[Hz]	mass ($M/M_\odot$)	Kerr parameter a/M
Hanford	$338.21^{+0.87}_{-0.73}$	$15.57^{+9.61}_{-8.86}$	$79.33^{+13.52}_{-9.65}$	$0.98^{+0.02}_{-0.04}$
Livingston	$339.96^{+2.77}_{-1.61}$	$13.92^{+10.27}_{-7.33}$	$81.02^{+11.59}_{-10.77}$	$0.98^{+0.01}_{-0.03}$

LIGO says (GW170104): $M = 48.7^{+5.7}_{-4.6}$ $a = 0.64^{+0.09}_{-0.2}$

Ringdown wave of GW150914, GW170814, GW170104

GW150914 (S/N = 23.7)

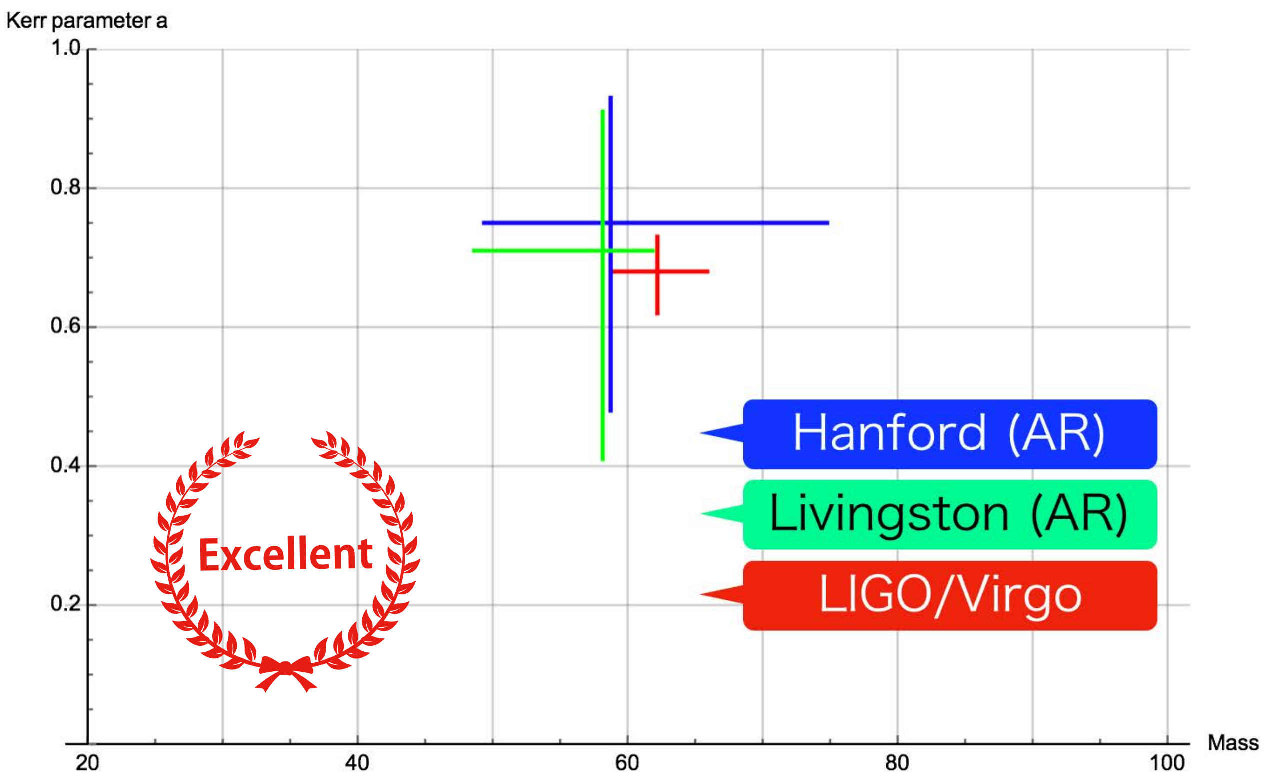

GW170814 (S/N = 18)

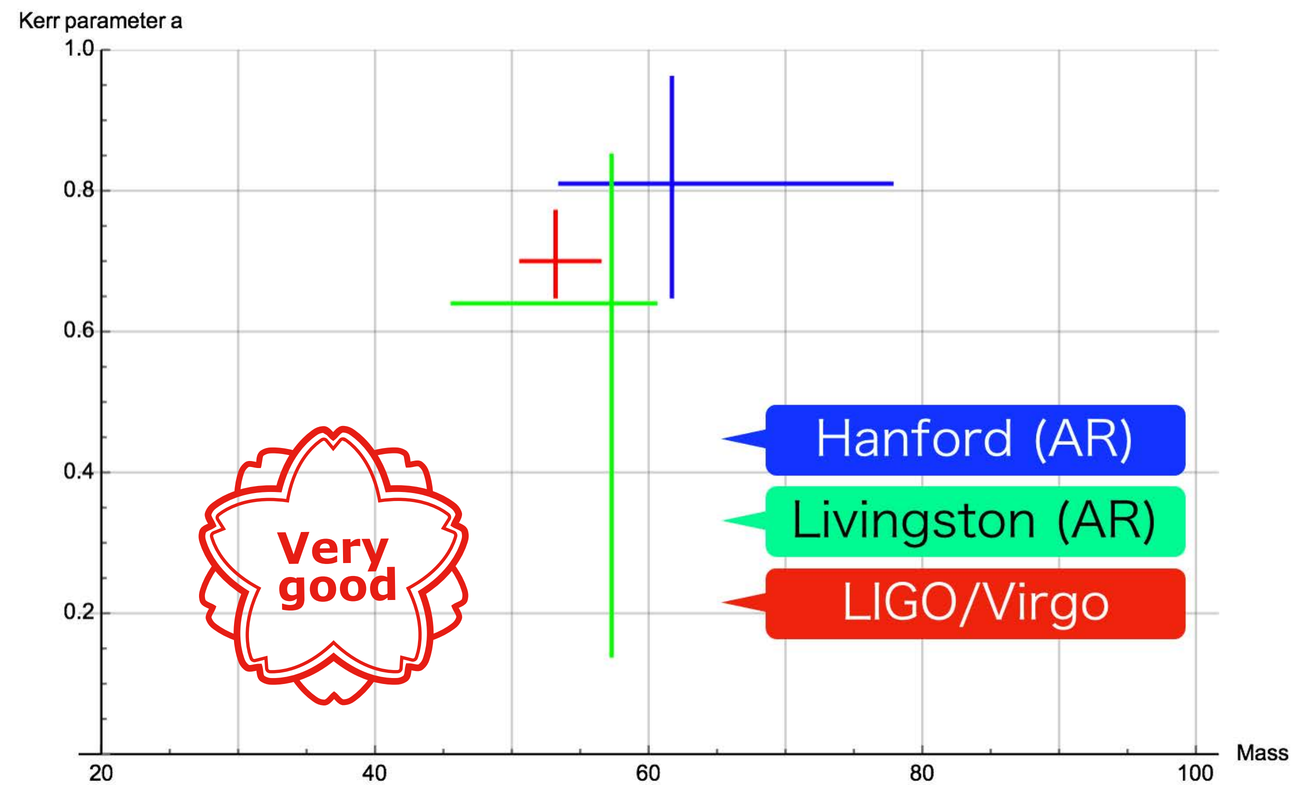

GW170104 (S/N = 13)

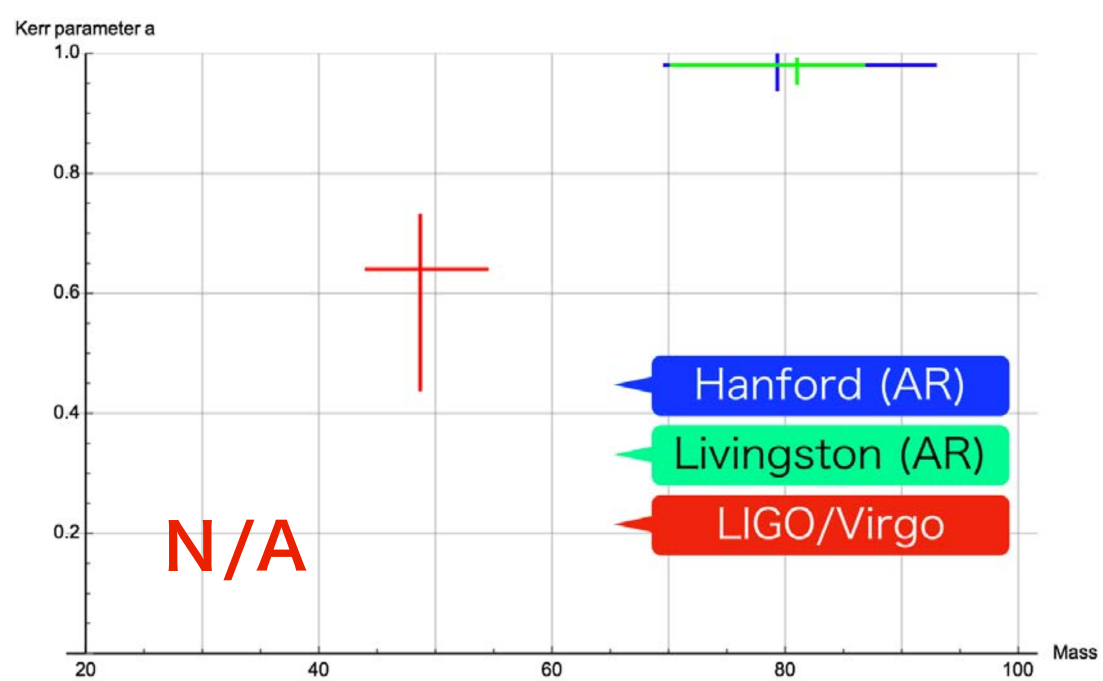

Summary & Outlook

自己回帰モデル *x(t)*

$$
\begin{aligned}
x_n &= a_1 x_{n-1} + a_2 x_{n-2} + \cdots + a_M x_{n-M} + \varepsilon \\
&= \sum_{j=1}^{M} a_j x_{n-j} + \varepsilon
\end{aligned}
$$

短いデータ (～ 30 pts) に対しても精度よく周波数・減衰率を特定できる.
シグナルを見つけるのにテンプレートは不要.

LIGO/Virgo の 3 実イベントデータに適用，リングダウン部分の抽出を試みた.

LIGO/Virgoのは発表している *(M, a)* と**GW150914, GW170814**よく一致
(S/N=23.7) (S/N=18)

S/Nの低い **GW170104** ではいまいち
(S/N=13)

★リングダウン部分だけを検出できれば，強い重力場の重力理論検証ができる.
他の方法と組み合わせ，検出データ数が稼げれば，相対論検証ができるだろう.

★テンプレートを使わない方法は，今後，未知の重力波シグナルの候補検出に役立つかも.

重力波観測の将来計画

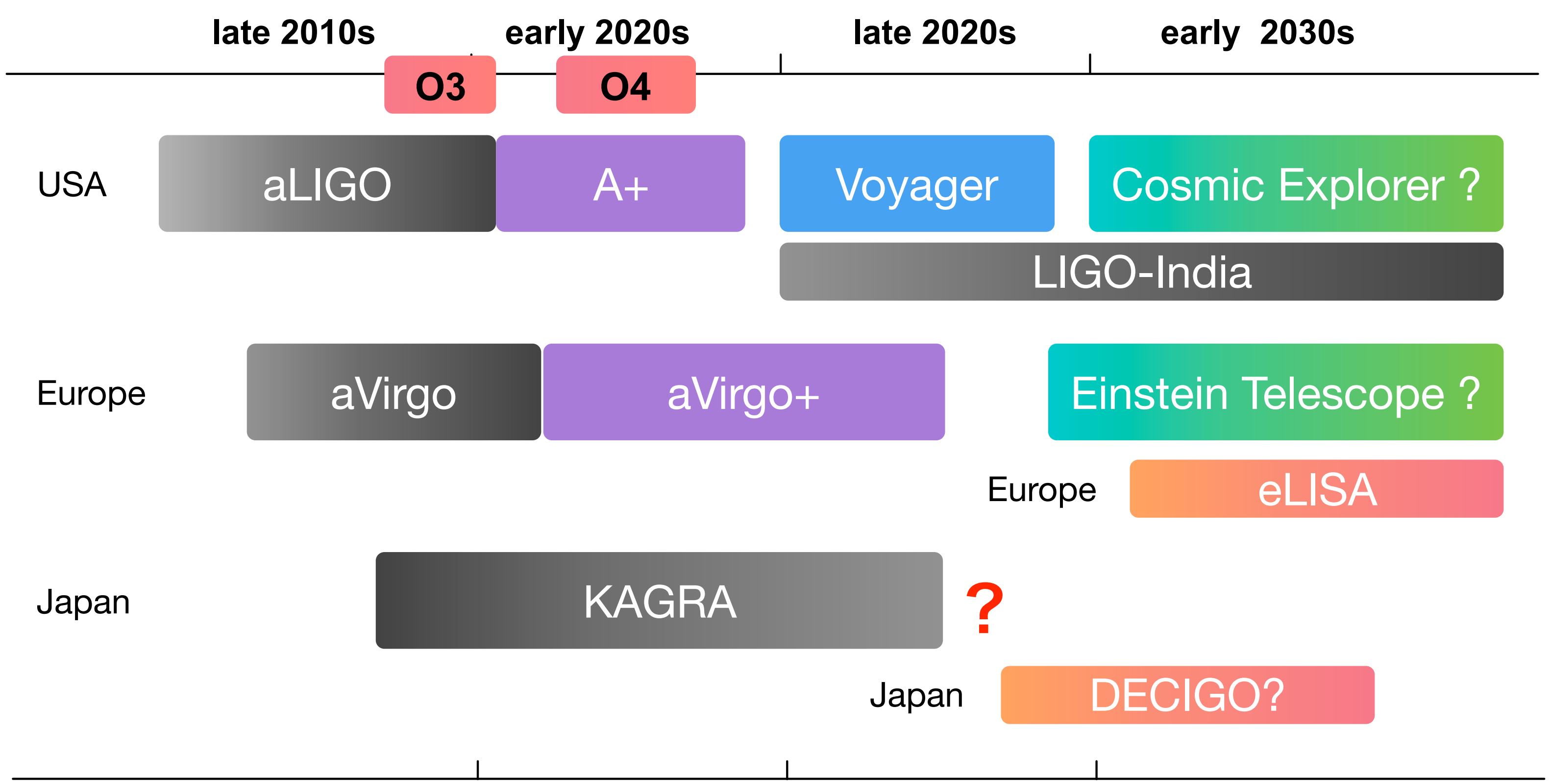

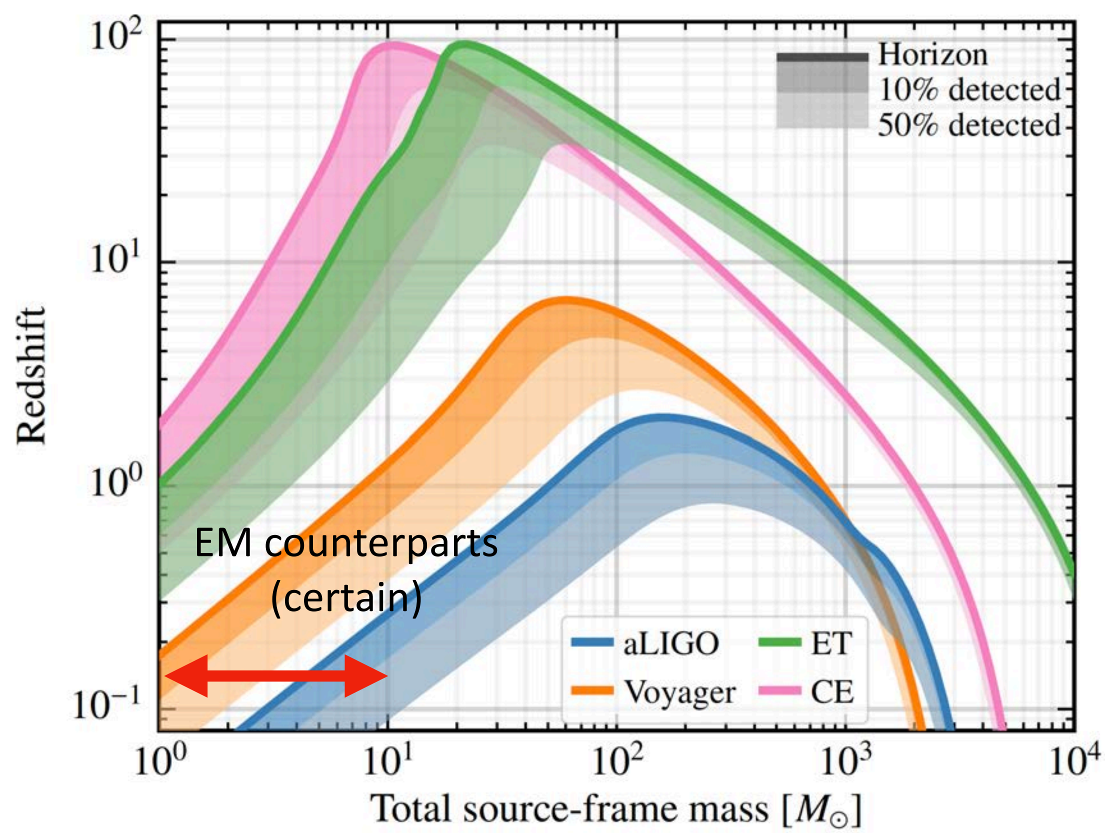

Evan Hall, MIT

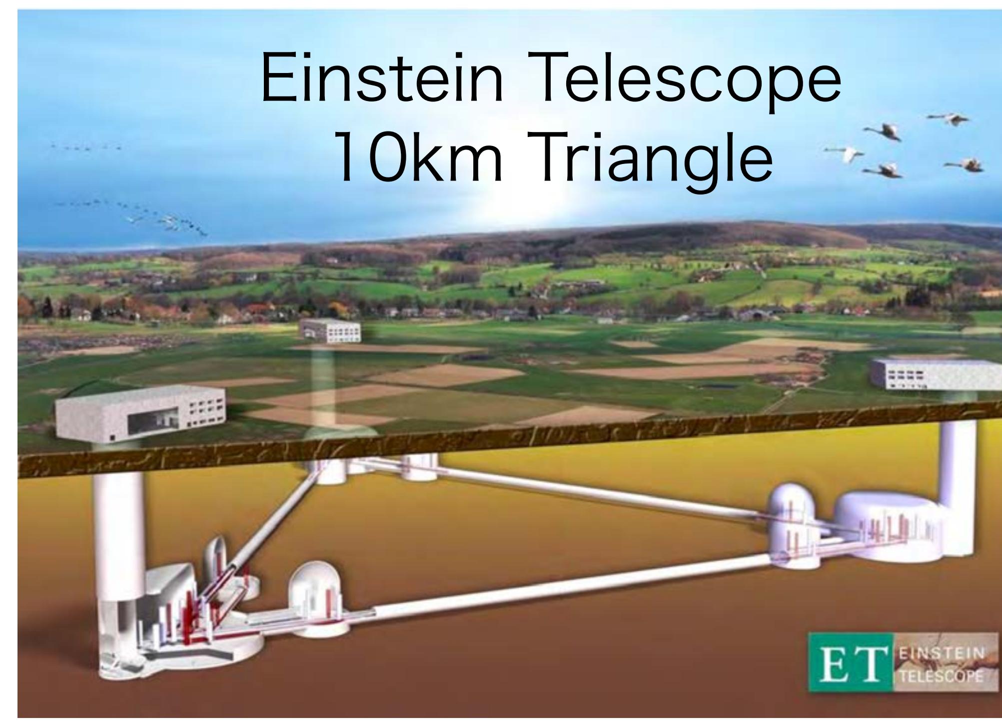

マルチ・メッセンジャー天文学の誕生

	宇宙線	ガンマ線	X 線	光			電磁波					
				紫外線	可視光線	赤外線	マイクロ波	超短波	短波	中波	長波	超長波
波長[m]	10^{-13}	10^{-10}	10^{-9}		3.8×10^{-7}	7.7×10^{-7}	10^{-4}	1	10	10^{2}	10^{3}	10^{4}
波長[nm]					380 770							
振動数[Hz]		3×10^{18}	3×10^{17}				3×10^{12}	3×10^{8}	3×10^{7}	3×10^{6}	3×10^{5}	3×10^{4}
利用例		医療／食品照射	医療／X線写真	殺菌	光学機器	赤外線写真	電子レンジ 携帯電話	FMラジオ テレビ	短波ラジオ	AMラジオ	飛行機の通信 電波時計	

ガンマ線 X線 可視光 赤外 電波

重力波

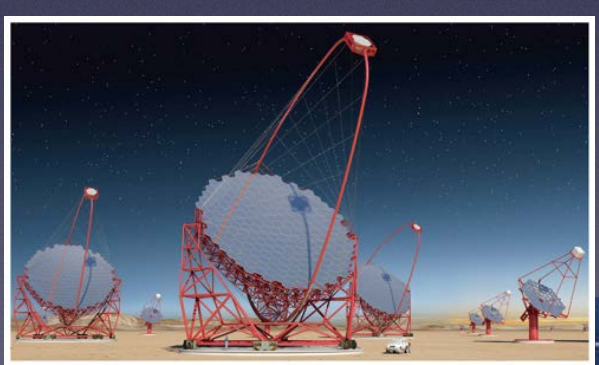



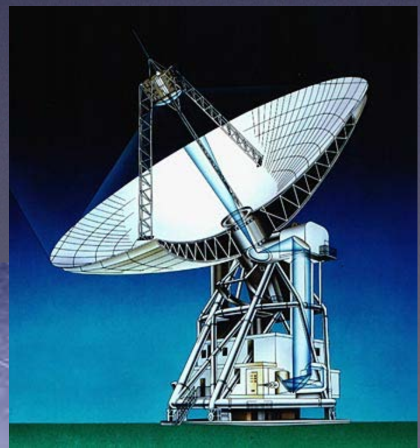
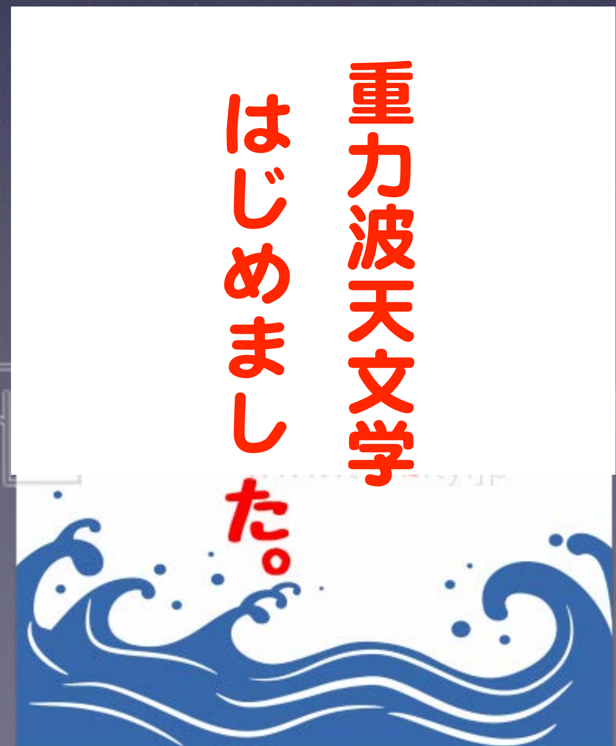

Black Widow Spider
Fermi Bubbles
Colosseum
Eiffel Tower
Einstein
Fermi Satellite
Godzilla
Golden Gate
Hulk
The Little Prince
Mjolnir
Mount Fuji
Castle
Obelisk
Pharos
Radio Telescope
Saturn V Rocket
Schrödinger's Cat
Starship Enterprise
TARDIS
Vasa

2018/10

Fermi衛星チーム，ガンマ線バースト天体カタログで21星座を命名

https://fermi.gsfc.nasa.gov/science/constellations/

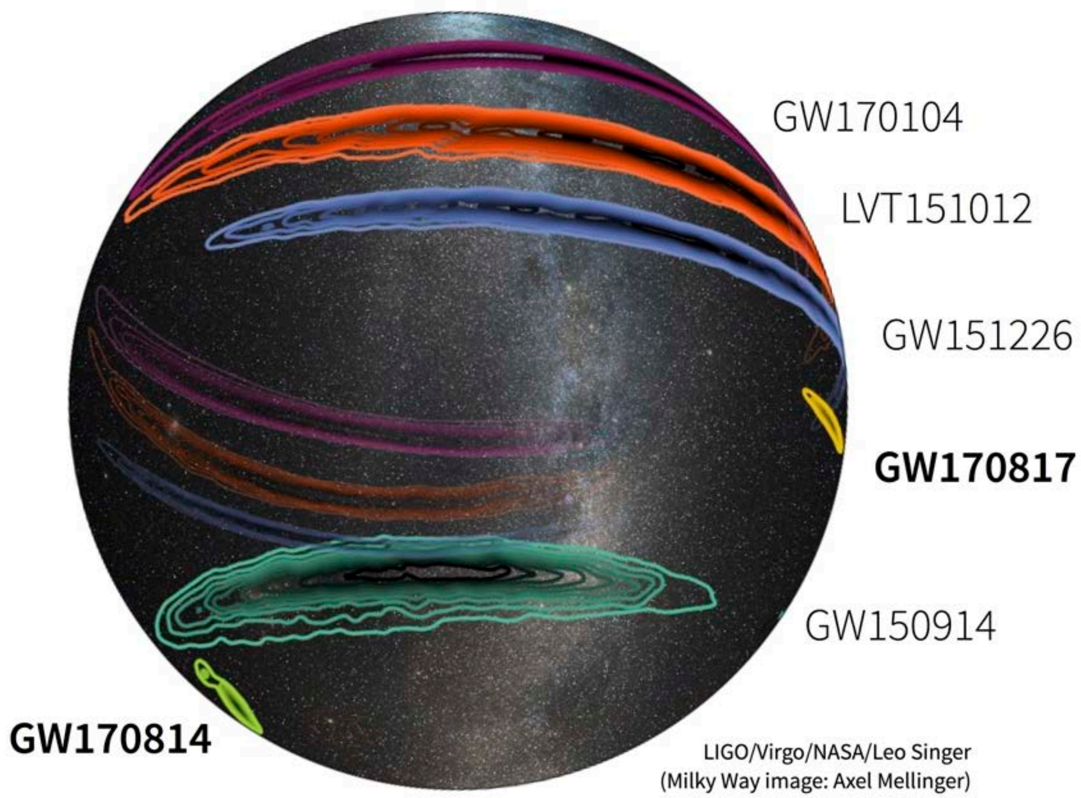

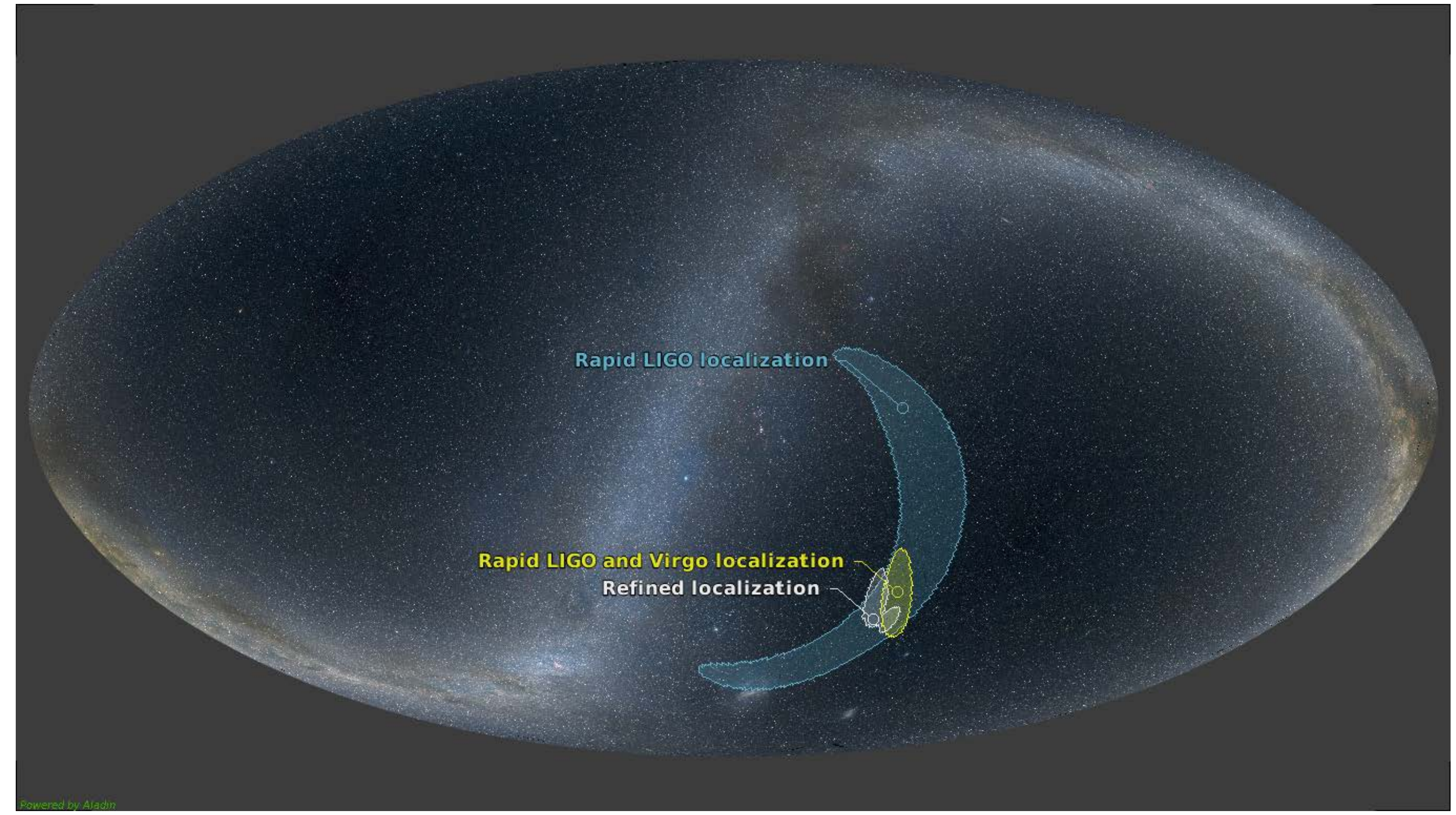

http://www.virgo-gw.eu/skymap.html

重力波源が特定されたのは，まだ１つ.

202x/xx
LIGO/Virgo/KAGRAチーム,
重力波天体カタログで108星座を命名

しかし
2019年の観測がはじまれば,
週に１回，BH-BH
月に１回，NS-NS

宇宙空間での観測がはじまれば,
1日に10回，BH-BH ??

まとめ

1．重力波観測時代がはじまった

BH-BH, NS-NS．次はBH-NS？ SN？

2．日本のKAGRAも2019年から実観測開始

LIGO/Virgoとの共同観測体制構築中．

3．データ解析には，まだまだ試すべきアイデアがたくさんある．

将来計画もたくさんある．　**新規参入，大歓迎！**